

SELECTED  
NOV 13 1995  
F

# Cornell University



IMPACT ON MULTILAYERED COMPOSITE PLATES

by

B.S. Kim and F. C. Moon



April, 1977

Final Report NASA CR 135247

# Theoretical and Applied Mechanics

19951109 069

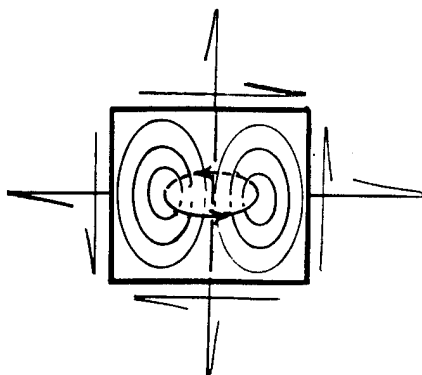
PLASTIC 277119

DISTRIBUTION STATEMENT A

Approved for public release  
Distribution Unlimited

Thurston Hall

Ithaca, New York



DTIC QUALITY INSPECTED 5

IMPACT ON MULTILAYERED COMPOSITE PLATES

by

B.S. Kim and F. C. Moon



April, 1977

Final Report NASA CR 135247

Accession For	
NTIS Cover	<input checked="" type="checkbox"/>
DTIC TAB	<input type="checkbox"/>
Unannounced	<input type="checkbox"/>
Justification	
By <i>DTIC AI memo</i>	
Distribution/ <i>11-2-95</i>	
Availability Codes	
Dist	Avail and/or Special
<i>A-1</i>	

1. Report No. NASA CRL35247	2. Government Accession No.	3. Recipient's Catalog No.	
4. Title and Subtitle Impact on Multi layered Composite Plates		5. Report Date 4/1977	
		6. Performing Organization Code	
7. Author(s) B.S. KIM and F.C. MOON		8. Performing Organization Report No.	
		10. Work Unit No.	
9. Performing Organization Name and Address Department of Theoretical and Applied Mech. Cornell University Ithaca, N.Y. 14853		11. Contract or Grant No. NSG-3080	
		13. Type of Report and Period Covered: Final Report 9/75-12/76	
12. Sponsoring Agency Name and Address National Aeronautics and Space Administration Washington, D.C., 20546		14. Sponsoring Agency Code	
		15. Supplementary Notes Project Manager: C.C. Chamis Materials and Structures Division NASA Lewis Research Center Cleveland, Ohio, 44135	
16. Abstract Stress wave propagation in a multilayer composite plate due to impact has been examined by means of the anisotropic elasticity theory. The plate is modelled as a number of identical anisotropic layers and the approximate plate theory of Mindlin is then applied each layer to obtain a set of difference-differential equations of motion. Dispersion relations for harmonic waves and correction factors are found. The governing equations are reduced to difference equations via integral transforms. With given impact boundary conditions these equations are solved for an arbitrary number of layers in the plate and the transient propagation of waves is calculated by means of a Fast Fourier Transform algorithm.  The multilayered plate problem is extended to examine the effect of damping layers present between two elastic layers. A reduction of the interlaminar normal stress is significant when the thickness of the damping layer is increased but it seems that the effect is mostly due to the softness of the damping layer. Finally the problem of a composite plate with a crack on the interlaminar boundary has been formulated.			
17. Key Words (Suggested by Author(s)) Multilayered Composite Plate, Approximate Plate Theory of Mindlin, Impact, Stress Wave, Dispersion Relation, Wave surface, Damping Layer, Crack, Fast Fourier Transform.		18. Distribution Statement Unclassified, unlimited	
19. Security Classif. (of this report) Unclassified	20. Security Classif. (of this page) Unclassified	21. No. of Pages	22. Price*

\* For sale by the National Technical Information Service, Springfield, Virginia 22151

## Contents

	<u>Page</u>
Preface and Summary	ii
Symbols Used	iv
I Introduction	1
II Impact on Multilayer Elastic Plate	5
III Impact of a Composite Plate with an Interlaminar Damping Layer	30
IV Impact on a Plate with a Crack	37
V Conclusion and Recommended Research	43
Reference	44
Figures	47
Appendix A - Flow Chart	72
Appendix B - Sample Computer Deck	76
Appendix C - Program and Sample Output	77

SYMBOLS USED

- $\Delta$ : Plate thickness (Nondimensional length unit)
- $b$ : A half of the layer thickness
- $N$ : Layer number in the plate
- $\rho$ : Density
- $t_0$ : Impact time
- $P_0(x_1, t)$ : Impact stress
- \*  $x_1(\eta), x_2(\xi)$ : Coordinate variables
- \*  $t(\tau)$ : Time variable
- $T_0$ : Nondimensional time unit =  $a/\sqrt{c_{66}/\rho}$
- \*  $\sigma_{ij}, \sigma(\Sigma), \tau(T), \sigma_{11}$ : Stress tensor and its components
- \*  $u_i, u(U), v(V)$ : Displacement vector and its components
- \*  $c_{ijkl}, c_{ij}(C_{ij})$ : Elastic Moduli ( $\hat{c}_{11} = c_{11} - \frac{c_{12}^2}{c_{22}}$ )
- $\lambda, \mu$ : Lamé's constants
- $\epsilon_{ij}, \epsilon_i$ : Infinitesimal strain tensor
- $\hat{A}$ : Laplace transform (in  $\tau$ ) and Fourier transform (in  $\eta$ ) of  $A$
- $P_n(\xi)$ : Legendre polynomial of  $\xi$
- \*  $k(\kappa)$ : Wave number
- \*  $\omega(\bar{\omega})$ : Frequency
- $\theta, \alpha, \beta$ : Phase shifts (wave number through the thickness)
- $C_D, C_S$ : Dilatational and shear wave speed
- $G^*(\omega) = G'(\omega) + iG''(\omega)$ : Complex modulus of elastomer
- $D$ : Thickness of viscoelastic layer
- $h$ : A half of the crack length
- \* Quantities in ( ) are nondimensional quantities.

## Preface and Summary

This report is the last of a series on the response of composite plates to impact forces. The motivation for these studies has been an attempt to understand the damage to aircraft jet engine fan blades by foreign object impact such as ice balls, stones, and birds. In addition, the National Aeronautics and Space Administration, sponsors of this research, have sought to develop computer codes from these analyses which will aid the fan blade designer in locating potential failure modes and positions and thus assist in optimizing fan blade fabrication to create greater impact tolerance.

The basic approach of the principal investigator in these studies has been to use wave propagation techniques to model the early response of composite plates to impact type forces. In using the wave method, the plate can be simplified in the analyses by neglecting reflections from edge boundaries far from the impact point. Thus, while the overall geometry of the plate is no longer included in the analysis, more sophisticated mathematical models near the point of impact have been used.

The basic model for the composite plate studies has been the anisotropic plate theory as extended by Mindlin [1] to account for wave phenomena. The plate equations were used as an approximation of the exact theory of elasticity because they lead to simpler computational schemes for evaluating average stresses and displacements in the plate.

Fourier and Laplace transform techniques have been used throughout these studies and inversion of the transforms has been accomplished with a fast Fourier transform algorithm. This algorithm is an effective computational tool but requires careful scaling of the impact problem in both space and time

variables. When it is properly used it can lead to calculations of thousands of stress values in a fraction of the time of conventional finite element schemes.

In summary, the use of plate models for the fan blade impact has avoided the analytical complexities of the exact theory of elasticity as well as the computational difficulties of finite element methods.

In earlier reports both central and edge impact of an anisotropic plate were studied, [ 2- 4 ]. In those reports only wave propagation in the plane of the plate was investigated. In another report [5] a multilayer plate model was developed in order to study impact induced wave propagation in both the thickness and inplane directions. In this final report further results are presented from the multilayer model. The composite plate has been modeled with as many as eight separate layers. Each layer may itself have several plies, so that effective anisotropic constants must be used for each layer in the analysis. The mathematical model exhibits wave propagation in both the thickness and inplane directions. Impact generated waves are shown to lead to interlaminar shear stresses and interlaminar tensile stresses during and after impact.

This report also presents an analysis of an impact damping mechanism. This consists of thin damping layer introduced between composite layers in the mathematical model. The resulting response due to impact shows that considerable reduction of stress can be achieved. However it appears that this stress reduction is linked to the lower elastic moduli of the damping sublayers and not the viscous nature of the sublayer.

Finally an attempt was made to analyze the impact of a plate with a crack. While the problem has been formulated, no progress was made on obtaining numerical answers to the crack problem.

## I. INTRODUCTION

The present research is a continuation of our previous work on the stress wave propagation in a laminated composite [2-5]. It has been motivated by the problem of the impact on jet engine fan blades caused by ingestions of foreign materials, such as birds and hailstones. The successful application of fiber-reinforced composite materials depends on the ability of these materials to withstand forces due to such impact.

The simplest approach to examine the dynamic behavior of a composite plate is based upon the work of White and Angona [6]. In their work, referred to as the effective modulus theory, the response of the composite plate to waves propagating normal to the laminate is predicted by a single constant wave speed, regardless of the internal structure of composites. Even though this theory is satisfactory for many problems, it fails in the case of some problems when the wave lengths become short. To overcome this limitation, Sun and et al. proposed a model which includes the effects of internal structure, such as the layer thickness [7]. In their work, referred to so the effective stiffness theory, displacements of both the reinforcing layer and the matrix layer are expressed as linear expansions about the midplanes of the layers and approximate equations of motion are derived for both layers. Then these approximate equations are required to satisfy the continuity conditions of displacement and stress components on every interface. Using this model the propagation of harmonic waves has been examined.

More recently a number of researchers have presented models for multilayer plates either by the discrete-continuum theory or the continuum mixture theory [8-14]. Many, however examined only the frequency-wave number dispersion relationship and stopped short of the transient

impact problem except for a few experimental or numerical works using the finite element method which sometimes show a considerable discrepancy from the experimental results.

In this report we present a new attempt to mathematically model the multilayer plate and develop a method by which we can examine the transient propagation of an impact wave in the plate, not only along the longitudinal direction but also through the thickness direction of the plate as well, using an inexpensive Fast Fourier Transform algorithm [3,15].

The composite plate under consideration for the first part of the present report is imagined to comprise  $N$  identical elastic layers. And each layer is made of a number of unidirectional plies lying alternately at a layup angle  $\pm\phi$  from the symmetry axis, as shown in Fig. 1. Then the elastic properties of the plate depend on the layup angle  $\phi$ . A key assumption for the first step of the work is that all the layers are identical. While restricting the application, this assumption allows us to formulate the problem using difference-differential equations due to a rather simple periodic structure of the plate. This technique for periodic structures has been widely used in the study of electrical transmission lines [16] and in the vibration of multistory buildings [17]. By means of an approximate plate theory of Mindlin [18], a set of approximate equations of motion is developed for a typical layer using the interlaminar stresses as explicit variables. The relative motion of a layer to the adjacent layers is related by phase shifts which represent the solution of the difference parts of equations. In this way the number of the layers can be increased without increasing the size of matrix in the numerical process of invert to satisfy the boundary conditions.

It is also well understood that a thin viscoelastic layer present between elastic layers can reduce the elastic impact energy significantly by dissipating the strain energy into heat [19,20]. In our previous work [5] an elastomer layer is presented between a composite half space and a protection strip on the edge on which the impact is applied. Numerical results of the work showed an appreciable reduction in the normal stress. As an extension of this research and the first part of this report we now examine the wave propagation in a composite plate made of two elastic layers and an elastomer layer. Generalization of this problem is straightforward by assuming that our new periodic composite layer is now made of an elastic sublayer and a viscoelastic sublayer lying alternately. We can now develop the approximate theory which includes both sublayers. For the second part of the present research we will examine the simplest case of this kind, i.e., an impact on a composite plate consisting of two elastic layers and an elastomer layer between them.

Another possible extension of the multilayer composite plate which can be found in frequent practice is discussed in the last part of this report. In this chapter a crack is introduced on the interface between two elastic layers which represent the final step before a failure occurs in the composite either by spalling or by excessive shear stress. Such crack problems constitute the main part of the study of fracture mechanics. A serious mathematical difficulty arises even in the static problems because of the mixed boundary conditions along the crack direction. The difficulty becomes more serious in the case of dynamic problems due to the diffraction of waves at the crack tip [21-24]. By employing the approximate equations of motion developed in the first part, the transient wave problem has been formulated and dual integral

equations are obtained after application of the mixed boundary conditions. But the resulting dual integral equations are not easy to solve and are under investigation at this time.

In the results presented in this report only a line impact has been examined. This has simplified the calculations and saved computer time in testing the model. The technique, however, can be extended to the two-dimensional or central impact problem. Since the impact speed is very high (~450 m/sec) and the impact time is short (< 100  $\mu$ sec), the impact can be in the range of the elastic-plastic impact or even in the range of the hydraulic impact. But the initial transmission of impact energy is propagated by elastic waves, as if in an unbounded plate, and it is useful to investigate the problem by means of the linear theory of anisotropic elasticity in an infinite composite plate.

## II. IMPACT ON MULTILAYER ELASTIC PLATE

### 1. Formulation

#### Basic Theory of Linear Anisotropic Elasticity

Cauchy's equations of motion in cartesian tensor form without body forces are given by

$$\sigma_{ij,i} = \rho \ddot{u}_j \tag{II-1}$$

$$\sigma_{ij} = \sigma_{ji}$$

where the repeated index implies summation on that index. A comma represents a partial differentiation with respect to the index following the comma and a superposed dot denotes a time derivative.

tensor is related to the infinitesimal strain tensor  $\epsilon_{ij}$  by

$$\sigma_{ij} = c_{ijkl} \epsilon_{kl} \text{ or } \sigma_i = c_{ij} \epsilon_j \tag{II-2}$$

The condensed elastic moduli  $c_{ij}$  has the following form for orthotropic materials

$$c_{ij} = \begin{bmatrix} c_{11} & c_{12} & c_{13} & 0 & 0 & 0 \\ c_{12} & c_{22} & c_{23} & 0 & 0 & 0 \\ c_{13} & c_{23} & c_{33} & 0 & 0 & 0 \\ 0 & 0 & 0 & c_{44} & 0 & 0 \\ 0 & 0 & 0 & 0 & c_{55} & 0 \\ 0 & 0 & 0 & 0 & 0 & c_{66} \end{bmatrix}$$

Analysis of a Layer

For a layer shown in Fig. 1 we employ the approximate plate theory of Mindlin [18] and the displacement field  $u$  is expanded in terms of the Legendre polynomials as

$$u(x_1, x_2, x_3, t) = \sum_{n=0}^{\infty} u^{(n)}(x_1, x_3, t) \cdot P_n(\xi) \quad (\text{II-3})$$

where  $\xi$  is the local coordinate along the thickness direction, normalized by  $b$ , a half layer thick.

Instead of solving Eq. (II-1) directly we solve a new approximate equation of motion which is obtained through a variational process by integration of Eq. (II-1) over the thickness  $\xi$  (see [1], [23]). The result is

$$b \cdot \sigma_{\alpha j}^{(n)} + [P_n(\xi) \cdot \sigma_{2j}]_{\xi=-1}^1 - \sigma_{2j}^{*(n)} = \frac{2\rho b}{2n+1} \ddot{u}_j^{(n)} : \begin{matrix} j = 1, 2, 3 \\ \alpha = 1, 3 \end{matrix} \quad (\text{II-4})$$

where

$$\sigma_{\alpha j}^{(n)} = \int_{-1}^1 P_n(\xi) \cdot \sigma_{\alpha j} d\xi$$

$$\sigma_{2j}^{*(n)} = \int_{-1}^1 \frac{dP_n(\xi)}{d\xi} \sigma_{2j} d\xi$$

By substituting the constitutive relation (II-2) for the displacement expansion (II-3) into the above approximate equations of motion, we can find governing equations of motion in terms of  $u_1^{(0)}, u_2^{(0)}, u_3^{(0)}, u_1^{(1)} \dots$ . The accuracy of this approximate theory depends on how many terms of the

displacement field we retain. Since the complexity in formulation increases rapidly with the number of terms included we keep terms only up to second order. Furthermore, we will examine harmonic waves propagating along the  $x_1$  and  $x_2$  directions so that we drop  $u_3^{(n)}$  terms and set  $\frac{\partial}{\partial x_3} \{ \} = 0$ . Next to get rid of the undesired coupling with higher modes we set  $\ddot{u}_1^{(2)} = \ddot{u}_2^{(2)} = 0$ . Then the resulting equations are

$$2b(c_{11}u_{1,11}^{(0)} + \frac{1}{b}c_{12}u_{2,1}^{(1)}) + (\sigma_{21}^+ - \sigma_{21}^-) = 2b\rho\ddot{u}_1^{(0)}$$

$$2bc_{66}(\frac{1}{b}u_{1,1}^{(1)} + u_{2,11}^{(0)}) + (\sigma_{22}^+ - \sigma_{22}^-) = 2b\rho\ddot{u}_2^{(0)}$$

$$\frac{2b}{3}(c_{11}u_{1,11}^{(1)} + \frac{3}{b}c_{12}u_{2,1}^{(2)}) - 2c_{66}(\frac{u_1^{(1)}}{b} + u_{2,1}^{(0)}) + (\sigma_{21}^+ + \sigma_{21}^-) = \frac{2}{3}b\rho\ddot{u}_1^{(1)}$$

$$\frac{2b}{3}(c_{66}u_{2,11}^{(1)} + \frac{3}{b}c_{66}u_{1,1}^{(2)}) - 2(c_{12}u_{1,1}^{(0)} + \frac{1}{b}c_{22}u_2^{(1)}) + (\sigma_{22}^+ + \sigma_{22}^-) = \frac{2}{3}b\rho\ddot{u}_2^{(1)}$$

$$(\sigma_{22}^+ - \sigma_{22}^-) - 2(c_{12}u_{1,1}^{(1)} + \frac{3}{b}c_{22}u_2^{(2)}) = 0$$

(II-5)

$$(\sigma_{21}^+ - \sigma_{21}^-) - 2(c_{66}u_{2,1}^{(1)} + \frac{3}{b}c_{66}u_1^{(2)}) = 0$$

where the sign + and - represent the stress components on the top and bottom surfaces of the layer under examination, i.e., at  $\xi = \pm 1$ . Here we notice that the first, fourth, and last equations are written in terms of  $u_i^{(n)}$ , where  $(n+i)$  is an odd integer and represents the thickness stretching motion (or symmetric motion). In the rest of the equations in which  $(n+i)$  is an even integer the displacements represent the flexural motion (or antisymmetric motion). Hence, this process has decoupled the

stretching motion from bending motion\*. To get rid of the 2nd order modes from Eq. (II-5) we solve the last two equations for  $u_2^{(2)}$  and  $u_1^{(2)}$ , and insert them into the remaining equations. Then Eq. (II-5) can be reduced as follows:

$$2b(c_{11}u_{1,1}^{(0)} + \frac{1}{b}c_{12}u_{2,1}^{(1)}) + (\sigma_{21}^+ - \sigma_{21}^-) = 2b\rho\ddot{u}_1^{(0)}$$

$$2b c_{66} (\frac{1}{b}u_{1,1}^{(1)} + u_{2,11}^{(0)}) + (\sigma_{22}^+ - \sigma_{22}^-) = 2b\rho\ddot{u}_2^{(0)} \quad (II-6)$$

$$\frac{2b\hat{c}_{11}}{3}u_{1,1}^{(1)} - 2c_{66}(\frac{u_1^{(1)}}{b} + u_{2,1}^{(0)}) + \frac{c_{12}b}{3c_{22}}(\sigma_{22}^+ - \sigma_{22}^-)_{,1} + (\sigma_{21}^+ + \sigma_{21}^-) = \frac{2}{3}b\rho\ddot{u}_1^{(1)}$$

$$-2(c_{12}u_{1,1}^{(0)} + \frac{1}{b}c_{22}u_2^{(1)}) + (\sigma_{22}^+ + \sigma_{22}^-) = \frac{2}{3}b\rho\ddot{u}_2^{(1)}$$

where  $\hat{c}_{11} = c_{11} - c_{12}^2/c_{22}$ .

Plate Analysis

In view of the Legendre polynomial expansion, the displacements on the both sides of a layer can be written as  $u_i^\pm = u_i^{(0)} \pm u_i^{(1)}$  since the governing equations for a layer, Eq. (II-6), only include terms up to the first order of expansion, i.e., a linear expansion. Remembering that this analysis is valid for any arbitrary layer in a plate, say the nth layer, equation (II-6) can be immediately written as

---

\* These two motions are, of course, coupled through the boundary conditions.

$$\begin{aligned} \rho(\ddot{u}_n + \ddot{u}_{n-1}) &= c_{11}(u_n + u_{n-1})_{,11} + \frac{c_{12}}{b}(v_n - v_{n-1})_{,1} + \frac{1}{b}(\tau_n - \tau_{n-1}) \\ \rho(\ddot{v}_n - \ddot{v}_{n-1}) &= -\frac{3}{b}c_{12}(u_n + u_{n-1})_{,1} - \frac{3}{b^2}c_{22}(v_n - v_{n-1}) + \frac{3}{b}(\sigma_n + \sigma_{n-1}) + (\tau_n - \tau_{n-1})_{,1} \\ \rho(\ddot{u}_n - \ddot{u}_{n-1}) &= \hat{c}_{11}(u_n - u_{n-1})_{,11} - \frac{3c_{66}}{b^2}(u_n - u_{n-1}) - \frac{3}{b}c_{66}(v_n + v_{n-1})_{,1} \\ &\quad + \frac{c_{12}}{c_{22}}(\sigma_n - \sigma_{n-1})_{,1} + \frac{3}{b}(\tau_n + \tau_{n-1}) \end{aligned} \tag{II-7}$$

$$\rho(\ddot{v}_n + \ddot{v}_{n-1}) = c_{66} \left\{ \frac{1}{b}(u_n - u_{n-1})_{,1} + (v_n + v_{n-1})_{,11} \right\} + \frac{1}{b}(\sigma_n - \sigma_{n-1})$$

where  $\sigma$  and  $\tau$  are used to represent  $\sigma_{22}$  and  $\sigma_{12}$  and  $u$  and  $v$  denote  $u_1$  and  $u_2$ , respectively. These equations are the approximate equations of motion of a layer written in the form of a difference-differential equation. For a plate made of  $N$  layer, the above equations contain  $4(N+1)$  unknowns  $(u_0, v_0, \tau_0, \sigma_0, \dots, u_N, v_N, \tau_N, \sigma_N)$  and offer  $4N$  equations. Since the additional four conditions are supplied by boundary conditions on the top and bottom surfaces, solutions of these equations can be found.

In Eq. (II-7) we notice some important points. The first point is that the longitudinal coordinate  $x_1$  and the time variable are continuous variables while the thickness coordinate  $x_2$  is now discrete. This enables us to use integral transforms in  $x_1$  and time variables so that we can arrive at pure difference equations after integral transforms. The second point concerns the continuity conditions of stress and displacement. We note that  $u$ ,  $v$ ,  $-\sigma_{22}$ , and  $\sigma_{12}$  have to be continuous across the layer boundary and these conditions are identically satisfied by

Eq. (II-7). But the normal stress tangential to the layer boundary is not necessarily continuous and Eq. (II-7) allows such a possibility. One can retain higher order terms in the displacement expansion given by Eq. (II-3) to give more accurate results. This can be achieved more easily by using Eq. (II-7) and increasing the number of layers in a plate under consideration. This process does not give any additional difficulties except a little more computer time.

## 2. Dispersion Relationships of Harmonic Waves

### Harmonic Waves

Before we examine the transient propagation of stress wave due to an impact we first investigate dispersion relations of harmonic waves in a composite plate governed by approximate equations of motion (II-7). For harmonic waves propagating along the  $x_1$  axis we assume

$$\{u_n, v_n, \sigma_n, \tau_n\} = \{U_n, V_n, \Sigma_n, T_n\} e^{i(kx_1 - \omega t)} \quad (\text{II-8})$$

Substituting this into the approximate equations of motion (II-7) we obtain

$$\begin{aligned} (\bar{\omega}^2 - c_{11}\kappa^2)(U_n + U_{n-1}) + c_{12}i\kappa(V_n - V_{n-1}) + b(T_n - T_{n-1}) &= 0 \\ -3c_{12}i\kappa(U_n + U_{n-1}) + (\bar{\omega}^2 - 3c_{22})(V_n - V_{n-1}) + i\kappa b(T_n - T_{n-1}) + 3b(\Sigma_n + \Sigma_{n-1}) &= 0 \\ 3c_{66}i\kappa(U_n - U_{n-1}) + (\bar{\omega}^2 - c_{66}\kappa^2)(V_n + V_{n-1}) + b(\Sigma_n - \Sigma_{n-1}) &= 0 \\ (\bar{\omega}^2 - \hat{c}_{11}\kappa^2 - 3c_{66})(U_n - U_{n-1}) - 3c_{66}i\kappa(V_n + V_{n-1}) + 3b(T_n + T_{n-1}) \\ + \frac{c_{12}}{c_{12}}i\kappa b(\Sigma_n - \Sigma_{n-1}) &= 0 \end{aligned} \quad (\text{II-9})$$

for  $n = 1, 2 \dots N$ . Here we set

$$\kappa = bk = k\left(\frac{\Delta}{2N}\right), \quad \Delta = 2bN$$

$$\omega^{-2} = \rho b^2 \omega^2 = \rho \omega^2 \left(\frac{\Delta}{2N}\right)^2$$

and  $\Delta$  is the total thickness of the plate. For a plate consisting of  $N$  layers, the boundary conditions require traction free surfaces, namely,  $T_0 = \Sigma_0 = T_N = \Sigma_N = 0$ . When these conditions are applied to equation (II-9) we obtain  $4N$  equations in terms of  $4N$  unknowns ( $U_0, V_0; U_n, V_n, T_n, \Sigma_n$  with  $n = 1, \dots, N-1; U_N, V_N$ ). By setting the coefficient matrix to be singular, required dispersion relationships can be obtained.

#### One-layer Plate

The dispersion relationship for a plate made of a single layer can be found by setting  $N = 1$  in equation (II-9) with  $\Sigma_0 = T_0 = \Sigma_1 = T_1 = 0$ . The resulting equations are now written in matrix form as follows:

$$\begin{bmatrix} (\omega^{-2} - c_{11}\kappa^2) & c_{12}i\kappa & 0 & 0 \\ -c_{12}i\kappa & \frac{1}{3}(-3c_{22} + \omega^{-2}) & 0 & 0 \\ 0 & 0 & c_{66}i\kappa & c_{66}\kappa^2 - \omega^{-2} \\ 0 & 0 & \hat{c}_{11}\kappa^2 + 3c_{66} - \omega^{-2} & 3c_{66}i\kappa \end{bmatrix} \cdot \begin{bmatrix} U_1 + U_0 \\ V_1 - V_0 \\ U_1 - U_0 \\ V_1 + V_0 \end{bmatrix} = \begin{bmatrix} 0 \\ 0 \\ 0 \\ 0 \end{bmatrix}$$

(II-10)

Then by setting the determinant of the coefficient matrix to zero we obtain

$$c_{11}k^2 - \frac{1}{3}(\omega^2 - 3c_{22})(\omega^2 - c_{11}k^2) = 0$$
$$c_{66}k^2 - \frac{1}{3}(\omega^2 - \hat{c}_{11}k^2 - 3c_{66})(\omega^2 - c_{66}k^2) = 0 .$$

(II-11)

Here we notice that the first relationship corresponds to the state of deformation of  $U_1 = U_0$  and  $V_1 = -V_0$ , which represents the thickness extension of the plate (or the symmetric mode), and the second describes the flexural deformation (or antisymmetric mode). The exact theory of plates gives an infinite number of dispersion relationships, but because this model only has two inertia points (namely  $n = 0, 1$ ), each of them having two components of displacement, we only have the first four relationships.

Dispersion relationships and corresponding phase velocities for an isotropic plate with Poisson's ratio  $1/4$  (namely  $\lambda = \mu$ ) are given in Fig. 2a and 2b up to the range where the wave length becomes equal to the plate thickness. Solid lines represent the symmetric modes and dotted lines the antisymmetric modes. As predicted by Mindlin and Medick the optical branch of the symmetric mode approaches the dilatation wave [18]. The acoustic branch of the antisymmetric mode starts from the bending motion and approaches the shear wave when the wave number  $k$  becomes larger and larger\*. Similar relationships for an anisotropic plate made of 55% graphite fiber-epoxy matrix with a layup angle of  $45^\circ$  are shown in Fig. 3a and 3b.

---

\* See section 5 for discussion about the large wave number limit.

Two-layer Plate

In this case we obtain eight equations by putting  $n = 1$  and  $2$  in equation (II-9). Boundary conditions require  $T_0 = \Sigma_0 = T_2 = \Sigma_2 = 0$ . By following the same procedure we find the dispersion relations as

$$\begin{aligned} & \{(\bar{\omega}^2 - c_{11}\kappa^2)(\bar{\omega}^2 - 3c_{22}) - 3c_{12}^2\kappa^2\}(\bar{\omega}^2 - \hat{c}_{11}\kappa^2 - 3c_{66} + \frac{c_{66}c_{12}}{c_{22}}\kappa^2) \\ & + 3(\bar{\omega}^2 - c_{11}\kappa^2)\{(\bar{\omega}^2 - c_{66}\kappa^2)(\bar{\omega}^2 - \hat{c}_{11}\kappa^2 - 3c_{66}) - 3c_{66}^2\kappa^2\} = 0 \end{aligned} \quad \text{(II-12)}$$

$$\begin{aligned} & \{(\bar{\omega}^2 - c_{66}\kappa^2)(\bar{\omega}^2 - \hat{c}_{11}\kappa^2 - 3c_{66}) - 3c_{66}^2\kappa^2\} \\ & + 3(\bar{\omega}^2 - c_{66}\kappa^2)\{(\bar{\omega}^2 - c_{11}\kappa^2)(\bar{\omega}^2 - 3c_{22}) - 3c_{12}^2\kappa^2\} = 0 \end{aligned}$$

Again the first equation represents the symmetric mode and is shown as solid lines in Fig. 4 and 5. The second equation is plotted with dotted lines representing the antisymmetric mode.

As expected we have six relationships since the this two-layer model is equivalent to a three-mass system with two degrees of freedom for each mass. When the wave number  $k\Delta$  increases the following are observed: for the symmetric mode the upper optical branch approaches the dilatation wave, whereas for the antisymmetric mode the lower optical branch approaches the shear wave\*.

---

\* See section 5 for discussions about the large wave number limit.

### N-Layer Plate

In general, we can obtain a  $2(N+1)$  order polynomial of  $\omega^{-2}$  by expanding a  $(4N) \times (4N)$  determinant and finding  $2(N+1)$  dispersion relationships. But, unfortunately, this process involves considerably complicated algebra and it may be necessary to develop a computer technique to find roots of an equation in determinant form (not in polynomial form).

A difference equation approach can be used to solve the  $N$  set of four simultaneous first order difference equations given by Eq. (II-9). This procedure is neat and can be generalized for any number of layers as discussed in the next section; but the last step of this approach, where a long polynomial is to be solved again, is not any simpler than the previous direct method.

### 3. Impact on an Elastic Composite Plate

#### Normalization and Integral Transforms of Governing Equations

The governing equations given by (II-7) are first nondimensionalized as follows:

$$\{U_n, V_n, \eta\} = \{u_n/\Delta, U_n/\Delta, x_1/\Delta\}$$

$$\{C_{ij}, T_n, \Sigma_n\} = \{c_{ij}/c_{66}, \tau_n/c_{66}, \sigma_n/c_{66}\}$$

$$\tau = t/T_0$$

where  $\Delta$  is the total thickness of the plate and  $T_0$  is the time required for the quasi-shear wave to travel the impact radius. Next we apply a Laplace transform in  $\tau$  and a Fourier transform in  $\eta$ , i.e.,

$$\hat{g}(s) = \int_0^{\infty} g(t) e^{-s\tau} d\tau$$

$$\bar{g}(k) = \frac{1}{\sqrt{2\pi}} \int_{-\infty}^{\infty} g(\eta) e^{ik\eta} d\eta$$

Then the resulting equations are

$$-(fs^2 + \frac{C_{11}}{2N} k^2) (\hat{U}_n + \hat{U}_{n-1}) - C_{12} ik (\hat{V}_n - \hat{V}_{n-1}) + (\hat{T}_n - \hat{T}_{n-1}) = 0$$

$$C_{12} ik (\hat{U}_n + \hat{U}_{n-1}) - (\frac{fs^2}{3} + 2NC_{22}) (\hat{V}_{n-1} - \hat{V}_{n-1}) + (\hat{\Sigma}_n + \hat{\Sigma}_{n-1}) - \frac{ik}{6N} (\hat{T}_n - \hat{T}_{n-1}) = 0$$

(II-13)

$$-C_{66} ik (\hat{U}_n - \hat{U}_{n-1}) - (fs^2 + \frac{C_{66}}{2N} k^2) (\hat{V}_n + \hat{V}_{n-1}) + (\hat{\Sigma}_n - \hat{\Sigma}_{n-1}) = 0$$

$$-(\frac{fs^2}{3} + \frac{\hat{C}_{11}}{6N} k^2 + 2NC_{66}) (\hat{U}_n - \hat{U}_{n-1}) + C_{66} ik (\hat{V}_n + \hat{V}_{n-1}) - \frac{C_{12} ik}{6NC_{22}} (\hat{\Sigma}_n - \hat{\Sigma}_{n-1}) + (\hat{T}_n - \hat{T}_{n-1}) = 0$$

where the normalization factor  $f$  is given as

$$f = \frac{1}{2N} \frac{\Delta^2 \rho}{c_{66} T_o^2} = \frac{b \Delta \rho}{c_{66} T_o^2} .$$

### Solution of Difference Equations

Since the simultaneous difference equations given are linear and all the coefficients are constants the solution [26] has to be

$$\{\hat{U}_n, \hat{V}_n, \hat{T}_n, \hat{\Sigma}_n\} = \{A, B, C, D\} e^{2i\theta n} \quad (\text{II-14})$$

where the phase shift  $\theta$  is complex, in general, and propagation through the thickness direction in the plate is characterized by  $\theta$ . Namely,  $\theta$  is the wave number in the thickness direction. By substituting solution (II-14) into the difference equation (II-13) we obtain a set of four simultaneous homogeneous equations through which the relationships among the constants A, B, C, and D have to be determined. If we set the resulting coefficient matrix of A, B, C, and D to be singular we obtain the following equation for phase shift  $\theta$ :

$$\begin{aligned} & \cos^4 \theta \left( f s^2 + \frac{C_{11} k^2}{2N} \right) \left( f s^2 + \frac{C_{66} k^2}{2N} \right) \\ & + \sin^4 \theta \left( \frac{f s^2}{3} + 2N C_{22} - \frac{C_{12} k^2}{6N} \right) \cdot \left( \frac{f s^2}{3} + \frac{\hat{C}_{11}}{6N} k^2 + 2N C_{66} - \frac{C_{66} C_{12}}{6N C_{22}} k^2 \right) \\ & + \cos^2 \theta \sin^2 \theta \left[ \left( f s^2 + \frac{C_{11} k^2}{2N} \right) \left\{ \frac{k^2}{6N} C_{66} + \frac{f s^2}{3} + 2N C_{22} - \left( \frac{k}{6N} \right)^2 \frac{C_{66}}{C_{22}} \left( f s^2 + \frac{C_{66} k^2}{2N} \right) \right\} \right. \\ & \left. - \left( C_{12} + C_{66} \right)^2 k^2 + \left( f s^2 + \frac{C_{66} k^2}{2N} \right) \left( \frac{f s^2}{3} + \frac{\hat{C}_{11}}{6N} k^2 + 2N C_{66} + \frac{C_{12}^2 k^2}{6N C_{22}} \right) \right] \quad (\text{II-15}) \\ & = a_1 \cos^4 \theta + a_2 \cos^2 \theta + a_3 = 0 . \end{aligned}$$

This equation implies that for a given wave number  $k$  along  $x_1$  and a frequency  $s$  ( $s$  represents the frequency for the case of harmonic waves), an infinite value of wave numbers exists for propagation through the thickness direction, but only four of them are sufficient to give all linearly independent solutions of the form of Eq. (II-14). If we denote the solution of the phase shift equation as

$$\cos^2 \beta = \frac{-a_2 + \sqrt{a_2^2 - 4a_1 a_3}}{2a_1} \tag{II-16}$$

$$\cos^2 \alpha = \frac{-a_2 - \sqrt{a_2^2 - 4a_1 a_3}}{2a_1}$$

the complete general solutions of difference equation (II-13) are

$$\begin{bmatrix} \hat{U}_n \\ \hat{V}_n \\ \hat{T}_n \\ \hat{\Sigma}_n \end{bmatrix} = \begin{bmatrix} A_1 \\ B_1 \\ C_1 \\ D_1 \end{bmatrix} e^{2i\beta n} + \begin{bmatrix} A_2 \\ B_2 \\ C_2 \\ D_2 \end{bmatrix} e^{-2i\beta n} + \begin{bmatrix} A_3 \\ B_3 \\ C_3 \\ D_3 \end{bmatrix} e^{2i\alpha n} + \begin{bmatrix} A_4 \\ B_4 \\ C_4 \\ D_4 \end{bmatrix} e^{-2i\alpha n} \tag{II-17}$$

Next, by substituting the above solutions into the original difference equations (II-13) we find the relationships among  $A_i$ ,  $B_i$ ,  $C_i$ , and  $D_i$ .

The results are

$$\begin{bmatrix} \hat{U}_n \\ \hat{V}_n \\ \hat{T}_n \\ \hat{\Sigma}_N \end{bmatrix} = \begin{bmatrix} X_1(\beta) E_1 \\ X_2(\beta) E_2 \\ X_3(\beta) E_3 \\ E_1 \end{bmatrix} \cdot \cos 2n\beta + i \begin{bmatrix} X_1(\beta) E_2 \\ X_2(\beta) E_1 \\ X_3(\beta) E_1 \\ E_2 \end{bmatrix} \cdot \sin 2n\beta \\
 + \begin{bmatrix} Y_1(\alpha) E_4 \\ Y_2(\alpha) E_3 \\ E_3 \\ Y_3(\alpha) E_4 \end{bmatrix} \cdot \cos 2n\alpha + i \begin{bmatrix} Y_1(\alpha) E_3 \\ Y_2(\alpha) E_4 \\ E_4 \\ Y_3(\alpha) E_3 \end{bmatrix} \cdot \sin 2n\alpha \quad (II-18)$$

where  $E_1 = D_1 + D_2$ ,  $E_2 = D_1 - D_2$ ,  $E_3 = C_3 + C_4$ ,  $E_4 = C_3 - C_4$  and

$$X_i(\beta) = - \frac{\Delta_i(\beta)}{\Delta(\beta)}$$

$$\begin{aligned}
 \Delta(\beta) = & (fs^2 + \frac{C_{11}k^2}{2n})(fs^2 + \frac{C_{66}k^2}{2n})\cos^3\beta \\
 & + \{ (fs^2 + \frac{C_{66}k^2}{2n})(\frac{fs^2}{3} + \frac{\hat{C}_{11}k^2}{6n} + 2nC_{66}) - C_{66}C_{12}k^2 - C_{66}^2k^2 \} \sin^2\beta \cdot \cos\beta
 \end{aligned}$$

$$\Delta_1(\beta) = ik \sin^2\beta \cos\beta \left\{ \frac{C_{12}}{6nC_{22}} (fs^2 + \frac{C_{66}k^2}{2n}) - (C_{12} + C_{66}) \right\} \quad (II-19)$$

$$\Delta_2(\beta) = i \sin^3\beta \left\{ \frac{C_{66}C_{12}k^2}{6nC_{22}} - (\frac{fs^2}{3} + \frac{\hat{C}_{11}k^2}{6n} + 2nC_{66}) \right\} - \cos^2\beta \sin\beta (fs^2 + \frac{C_{11}k^2}{2n})$$

$$\begin{aligned}
 \Delta_3(\beta) = & k \sin^3\beta \left\{ (\frac{fs^2}{3} + \frac{\hat{C}_{11}k^2}{6n} + 2nC_{66})C_{12} - \frac{C_{12}^2k^2}{6nC_{22}} C_{66} \right\} \\
 & + k \sin\beta \cos^2\beta \left\{ \frac{C_{12}}{6nC_{22}} (fs^2 + \frac{C_{11}k^2}{2n}) \cdot (fs^2 + \frac{C_{66}k^2}{2n}) - (fs^2 + \frac{C_{11}k^2}{2n})C_{66} \right\}
 \end{aligned}$$

and

$$Y_i(\alpha) = - \frac{\bar{\Delta}_i(\alpha)}{\bar{\Delta}(\alpha)}$$

$$\begin{aligned} \bar{\Delta}(\alpha) = & i \cos^2 \alpha \cdot \sin \alpha \{ C_{66} k^2 (C_{12} + C_{66}) - (fs^2 + \frac{C_{66} k^2}{2n}) \cdot (\frac{fs^2}{3} + \frac{\hat{C}_{11} k^2}{6n} \\ & + 2nC_{66} + \frac{12k^2}{6nC_{22}}) \} + i \sin^3 \alpha (\frac{fs^2}{3} + 2nC_{22}) \\ & \times (\frac{C_{66} C_{12} k^2}{6nC_{22}} - \frac{fs^2}{3} - \frac{C_{11} k^2}{6n} - 2nC_{66}) \end{aligned}$$

$$\begin{aligned} \bar{\Delta}_1(\alpha) = & \cos^3 \alpha (fs^2 + \frac{C_{66} k^2}{2n}) \\ & + \sin^2 \alpha \cdot \cos \alpha \{ -(\frac{k}{6n})^2 \frac{C_{12}}{C_{22}} (fs^2 + \frac{C_{66} k^2}{2n}) + \frac{k^2}{6n} C_{66} + (\frac{fs^2}{3} + 2nC_{22}) \} \end{aligned}$$

$$\bar{\Delta}_2(\alpha) = k \cdot \cos^2 \alpha \sin \alpha (C_{12} + C_{66}) \quad (II-20)$$

$$+ k \sin^3 \alpha \{ \frac{1}{6n} (\frac{fs^2}{3} + \frac{\hat{C}_{11} k^2}{6n} + 2nC_{66}) - (\frac{k}{6n})^2 \frac{C_{12} C_{66}}{C_{22}} \}$$

$$\begin{aligned} \bar{\Delta}_3(\alpha) = & ik \sin^2 \alpha \cos \alpha \{ \frac{C_{66} k^2}{6n} - \frac{1}{6n} (\frac{fs^2}{3} + \frac{\hat{C}_{11} k^2}{6n} + 2nC_{66}) (fs^2 + \frac{C_{66} k^2}{2n}) \\ & + C_{66} k (\frac{fs^2}{3} + 2nC_{22}) \} + ik \cos^3 \alpha \{ -C_{12} (fs^2 + \frac{C_{66} k^2}{2n}) \}. \end{aligned}$$

Equations (II-18) with (II-19,20) and the phase shifts  $\alpha$  and  $\beta$  given by (II-16) constitute the final form of the general solutions of the difference equations (II-13).

In Eqs. (II-19,20) we notice that when  $k \rightarrow 0$  we have  $X_1(\beta) = X_3(\beta) = Y_2(\alpha) = Y_3(\alpha) = 0$ . Namely the propagation of the normal stress (with phase shift  $\beta$ ) and the propagation of the shear stress (with phase shift  $\alpha$ ) are completely decoupled. This occurs when the waves are propagating only through the thickness direction [27].

#### Impact Boundary Condition

Boundary conditions for an impact can be described by any two conditions among  $u_o, v_o, \sigma_o,$  and  $\tau_o$  and another two conditions from  $u_N, v_N, \sigma_N,$  and  $\tau_N$ . For our present problem we have chosen a line impact by a normal stress along the  $x_3$  axis (Figure 1), i. e.,

$$\sigma_o = -\frac{P_o}{4} \left(1 - \cos \frac{2\pi t}{t_o}\right) \left(1 + \cos \frac{\pi x}{a}\right) : |x| \leq a \text{ and } 0 \leq t \leq t_o$$

$$= 0 : |x| > a \text{ or } t > 0 \text{ or } t > t_o$$

$$\tau_o = \sigma_N = \tau_N = 0 . \quad (\text{II-21})$$

Hence, the boundary conditions for the present impact problem lead to the following equation

$$\begin{bmatrix} 0 & , & X_3(\beta) & , & 1 & , & 0 \\ 1 & , & 0 & , & 0 & , & Y_3(\alpha) \\ iX_3(\beta)\sin 2\beta N & , & X_3(\beta)\cos 2\beta N & , & \cos 2\alpha N & , & i\sin 2\alpha N \\ \cos 2\beta N & , & i\sin 2\beta N & , & iY_3(\alpha)\sin 2\alpha N & , & Y_3(\alpha)\cos 2\alpha N \end{bmatrix} \begin{bmatrix} E_1 \\ E_3 \\ E_3 \\ E_4 \end{bmatrix} = \begin{bmatrix} 0 \\ q \\ 0 \\ 0 \end{bmatrix} \quad (\text{II-22})$$

where  $q$  is the integral transform of the impact function (II-21)\*.

Solving the above equations for  $E_i$ 's we can have

$$\begin{aligned} E_i &= \frac{D_i}{D} q \\ D &= \{1 + X_3^2(\beta)Y_3^2(\alpha)\}\sin 2\alpha N \cdot \sin 2\beta N + 2X_3(\beta)Y_3(\alpha)(\cos 2\alpha N \cdot \cos 2\beta N - 1) \\ D_1 &= X_3(\beta)Y_3(\alpha)(\cos 2\alpha N \cdot \cos 2\beta N - 1) + \sin 2\alpha N \cdot \sin 2\beta N \\ D_2 &= i\{\cos 2\beta N \cdot \sin 2\alpha N - X_3(\beta)Y_3(\alpha)\cos 2\alpha N \cdot \sin 2\alpha N\} \\ D_3 &= iX_3(\beta)\{X_3(\beta)Y_3(\alpha)\sin 2\beta N \cdot \cos 2\alpha N - \cos 2\beta N \cdot \sin 2\alpha N\} \\ D_4 &= X_3(\beta)\{X_3(\beta)Y_3(\alpha)\sin 2\alpha N \cdot \sin 2\beta N + \cos 2\beta N \cdot \cos 2\alpha N - 1\} \end{aligned} \quad (\text{II-23})$$

Substituting the  $E_i$ 's into the general solution (II-18) we can find the complete solutions which satisfy the impact boundary conditions given by (II-21). In other words, for given values of  $k$  and  $s$  we first find the phase shift  $\alpha$  and  $\beta$  from (II-15,16) and with these we can find solutions in integral transform from equations (II-18,23) which are the final solutions under impact. After  $\hat{U}_n, \hat{V}_n, \hat{T}_n$  and  $\hat{\Sigma}_n$  are calculated

\* Allowing the determinant of the coefficient matrix to vanish leads to dispersion relations of an N-layer plate, namely  $\mathcal{D}(\alpha, \beta) = 0$ . Then,  $\alpha$  and  $\beta$  are obtained from (II-15,16) which gives the complete dispersion relationships.

with a given impact function  $q$ , they can be inverted easily by means of the fast Fourier transform routine [3,20] to give the complete displacement and the stress fields after impact.

### Tangential Normal Stress

As discussed following Eq. (II-7), the tangential normal stress does not appear explicitly in the approximate equations of motion. Therefore, this component of the stress has to be calculated from the constitutive equation. Namely,

$$\begin{aligned}\sigma_{11_0} &= c_{11}u_{0,1} + \frac{c_{12}}{2b}(v_1 - v_0) \\ \sigma_{11_n} &= c_{11}u_{n,1} + \frac{c_{12}}{2b}(v_n - v_{n-1}) \quad 1 \leq n \leq N\end{aligned}$$

or after normalization and integral transform they are

$$\begin{aligned}\hat{\sigma}_{11_0} &= -ikC_{11}\hat{U}_0 + N \cdot C_{12}(\hat{V}_1 - \hat{V}_0) & \text{(II-24)} \\ \hat{\sigma}_{11_n} &= -ikC_{11}\hat{U}_n + N \cdot C_{12}(\hat{V}_n - \hat{V}_{n-1}) \quad 1 \leq n \leq N\end{aligned}$$

Then once the displacement field is computed the tangential normal stress can be obtained from the above equation and inverted.

#### 4. Some Numerical Results

The analysis discussed in the previous section includes the transient propagation in all directions but suitable choices of impact time, impact radius, sizes of time and distance steps are essential to make good use of the fast Fourier transform. For example, if we take a large time increment with a relatively thin plate propagation through the thickness will not be seen. For this matter we have examined several different cases.

##### Case 1: Longitudinal propagation

Propagation of impact generated waves along the longitudinal direction is examined for an isotropic plate (steel plate:  $\lambda = \mu = 1.2 \times 10^7$  psi) employing a two-layer model. For these calculations we used an impact time  $t_0 = 10$   $\mu$ sec, plate thickness  $\Delta = 1$  cm, and impact radius  $a = 4$  cm. Some of the results at a few different time sequences are shown in Fig. 6 a-f.

In these figures we can see two distinct states of propagation and corresponding wave fronts: one for horizontal displacements ( $u$ ) and longitudinal normal stresses ( $\sigma_{11}$ ), and another for vertical displacements ( $v$ ) and shear stresses ( $\tau$ ). In other words, the initial signals of the horizontal displacements and longitudinal normal stresses propagate through the plate with longitudinal wave speed at amplitudes that are relatively small. But the major parts of their signals are due to a bending wave propagating with shear stresses and vertical displacements with a lower velocity. When the group velocities of these waves are calculated from the numerical results, they are about 5 mm/ $\mu$ sec and 3 mm/ $\mu$ sec, respectively, while the phase velocities of the unbounded

medium of this material are  $C_d = \sqrt{(\lambda+2\mu)/\rho} = 5.61 \text{ mm}/\mu\text{sec}$  and  $C_s = \sqrt{\mu/\rho} = 3.25 \text{ mm}/\mu\text{sec}$ .

### Case 2: Propagation Through Thickness

To examine the propagation through the thickness it is necessary to have a sufficient number of layers in a plate. It is also essential to make the time step relatively small compared to the layer thickness. To do this we increase the thickness of the plate and the number of layers and reduce the impact time.

In Figs. 7 and 8 propagation of the transverse normal stress in the same plate ( $\Delta = 4 \text{ cm}$ ,  $t_0 = 2\mu\text{sec}$ ,  $a = 40 \text{ cm}$ ; 4-layer model) is shown at different time sequences. As seen in Fig. 7, the transverse normal stress is initially compressive due to the impact and a compression wave propagates through the thickness. But later it becomes a tension wave after reflection from the free surface and the tension wave propagates back to the impact surface. In Fig. 8 we see the change of the transverse normal stress and the interlaminar shear stress with time for the same impact conditions as in Fig. 7.

Similar results are also shown for the case of an anisotropic plate in Fig. 9 (55% graphite fibers-epoxy matrix, layup angle =  $15^\circ$ ;  $\Delta = 1 \text{ cm}$ ,  $t_0 = 2\mu\text{sec}$ ,  $a = 2 \text{ cm}$ ; 8-layer model). Here we again notice a clear delay in time for waves to travel from one layer to the next one. Another important point is that the shape of the impact stress is relatively well preserved during the initial stage of propagation but changes immediately afterwards. The distortion of the shape becomes more serious with further propagation due to reflection, thus, showing the highly dispersive nature of the harmonic waves in the approximate plate theory.

When the group velocities are calculated from these results, we find 6.32 mm/ $\mu$ sec for the dilatation wave and 3.33 mm/ $\mu$ sec for the shear wave in the case of the isotropic plate and 2.5 mm/ $\mu$ sec for the quasi-dilatation wave of the anisotropic plate. Their expected values are, respectively, 5.61, 3.25, and 2.36 mm/ $\mu$ sec. In other words, waves going through the thickness are traveling faster than expected.

### Case 3. Wave Surfaces

In the previous two cases we examined the transient waves propagating dominantly along either the  $x_1$  axis or through the thickness direction by suitable choices of the plate geometry and impact condition. Now we examine the combined effect, simultaneous propagation in both directions. This effect is shown in Fig. 10 (isotropic plate;  $\Delta = 4$  cm,  $t_0 = 4\mu$ sec,  $a = 4$  cm; 4-layer model) where the transverse normal stress generated from the line source due to impact not only spreads out in all directions but also reflects from the free surface.

When the plate is anisotropic, the situation is more complex in the sense that waves are neither dilatation nor shear but they are coupled together (now called quasi-dilatational or quasi-shear waves). Due to the coupling, phase velocities of the anisotropic wave vary from one direction to another, resulting in complicated shapes for the velocity surfaces and wave fronts [2]. For an anisotropic plate (made of 55% graphite fiber-epoxy matrix with layup angle  $45^\circ$ ) the velocity surfaces and the wave surfaces are shown in Fig. 11. The stress state at 10  $\mu$ sec after the impact on the same plate ( $\Delta = 4$  cm,  $t_0 = 4\mu$ sec,  $a = 2$  cm; 8-layer model) with the corresponding wave fronts are shown in Fig. 12a. In the

propagation of the quasi-longitudinal wave we notice that the longitudinal propagation is well bounded by the quasi-dilatational wave surface but the transverse propagation is not. The shear wave is not bounded by the quasi-shear wave front in either direction.

This interesting phenomenon of higher propagation speeds through the thickness is related to the dispersion relationship at short wave length limits; it is discussed in the next section.

## 5. Correction Factor and Conclusion

### Correction Factor

According to the present model of a multilayer plate, one of the antisymmetric modes of the dispersion relationships approaches the shear speed when the wave length becomes shorter and shorter, as mentioned in Section 2. It is well understood that such a limit is incorrect, i.e., in the limit of short wave length there should be a Rayleigh wave instead of a shear wave. Such a discrepancy can be eliminated by introduction of proper correction factors, as shown by Mindlin and Medick [18]. Correction factors can be found by examining either the large wave number limit or the cut-off frequencies of both the exact theory and the present approximate theory. Since these two ways lead us to the same results we will find the factors by matching the cut-off frequencies of the two theories.

The cut-off frequencies of the exact theory for an isotropic plate can be obtained from the well-known Rayleigh-Lam's equation. The lowest cut-off frequencies are  $\frac{\pi}{\Delta} \sqrt{(\lambda+2\mu)/\rho}$  for the symmetric mode and  $\frac{\pi}{\Delta} \sqrt{\mu/\rho}$  for the antisymmetric mode. The corresponding cut-off frequencies of our approximate theory are  $\frac{2}{\Delta} \sqrt{3c_{22}/\rho}$  and  $\frac{2}{\Delta} \sqrt{3c_{66}/\rho}$ \*. Hence, we notice that replacing  $c_{22}$  by  $c_{22}\pi^2/12$  and  $c_{66}$  by  $c_{66}\pi^2/12$  makes the two theories have the same two lowest cut-off frequencies. Furthermore the shear wave observed in the short wave length limit of the present approximation becomes a wave with a speed of  $\frac{\pi}{\sqrt{12}} \sqrt{\mu/\rho}$ , i.e., the Rayleigh wave.

Another important consequence of the correction factor is to reduce propagation speeds through the thickness, which are related to  $\sqrt{c_{22}/\rho}$

---

\* The lowest two cut-off frequencies are found from Eq. (II-11) and they are independent of the layer number in the plate under investigation.

and  $\sqrt{c_{66}/\rho}$ , with a factor of  $\pi/\sqrt{12}$ . Propagation of the maximum value of the interlaminar normal stress through the thickness is examined with and without correction factors and the results are shown in Fig. 13.

Without the correction factor the propagation speed in a composite plate is roughly about 2.60 mm/ $\mu$ sec obtained from the numerical results used in Fig. 12.

When the same plate is subjected to identical impact conditions this reduces to about 2.41 mm/ $\mu$ sec with the correction factor. Comparing this with the group velocity in an unbounded composite space (= 2.36 mm/ $\mu$ sec) the agreement of the present approximate theory is remarkable. Similar results are also observed in the case of shear and quasi-shear waves. When these correction factors are introduced in the previous cases, shown in Figs. 8, 9, and 12, all the signals propagating through the thickness are now well bounded within the corresponding wave fronts, as shown in Fig. 12b and from this we can notice the importance of the correction factors.

#### Discussion and Computation Time

It is interesting to compare the computation time of this model with some other methods, such as the finite element method or the finite difference method. In the case of an 8-layer anisotropic plate model, from which Figs. 9 and 12 are produced, we have

9 steps along the thickness: 8-layer model;

32 step along the  $x_1$  direction: 64 points are used in practice but only half of them are useful because of the symmetry of the problem,

32 steps in time;

2 displacement components at each point.

Therefore the total number of the unknowns, which are the basic unknowns either in case of the finite difference or finite element methods, is

18,432. After these primary variables are calculated, 27,648 secondary variables (three stress components at each points) have to be calculated again. According to our present model all these processes require only 200 K of computer space without using magnetic tapes or any kind of additional storage space and only 1 minute 6 seconds for CPU time in the IBM 370-168 model including compiling, linkage editing, I/O and execution.

### Conclusion

The present theory is a generalization of Mindlin's approximate plate theory applied to a multilayer plate under an impact. By combined use of the finite difference technique in the thickness direction and the fast Fourier transform in the plane of plate and time, this model can be very useful for the study of wave propagation in a composite plate under impact forces. However, reasonable attention in usage of the fast Fourier transform is required to avoid spurious data. From the limited numerical data obtained from this model it appears that the anisotropy in the plate will lead to a considerable interlaminar shear which might lead to ply bonding failures. The model also shows that for short enough impact times, an interlaminar tension can develop as one would expect, which might also account for interlaminar ply failure.

### III. IMPACT OF A COMPOSITE PLATE WITH AN INTERLAMINAR DAMPING LAYER

#### 1. Description of Problem

##### Geometry of Plate

As an extension of the multilayer plate discussed in Chapter II we now examine the impact and the consequent stress wave propagation in a composite plate with viscoelastic damping layers. Possible models for damping mechanisms in plates are shown in Fig. 14. We will formulate a model made of an alternating number of elastic and viscoelastic layers, as shown in Fig. 14-c. As long as the layer structure of the plate is periodic, the main part of the analysis in Chapter II for an elastic plate is valid with additional equations for viscoelastic layers.

##### Viscoelastic Property of Elastomer

The mechanical properties of an elastomer are usually expressed in terms of a complex modulus depending on the frequency, i.e.,

$$G^*(\omega) = G'(\omega) + iG''(\omega) . \quad (\text{III-1})$$

With this the constitutive equation is written as

$$\bar{\sigma}_{ij}(\omega) = G^*(\omega)\bar{\epsilon}_{ij}(\omega) \quad (\text{III-2})$$

in the frequency space where  $\bar{\sigma}_{ij}(\omega)$  and  $\bar{\epsilon}_{ij}(\omega)$  are respectively the Fourier transforms of  $\sigma_{ij}$  and  $\epsilon_{ij}$  in time\* [29].

---

\* For (III-2) the Fourier transform is defined as

$$\bar{f}(\omega) = \frac{1}{\sqrt{2\pi}} \int_{-\infty}^{\infty} f(t)e^{-i\omega t} dt .$$

The constitutive relation (III-2) with the complex modulus (III-1) implies the following constitutive equation in a time space:

$$\underline{\underline{\sigma}}(x,t) = \int_{-\infty}^t G(t-\tau) \underline{\underline{\dot{\epsilon}}}(x,\tau) d\tau \quad (\text{III-3})$$

where the relaxation function  $G(t)$  is related with the complex modulus  $G^*(\omega)$  as

$$G^*(\omega) = \frac{1}{i\omega} \int_0^{\infty} G(t) e^{-i\omega t} dt \quad (\text{III-4})$$

Therefore, when the complex modulus  $G^*(\omega)$  is obtained by experiments, usually by means of harmonic excitation of strain, the relaxation function  $G(t)$  can be found by inversion of equation (III-4).

The viscoelastic property of the elastomer under consideration has been extensively investigated (e.g. [19]) and its complex modulus is given in Fig. 15. This complex modulus can be reasonably well described by a three parameter equation as

$$G'(\omega) = a - \frac{6}{\omega^2 + c} \quad (\text{III-5})$$

These three parameters are obtained from another set of parameters: the maximum values of  $G'(\omega)$  when  $\omega \rightarrow \infty$ , the maximum value of  $G''(\omega)/G'(\omega)$  and the  $\omega_0$  at which  $G''(\omega)/G'(\omega)$  becomes the maximum. Therefore, if we characterize the complex modulus by proper choice of  $G'(\omega)$ ,  $\omega_0$  and the maximum of  $G''(\omega_0)/G'(\omega_0)$ , the relaxation functions are completely described.

## 2. Formulation

### Elastic Layer

In Fig. 16 a typical viscoelastic layer (nth) is shown between two adjacent elastic layers (nth and (n+1)th) with appropriate discretization. The approximate equations of motion for the nth elastic layer given by Eq. (II-7) are still valid. But remembering the new discretizing notation in Fig. 16 we now have to replace  $( )_n$  and  $( )_{n-1}$  by  $( )_n^-$  and  $( )_{n-1}^+$ , respectively. The results are

$$\begin{aligned} \rho(\ddot{u}_n^- + \ddot{u}_{n-1}^+) &= c_{11}(u_n^- + u_{n-1}^+)_{,11} + \frac{c_{12}}{b}(v_n^- - v_{n-1}^+)_{,1} + \frac{1}{b}(\tau_n^- - \tau_{n-1}^+) \\ \rho(\ddot{v}_n^- - \ddot{v}_n^+) &= -\frac{3c_{12}}{b}(u_n^- + u_{n-1}^+)_{,1} - \frac{3c_{22}}{b^2}(v_n^- - v_{n-1}^+) + \frac{3}{b}(\sigma_n^- + \sigma_{n-1}^+) + (\tau_n^- - \tau_{n-1}^+)_{,1} \\ \rho(\ddot{u}_n^- - \ddot{u}_{n-1}^+) &= \hat{c}_{11}(u_n^- - u_{n-1}^+)_{,11} - \frac{3c_{66}}{b^2}(u_n^- - u_{n-1}^+) - \frac{3c_{66}}{b}(v_n^- + v_{n-1}^+)_{,1} \\ &\quad + \frac{c_{12}}{c_{22}}(\sigma_n^- - \sigma_{n-1}^+)_{,1} + \frac{3}{b}(\tau_n^- + \tau_{n-1}^+) \\ \rho(\ddot{v}_n^- + \ddot{v}_{n-1}^+) &= c_{66}\left\{\frac{1}{b}(u_n^- - u_{n-1}^+)_{,1} + (v_n^- + v_{n-1}^+)_{,11}\right\} + \frac{1}{b}(\sigma_n^- - \sigma_{n-1}^+) \end{aligned} \quad (\text{III-6})$$

### Viscoelastic Layer

Since the thickness of the elastomer is thin compared with the elastic layer, we can assume that the stress field is uniform through the thickness of the elastomer. In other words, we have  $\sigma_n^- = \sigma_n^+ = \sigma_n$  and  $\tau_n^- = \tau_n^+ = \tau_n$  for (III-6). Therefore, the following compatibility conditions for the

elastomer can be obtained immediately:

$$\epsilon_{12(n)} = \frac{1}{4} \frac{\partial}{\partial x_1} (v_n^+ + v_n^-) + \frac{1}{2D} (u_n^+ - u_n^-) \quad (\text{III-7})$$

$$\epsilon_{22(n)} = \frac{1}{D} (v_n^+ - v_n^-)$$

where  $D$  is the thickness of the elastomer.

We further assume that the dissipation is mostly due to shear motion, i.e., that the normal component of the continuous traction vector is transmitted through the viscoelastic layer purely elastically. Therefore, by combining (III-7) with (III-3) we find

$$\sigma_n = \frac{E}{D} (v_n^+ - v_n^-) \quad (\text{III-8})$$

$$\tau_n = \int_{-\infty}^t G(t-\tau) \left\{ \frac{1}{2} \frac{\partial}{\partial x_1} (\dot{v}_n^+ + \dot{v}_n^-) + \frac{1}{D} (\dot{u}_n^+ - \dot{u}_n^-) \right\} d\tau$$

These two equations and four more from Eq. (III-6) are the complete equations needed to solve the impact on a composite plate with elastomer. For a plate made of  $N$  elastic layers and  $(N-1)$  viscoelastic layers Eq. (III-6) provides  $4N$  equations and (III-8) gives  $2(N-1)$  equations. Since the total number of the unknowns are now  $6N+2$  ( $u_0, v_0, \sigma_0, \tau_0; u_1^-, v_1^-, u_1^+, v_1^+, \sigma_1, \tau_1; \dots \dots; u_{N-1}^-, v_{N-1}^-, u_{N-1}^+, v_{N-1}^+, \sigma_{N-1}, \tau_{N-1}; u_N, v_N, \sigma_N, \tau_N$ ) we can solve this system of equations with four additional conditions supplied by the suitable boundary conditions.

Here we notice that the governing equations are now a set of six difference-integro-partial differential equations. These equations can be

reduced to difference equations after appropriate integral transforms and the resulting difference equations can be handled rather simply, as in the previous chapter.

### 3. Numerical Results and Discussion

#### Impact on Plate

For the report we examine the impact on a plate consisting of two elastic layers and a viscoelastic layer, as shown in Fig. 17, with an impact function

$$\begin{aligned} \sigma_o &= P_o \left\{ 1 - \left( \frac{x_1}{a} \right)^2 \right\} \sin \frac{\pi t}{t_o} & ; & \quad |x_1| < a \quad \text{and} \quad 0 < t < t_o \\ &= 0 & ; & \quad |x_1| > a \quad \text{or} \quad t > t_o, \quad \text{or} \quad t < 0 \end{aligned} \tag{III-9}$$

with all other stress components vanishing on both surfaces of the plate. Now by putting  $n = 1$  and  $2$  into Eq. (III-6) we have eight equations and two more equations are obtained from Eq. (III-8). We again normalize these equations and take the integral transform, as in Chapter II. The resulting equations are:

$$\begin{aligned}
 &-(fs^2 + \frac{C_{11}}{\Delta}bk^2)(\hat{U}_1^- + \hat{U}_0^-) - C_{12}ik(\hat{V}_1^- - \hat{V}_0^-) + \hat{T}_1 = 0 \\
 &3C_{12}ik(\hat{U}_1^- + \hat{U}_0^-) - (fs^2 + \frac{3C_{22}\Delta}{b})(\hat{V}_1^- - \hat{V}_0^-) + 3\hat{\Sigma}_1 - ik\frac{b}{\Delta}\hat{T}_1 = -3\hat{\Sigma}_0 \\
 &-(fs^2 + \frac{b}{\Delta}C_{66}k^2)(\hat{V}_1^- + \hat{V}_0^-) - C_{66}ik(\hat{U}_1^- - \hat{U}_0^-) + \hat{\Sigma}_1 = \hat{\Sigma}_0 \\
 &-(fs^2 + \frac{b}{\Delta}C_{11}k^2 + \frac{\Delta}{b}3C_{66})(\hat{U}_1^- - \hat{U}_0^-) + 3C_{66}ik(\hat{V}_1^- + \hat{V}_0^-) - \frac{C_{12}}{C_{22}}\frac{b}{\Delta}ik\hat{\Sigma}_1 + 3\hat{T}_1 = -\frac{C_{12}}{C_{22}}\frac{b}{\Delta}ik\hat{\Sigma}_0 \\
 &-(fs^2 + \frac{C_{11}}{\Delta}bk^2)(\hat{U}_2^+ + \hat{U}_1^+) - C_{12}ik(\hat{V}_2^+ - \hat{V}_1^+) - \hat{T}_1 = 0 \\
 &3C_{12}ik(\hat{U}_2^+ + \hat{U}_1^+) - (fs^2 + \frac{3C_{22}\Delta}{b})(\hat{V}_2^+ - \hat{V}_1^+) + 3\hat{\Sigma}_1 + \frac{b}{\Delta}ik\hat{T}_1 = 0 \\
 &-(fs^2 + \frac{b}{\Delta}C_{66}k^2)(\hat{V}_2^+ + \hat{V}_1^+) - C_{66}ik(\hat{U}_2^+ - \hat{U}_1^+) - \hat{\Sigma}_1 = 0 \\
 &-(fs^2 + \frac{b}{\Delta}C_{11}k^2 + \frac{\Delta}{b}3C_{66})(\hat{U}_2^+ - \hat{U}_1^+) + 3C_{66}ik(\hat{V}_2^+ + \hat{V}_1^+) + \frac{C_{12}}{C_{22}}\frac{b}{\Delta}ik\hat{\Sigma}_1 + 3\hat{T}_1 = 0 \\
 \\
 &\hat{\Sigma}_1 = E\frac{\Delta}{D}(\hat{V}_1^+ - \hat{V}_1^-) \\
 &\hat{T}_1 = \bar{G}(s)\{\frac{\Delta}{D}(\hat{U}_1^+ - \hat{U}_1^-) - \frac{ik}{2}(\hat{V}_1^+ + \hat{V}_1^-)\}
 \end{aligned}
 \tag{III-10}$$

where  $\bar{G}(s)$  is the Laplace transform of the relaxation function  $G(t)$  with respect to  $\tau = t/T_0$  and we have used the boundary conditions  $\tau_0 = \tau_2 = \sigma_2 = 0$ . From the above 10 equations we can find 10 unknowns  $(\hat{U}_0^-, \hat{V}_0^-, \hat{U}_1^-, \hat{V}_1^-, \hat{U}_1^+, \hat{V}_1^+, \hat{\Sigma}_1, \hat{T}_1; \hat{U}_2^-, \hat{V}_2^-)$  with given impact function  $\hat{\Sigma}_0$  and once these are calculated the displacement and the stress fields can be computed by inversions of the integral transforms by means of the FFT algorithm.

### Numerical Results

For the present computation we have used the Young's modulus  $E = .7 \times 10^4$  psi and the shear modulus  $G'(\omega) = .817 \times 10^4 - \frac{2.41 \times 10^{12}}{3 \times 10^4 + \omega^2}$  for the elastomer where  $\omega$  is given in hertz. The  $G'(\omega)$  in this case implies that  $G'(\infty) = .817 \times 10^4$  psi and  $\max(G''(\omega)/G'(\omega)) = 3.3$  at  $\omega_0 = 800$  Hz.

The propagation of stress wave in this case is quite similar to that of the composite plate without an elastomer layer except the peak values of the interlaminar stress. Values of the peak stress with different thickness of the elastomer layer are plotted with those of the purely elastic plate in Fig. 18. As we can see in this figure the interlaminar shear stress has increased by a small amount while a reduction of the normal stress is considerable when the elastomer layer becomes thicker and thicker. From this result it is obvious that the reduction of the normal component of stress can be achieved by introducing such a soft and energy-dissipating elastomer layer.

### Discussion

In addition to the simple reduction of the normal stress it is also observed that the amount of reduction increases with the value of  $G''(\omega)/G'(\omega)$  and the location of  $\omega_0$  at which  $G''(\omega)/G'(\omega)$  becomes the maximum value. In other words, we can make the dissipation effect more serious by choosing an elastomer whose  $G''(\omega)/G'(\omega)$  becomes maximum at  $\omega_0$  around which the most of the impact energy is carried out.

It is also believed that a further dissipation effect will be possible if we make the transmission of the normal stress viscoelastic across the elastomer layer, which we have assumed is elastic for this report.

#### IV. IMPACT ON A PLATE WITH A CRACK

##### 1. Introduction

When the impact stress is low, the impact is elastic and the stresses in the plate can be described by elastic wave propagation. When the stress is increased beyond a certain limit then the impact damage occurs. Elastic-plastic impact is complicated for two reasons, namely, unloading and loading must be treated differently, and the strain rate effect [30] must be included. If the impact stress is increased further to a certain level where the induced stress is higher than the strength of a target material then penetration begins to occur. In this limit the target material sometimes behaves as a fluid and such a state of impact is known as a hydraulic impact [31]. Another failure mode is the occurrence of interlaminar cracks.

Investigation of the stress state in solids with cracks falls in the category of so-called fracture mechanics and has been under an extensive scrutiny since the famous enunciation by Griffith [32]. Presence of cracks inside a material usually leads us to a mixed boundary value problem and only a limited class of problems can be solved [33,34]. In the case of dynamic loading the problem becomes more difficult due to the scattering of the stress wave by the crack [21-24]. In this report we will formulate the problem of a plate with a crack which is subject to a dynamic loading.

Our original goal was to study the effect of interlaminar cracks in composite plates in response to impact loads. Debugging problems in other parts of this report, however, used valuable time originally set aside for this problem. The following section is an attempt to illustrate the

use of the Mindlin plate theory for the study of interlaminar cracks and to point out the mathematical difficulties that must be overcome in solving the problem.

## 2. Formulation

### Description of Problem

The plate under consideration has a crack on the midplane running from  $x_1 = -h$  to  $+h$  as shown in Fig. 19. Stress can be applied either on the surface of the plate or on the crack surface. In the former case the crack surfaces can be in contact and the boundary conditions become more complex due to the partial continuity of stresses and displacements during the contact. For the present report to illustrate the mathematical difficulties we assume that the crack surface is subject to a known compressive impact.

### Governing Equation and Boundary Conditions

We can formulate this crack problem by assuming that the lower and the upper half plates are made of a number of layers but for simplicity we consider the plate to consist of two identical layers and the crack to be present on the interface of these two layers. Following the notation shown in Fig. 19 we have the governing equations identical to Eq. (III-6) with  $n = 1$  and  $2$ . The boundary condition requires that both plate surfaces remain traction free. The crack surface is subject to a prescribed impact condition while the displacement and stress are continuous along the layer boundary outside the crack. Namely, we have

$$\begin{aligned} \sigma_0 &= \tau_0 = \sigma_2 = \tau_2 = 0 \\ \left. \begin{aligned} \sigma_1^+ &= \sigma_1^- = -P_0(x_1, t) \\ \tau_1^+ &= \tau_1^- = 0 \end{aligned} \right\} |x| < h \end{aligned} \quad (IV-1)$$
$$\left. \begin{aligned} u_1^+ &= u_1^- , & v_1^+ &= v_1^- \\ \sigma_1^+ &= \sigma_1^- , & \tau_1^+ &= \tau_1^- \end{aligned} \right\} |x| > h .$$

Due to the twofold symmetry of the problem we now have  $u_0 = u_2$ ,  $v_0 = -v_2$ ,  $\tau_1^+ = \tau_1^- = 0$  and we can set  $u_1^+ = u_1^- = u_1$ ,  $-v_1^+ = v_1^- = v_1$ . Thus, the eight equations obtained from Eq. (III-6) are now reduced to

$$\begin{aligned} \rho(\ddot{u}_1 + \ddot{u}_0) &= c_{11}(u_1 + u_0)_{,11} + \frac{c_{12}}{b}(v_1 - v_0)_{,1} \\ \rho(\ddot{v}_1 - \ddot{v}_0) &= -\frac{3c_{12}}{b}(u_1 + u_0)_{,1} - \frac{3c_{22}}{b^2}(v_1 - v_0) + \frac{3\sigma}{b} \\ \rho(\ddot{u}_1 - \ddot{u}_0) &= \hat{c}_{11}(u_1 - u_0)_{,11} - \frac{3c_{66}}{b^2}(u_1 - u_0) - \frac{3c_{66}}{b}(v_1 + v_0)_{,1} + \frac{c_{12}}{c_{22}}\sigma_{,1} \\ \rho(\ddot{v}_1 + \ddot{v}_0) &= c_{66}\left\{\frac{1}{b}(u_1 - u_0)_{,1} + (v_1 + v_0)_{,11}\right\} + \frac{\sigma}{b} \end{aligned} \quad (IV-2)$$

and the boundary condition is now

$$\left. \begin{aligned} \sigma &= -P_o(x_1, t) & |x_1| < h \\ v_1 &= 0 & |x_1| > h \end{aligned} \right\} \text{ along } x_2 = 0 \quad (IV-3)$$

### Dual Integral Equation

We now normalize the governing equation (IV-2) and take the integral transform. Then we have

$$\begin{bmatrix} (fs^2 + \frac{b}{\Delta}c_{11}k^2), & c_{12}ik & , & 0 & , & 0 \\ -3C_{12}ik & , & (fs^2 + \frac{3\Delta}{b}c_{22}), & 0 & , & 0 \\ 0 & , & 0 & , & C_{66}ik & , & (fs^2 + \frac{b}{\Delta}c_{66}k^2) \\ 0 & , & 0 & , & (fs^2 + \frac{b}{\Delta}\hat{c}_{11}k^2 + \frac{3\Delta}{b}c_{66}), & -3C_{66}ik \end{bmatrix} \begin{bmatrix} \hat{u}_1 + \hat{u}_0 \\ \hat{v}_1 - \hat{v}_0 \\ \hat{u}_1 - \hat{u}_0 \\ \hat{v}_1 + \hat{v}_0 \end{bmatrix} = \begin{bmatrix} 0 \\ 3\hat{\Sigma} \\ \hat{\Sigma} \\ -\frac{C_{12}}{C_{22}}\frac{b}{\Delta}ik\hat{\Sigma} \end{bmatrix} \quad (IV-4)$$

and these can be solved for  $\hat{U}_0$ ,  $\hat{U}_1$ ,  $\hat{V}_0$ , and  $\hat{V}_1$  in terms of  $\hat{\Sigma}$ . Since the mixed boundary conditions are given by  $\sigma$  and  $v_1$  we solve  $\hat{V}_1$  as

$$\hat{V}_1 = K(s,k)\hat{\Sigma} \quad (\text{IV-5})$$

with

$$K(s,k) = \frac{1}{2} \left[ \frac{3}{A} (fs^2 + \frac{b}{\Delta} C_{11} k^2) + \frac{1}{B} \left\{ \frac{C_{12}}{C_{22}} \frac{b}{\Delta} C_{66} k^2 - (fs^2 + \frac{b}{\Delta} \hat{C}_{11} k^2 + \frac{3b}{\Delta} C_{66}) \right\} \right]$$

$$A = \text{Det} \begin{vmatrix} (fs^2 + \frac{b}{\Delta} C_{11} k^2) & , & C_{12} ik \\ -3C_{12} ik & , & (fs^2 + \frac{3\Delta}{b} C_{22}) \end{vmatrix} \quad (\text{IV-6})$$

$$B = \text{Det} \begin{vmatrix} C_{66} ik & , & (fs^2 + \frac{b}{\Delta} C_{66} k^2) \\ (fs^2 + \frac{b}{\Delta} \hat{C}_{11} k^2 + \frac{3\Delta}{b} C_{66}) & , & -3C_{66} ik \end{vmatrix}$$

Next we take the inverse transform of  $\hat{\Sigma}$  and  $\hat{V}_1$ , and apply the mixed boundary condition given in Eq. (IV-3). Since the boundary conditions are for all times  $t > 0$  we only take the inverse Fourier transform to apply the boundary conditions, i.e.,

$$\hat{\Sigma}(\eta,s) = \frac{1}{\sqrt{2\pi}} \int_{-\infty}^{\infty} \hat{\Sigma} e^{-ik\eta} dk \quad (\text{IV-7})$$

$$\hat{V}_1(\eta,s) = \frac{1}{\sqrt{2\pi}} \int_{-\infty}^{\infty} K(s,k) \hat{\Sigma} e^{-ik\eta} dk$$

Application of the boundary condition given by Eq. (IV-3) results in the following integral equation:

$$-\hat{P}_o(\eta, s) = \frac{1}{\sqrt{2\pi}} \int_{-\infty}^{\infty} \hat{\Sigma} e^{-ik\eta} dk \quad : \quad |\eta| < h/\Delta \quad (IV-8)$$

$$0 = \frac{1}{\sqrt{2\pi}} \int_{-\infty}^{\infty} K(s, k) \hat{\Sigma} e^{-ik\eta} dk \quad : \quad |\eta| > h/\Delta$$

for an unknown function  $\hat{\Sigma}$ .

### 3. Discussion

The integral equations of the type given in Eq. (IV-8) are known as dual integral equations, each of which has its own region of application and occur in mixed boundary value problems [35]. There are a number of ways to solve this type of integral equations, such as by reduction to a single Fredholm integral equation or by using the Wiener-Hopf technique [36]. Finding the solution depends on the kernel and in general it is rather difficult to do except for some special cases such as for Bessel kernels or trigonometric kernels.

Once the unknown function  $\hat{\Sigma}$  is determined the other variables  $(\hat{U}_o, \hat{U}_1, \hat{V}_o, \hat{V}_1)$  can be computed by solving the algebraic equation (IV-4) and the complete displacement can be found by inversions of the integral transform.

The problem formulated in this chapter is the simplest impact problem in that the contact of the crack surface does not occur and that it has a twofold symmetry. But it is expected that the critical response of the plate, particularly the stress field near the crack, can be a guideline for a more complex problem.

## V. CONCLUSION AND RECOMMENDED RESEARCH

The present theory is a generalization of Mindlin's approximate theory of plate applied to a multilayer plate under impact. By combined use of the finite difference technique in the thickness direction and integral transforms this model has been shown to be very effective for wave propagation analyses.

This model is extended to examine the effects of an elastomer layer between elastic layers of the plate. The reduction of interlaminar normal stress is significant due to the damping layer but further investigation seems necessary to determine the nature of the reduction.

The presence of a crack in the plate has been formulated. The resulting equations are given by dual integral equations which, as in many cases, are rather difficult to solve.

The basic idea of the periodic structure of the multilayer plate, where the governing equations are derived for each layer and given by a set of difference-differential equations, may be useful to handle different types of problems, such as heat conduction and thermoelastic problems in composite plates.

### References

- [1] Mindlin, R.D., - "High Frequency Vibrations of Crystal Plates", Quart. Appl. Math., Vol. 19, p. 51-61 (1961).
- [2] Moon, F.C., - "Wave Surfaces Due to Impact on Anisotropic Plates", J. Composite Materials, Vol. 6, p. 62 (1972).
- [3] Moon, F.C. and Kang, C.K., - "Analysis of Edge Impact Stresses in Composite Plates", TR to NASA Lewis Research Center, Princeton University (1974).
- [4] Moon, F.C., - "One Dimensional Transient Waves in Anisotropic Plate", J. Appl. Mech., Trans. ASME, p. 485 (1973).
- [5] Moon, F.C., Kim, B.S. and Fang - Landau, S.R., - "Impact of Composite Plates: Analysis of Stresses and Forces", TR to NASA Lewis Research Center, Princeton University (1976).
- [6] White, J.E. and Angona, F.A., - "Elastic Wave Velocities in Laminated Media", J. Acoust. Soc. Am., Vol. 27, p. 310 (1955).
- [7] Sun, C.T., Achenbach, J.D. and Herrmann, G., - "Continuum Theory for a Laminated Media", J. Appl. Mech., Trans. ASME, p. 467 (1968).
- [8] Nayfeh, A.H. and Gurtman, G.A., - "A Continuum Approach to the Propagation of Shear Waves in Laminated Wave Guides", J. Appl. Mech., Trans. ASME, p. 106 (1974).
- [9] Hegemier, G.A., Gurtman, G.A. and Nayfeh, A.M., - "A Continuum Mixture Theory of Wave Propagation in Laminated and Fiber Reinforced Composites", Int. J. Solids Struc., Vol. 9, p. 395 (1973).
- [10] Chao, T. and Lee, P.C.Y., - "Discrete Continuum Theory for Periodically Layered Composite Materials", J. Acoust. Soc. Am., Vol. 57, p. 78 (1975).
- [11] Lee, P.Y.C. and Nikodem, Z., - "An Approximate Theory for High Frequency Vibrations of Elastic Plates", Int. J. Solids Struc., Vol. 8, p. 581 (1972).
- [12] Dong, S.B. and Nelson, R.B., - "On Natural Vibrations and Waves in Laminated Orthotropic Plates", J. Appl. Mech., Trans. ASME, p. 739 (1972).
- [13] Hegemier, G.A. and Nayfeh, A.H., - "A Continuum Theory for Wave Propagation in Laminated Composites, Case 1: Propagation Normal to the Laminates", J. Appl. Mech., Trans. ASME, p. 503 (1973).
- [14] Hegemier, G.A. and Nayfeh, A.H., - "A Continuum Theory for Wave Propagation in Laminated Composites, Case 2: Propagation Parallel to the Laminates" J. Elasticity, Vol. 3, p. 125-140 (1973).

- [15] Cooley, J.W., Lewis, P.A.W. and Welch, P.D., - "The Fast Fourier Transform Algorithm: Programming Considerations in the Calculation of sine, cosine and Laplace Transforms", J. Sound Vib., Vol. 12, p. 315-337 (1970).
- [16] Brillouin, L. - Wave Propagation in Periodic Structures, Dover, N.Y. (1946).
- [17] Thomson, W.T., - Vibration Theory and Application, Prentice Hall, N.J. (1965).
- [18] Mindlin, R.D. and Medick, M.A., - "Extensional Vibrations of Elastic Plates", J. Appl. Mech., Trans. ASME, p. 561 (1959).
- [19] Yan, M.J. and Dowell, E.H., - "High Damping Measurements and Preliminary Evaluation of an Equation for Constrained Layer Damping", AIAA Journal, Vol. 11, p. 388 (1973).
- [20] Nakra, B.C. and Grootenhuis, P., - "Structural Damping Using a Four Layer Sandwich", J. Eng. Ind., Trans. ASME, p. 81 (1972).
- [21] Achenback, J.D., - "Crack Propagation Generated By a Horizontally Polarized Shear Wave", J. Mech. Phys. Solids, Vol. 18, p. 245 (1970).
- [22] Achenback, J.D. and Nuismer, R., - "Fracture Generated by a Dilatational Wave", Int. J. Frac. Mech., Vol. 7, p. 77 (1971).
- [23] Nuismer, R.J. and Achenback, J.D., - "Dynamically Induced Fracture", J. Mech. Phys. Solids, Vol. 20, p. 203 (1972).
- [24] Keer, L.M. and Luong, W.C., - "Diffraction of Waves and Stress Intensity Factors in a Cracked Layered Composite", J. Acoust. Soc. Am., Vol. 56, p. 1681 (1974).
- [25] Levy, H. and Lessman, F., - Finite Difference Equations, MacMillan Co. (1961).
- [26] Kim, B.S. and Moon, F., - "Impact on a Laminated Half Space", to be published.
- [27] Premont, E.J. and Stubenrauch, K.R., - "Impact Resistance of Composite Fan Blades", Tech. Rep. to NASA Lewis Research Center, NASA CR-134515, Pratt and Whitney Aircraft (1973).
- [28] Novak, R.C., - "Multi-Fiber Composites", Tech. Rep. to NASA Lewis Research Center, NASA OR-135062, United Technology (1976).
- [29] Christensen, R.M., - Theory of Viscoelasticity, Academic Press, N.Y. (1971).
- [30] Christescu, N., - Dynamic Plasticity, North-Holland, New York (1967).
- [31] Birkhoff, A. et al., - "Explosives with Lined Cavities", J. Appl. Phys. Vol. 19, p. 563 (1948).

- [32] Griffith, A., - "Phenomenon of Rupture and Flaw in the Solids",  
Phil. Trans. Roy. Soc. (London), Vol. A221, p. 163 (1921).
- [33] Liebowitz, H., (Ed.) - Fracture, Vol. 2, Academic Press, N.Y. (1968).
- [34] Sneddon, I.N. and Lowengrub, M. - Crack Problems in the Classical  
Theory of Elasticity, John Wiley and Sons, New York (1969).
- [35] Sneddon, I.N., - Mixed Boundary Value Problems in Potential Theory,  
North-Holland, Amsterdam (1966).
- [36] Noble, B., - Method Based On the Wiener-Hopf Technique, Pergamon  
Press, New York (1958).

## Figures

1. Composite Plate and Layer
- 2 a,b. Dispersion Relationship and Phase Velocity for Isotropic Plate:  
One-layer Model ( $\lambda = \mu$ ).
- 3 a,b. Dispersion Relationship and Phase Velocity for Composite Plate:  
One-layer Model (55% Graphite Fiber-Epoxy Matrix, Layup Angle  $45^\circ$ ).
- 4 a,b. Dispersion Relationship and Phase Velocity for Isotropic Plate:  
Two-layer Model ( $\lambda = \mu$ ).
- 5 a,b. Dispersion Relationship and Phase Velocity for Composite Plate:  
Two-layer Model (55% Graphite Fiber-Epoxy Matrix, Layup Angle  $45^\circ$ ).
- 6 a-f. Longitudinal Propagation Impact Stress in Isotropic Plate:  
Two-layer Model ( $\lambda = \mu = 1.2 \cdot 10^7$  psi;  $\Delta = 1$  cm,  $t_0 = 10$   $\mu$ sec,  
 $a = 4$  cm).
7. Transverse Propagation of Normal Stress in Isotropic Plate:  
4-layer Model ( $\lambda = \mu = 1.2 \cdot 10^7$  psi;  $\Delta = 4$  cm,  $t_0 = 2$   $\mu$ sec,  $a = 40$  cm).
8. Transverse Propagation of Normal and Shear Stress in Isotropic Plate:  
(Same as in Fig. 7).
9. Transverse Propagation of Normal Stress in Composite Plate:  
8-layer Model (55% Graphite Epoxy-Fiber Matrix, Layup Angle  $15^\circ$ ;  
 $\Delta = 1$  cm,  $t_0 = 2$   $\mu$ sec,  $a = 2$  cm).
10. Two Dimensional Propagation of Normal Stress in Isotropic Plate:  
4-layer Model ( $\lambda = \mu = 1.2 \cdot 10^7$  psi;  $\Delta = 4$  cm,  $t_0 = 4$   $\mu$ sec,  $a = 4$  cm).
11. Velocity Surface and Wave Surface of Composite Plate (55% Graphite  
Fiber-Epoxy Matrix, Layup Angle  $45^\circ$ ).
- 12a,b. Comparison of Theoretical Wave Front and Numerical Wave Front of  
Composite Plate 10  $\mu$ sec after Impact: 55% Graphite Fiber-Epoxy  
Matrix (For Numerical Results; 8-layer Model,  $\Delta = 4$  cm,  $t_0 = 4$   $\mu$ sec,  
 $a = 2$  cm). Without and with Correction Factors.
13. Effect of Correction Factor on Transverse Propagation of Peak  
Value of Normal Stress: 8-layer Model (55% Graphite Fiber-Epoxy  
Matrix, Layup Angle  $45^\circ$ ;  $\Delta = 4$  cm,  $t_0 = 4$   $\mu$ sec,  $a = 2$  cm).
14. Viscoelastic Impact Energy Absorbing Models.
- 15a,b. Complex Modulus of Elastomer.
16. Plate with Viscoelastic Layers.
17. Impact of Plate Made of 2 Elastic Layers and a Viscoelastic Layer.

18. Peak Value of Interlaminar Stress Vs Elastomer thickness (Two Elastic Layers and a Viscoelastic Layer: ( $\Delta = 1$  cm,  $t_0 = 10$   $\mu$ sec,  $a = 4$  cm).
19. Composite Plate with Crack.

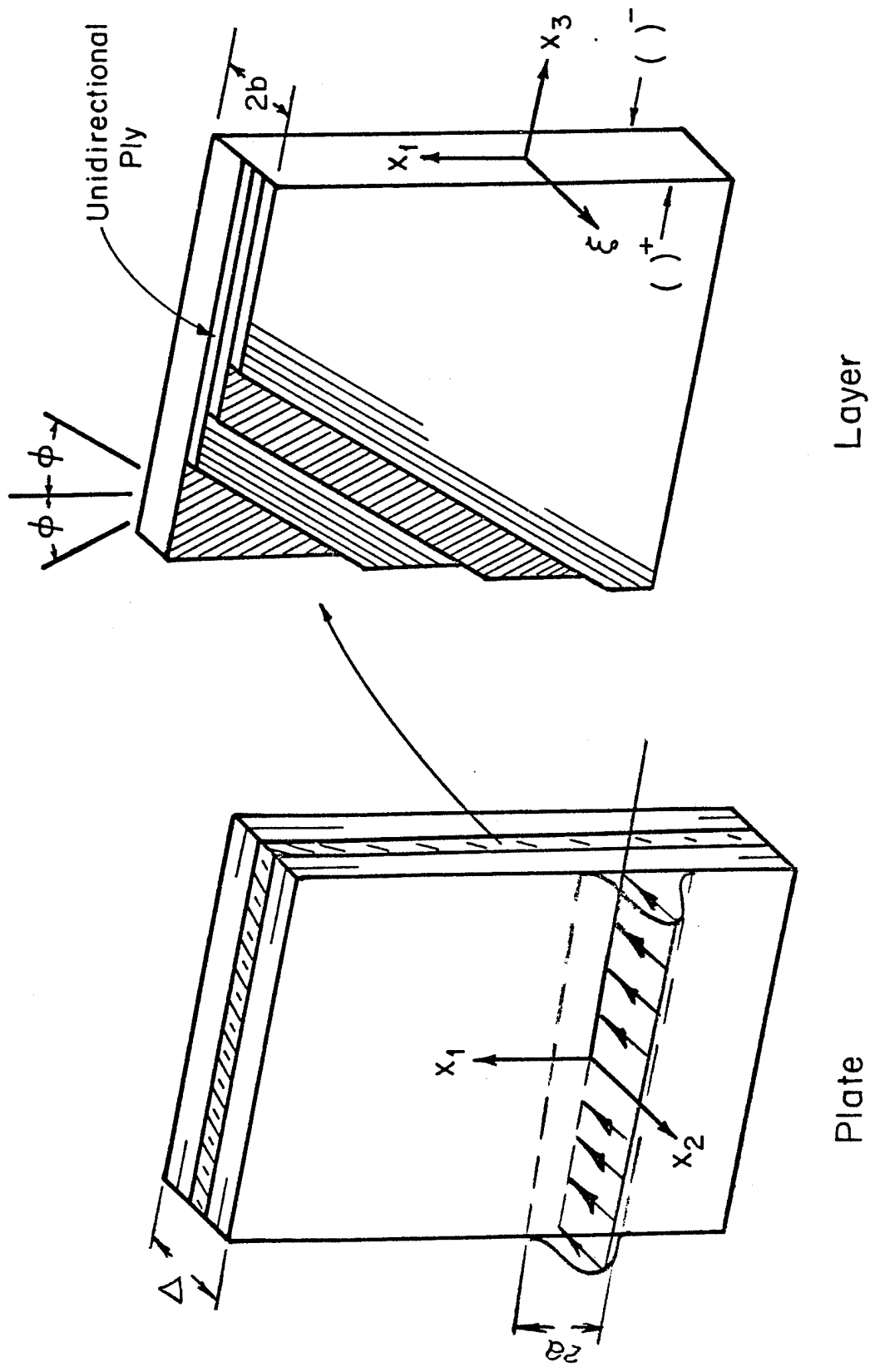


Figure 1. Multilayered Composite Plate and Layer

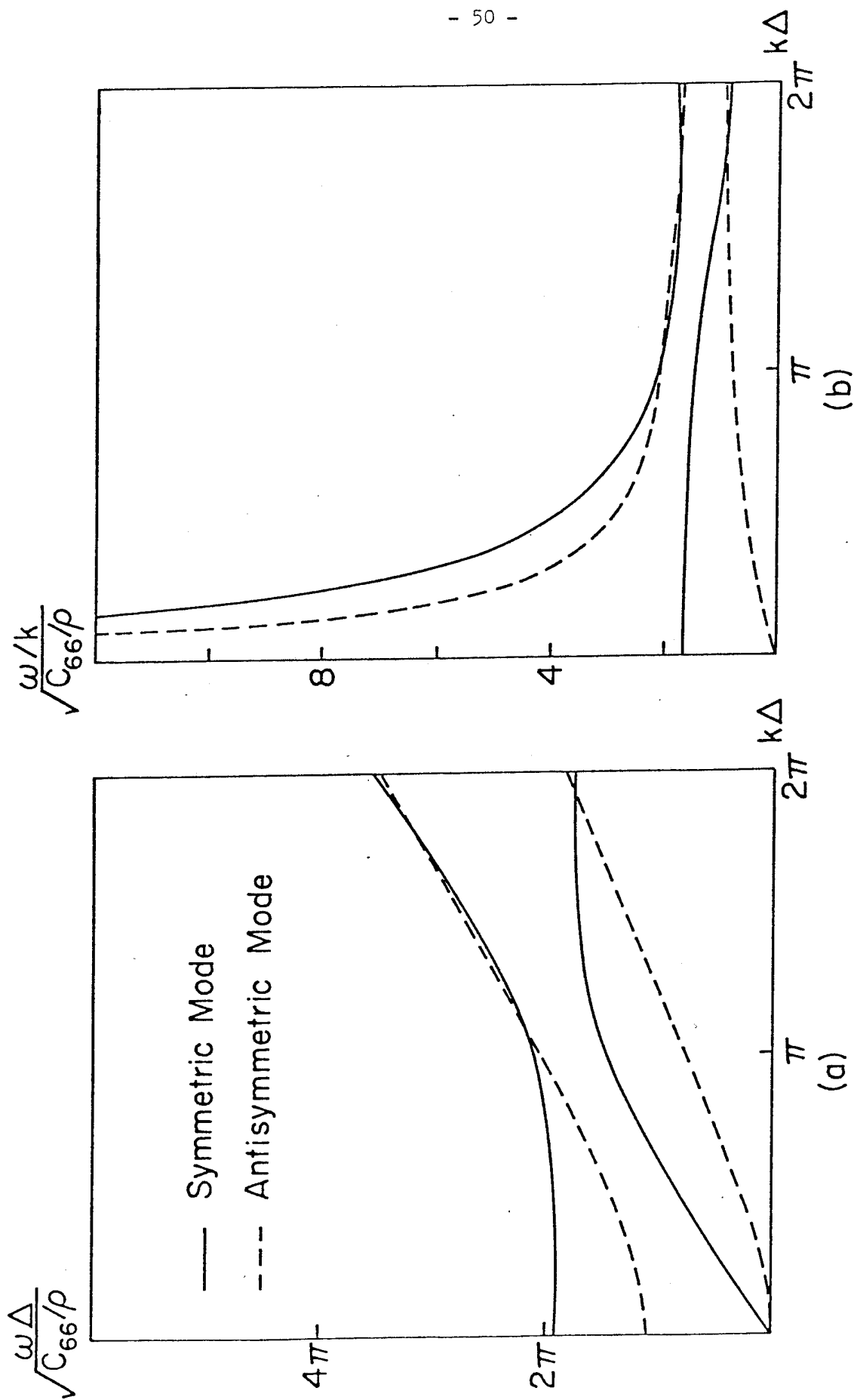


Figure 2. Dispersion Relationship and Phase Velocity of Isotropic Plate:  
One-Layer Model ( $\lambda = \mu$ , Poisson's Ratio = 1/4)

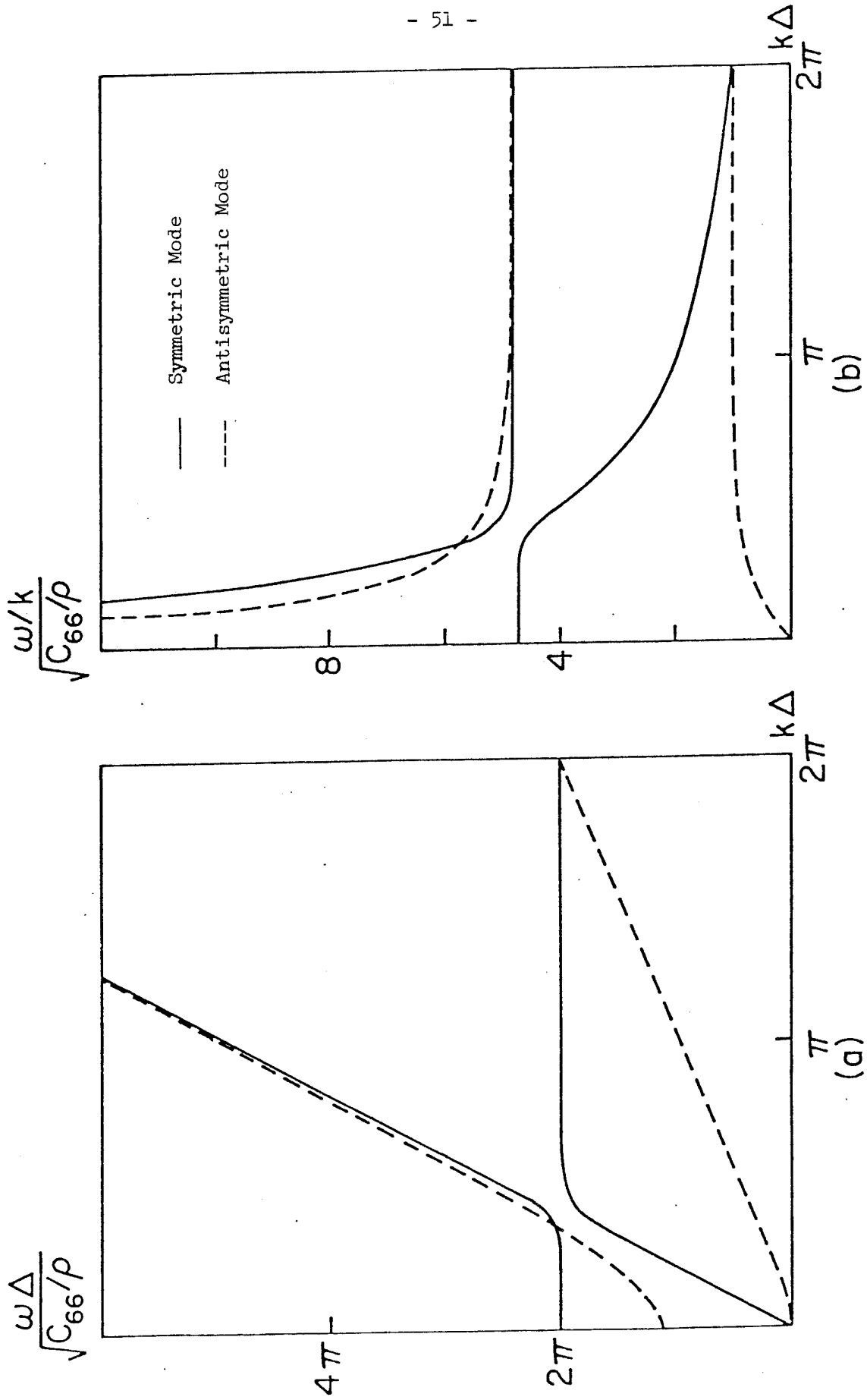


Figure 3. Dispersion Relationship and Phase Velocity of Composite Plate: One-Layer Model (55% Graphite Fiber - Epoxy Matrix; Layup Angle = 45°)

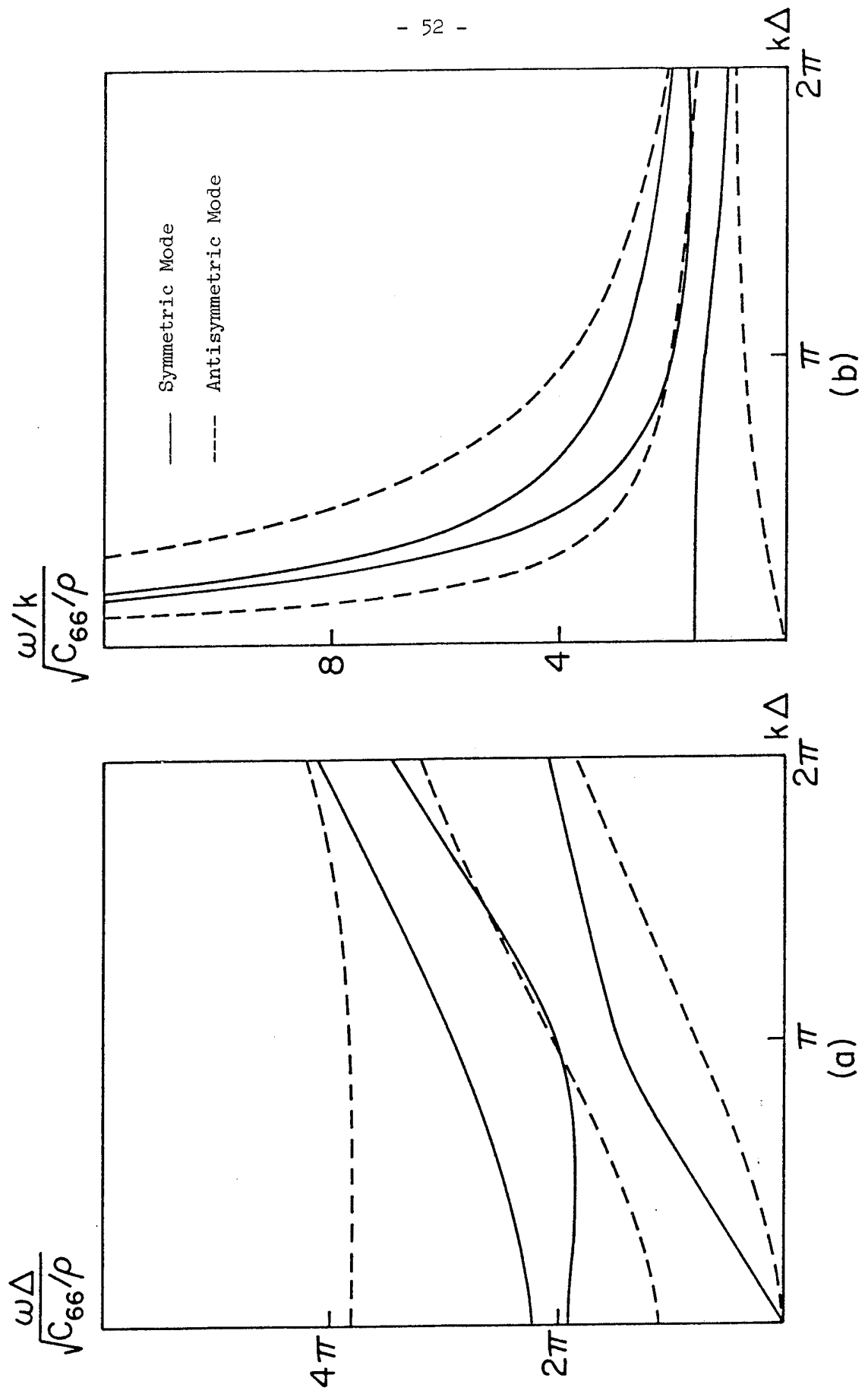


Figure 4. Dispersion Relationship and Phase Velocity of Isotropic Plate:  
Two-layer Model ( $\lambda = \mu$ , Poisson's Ratio = 1/4)

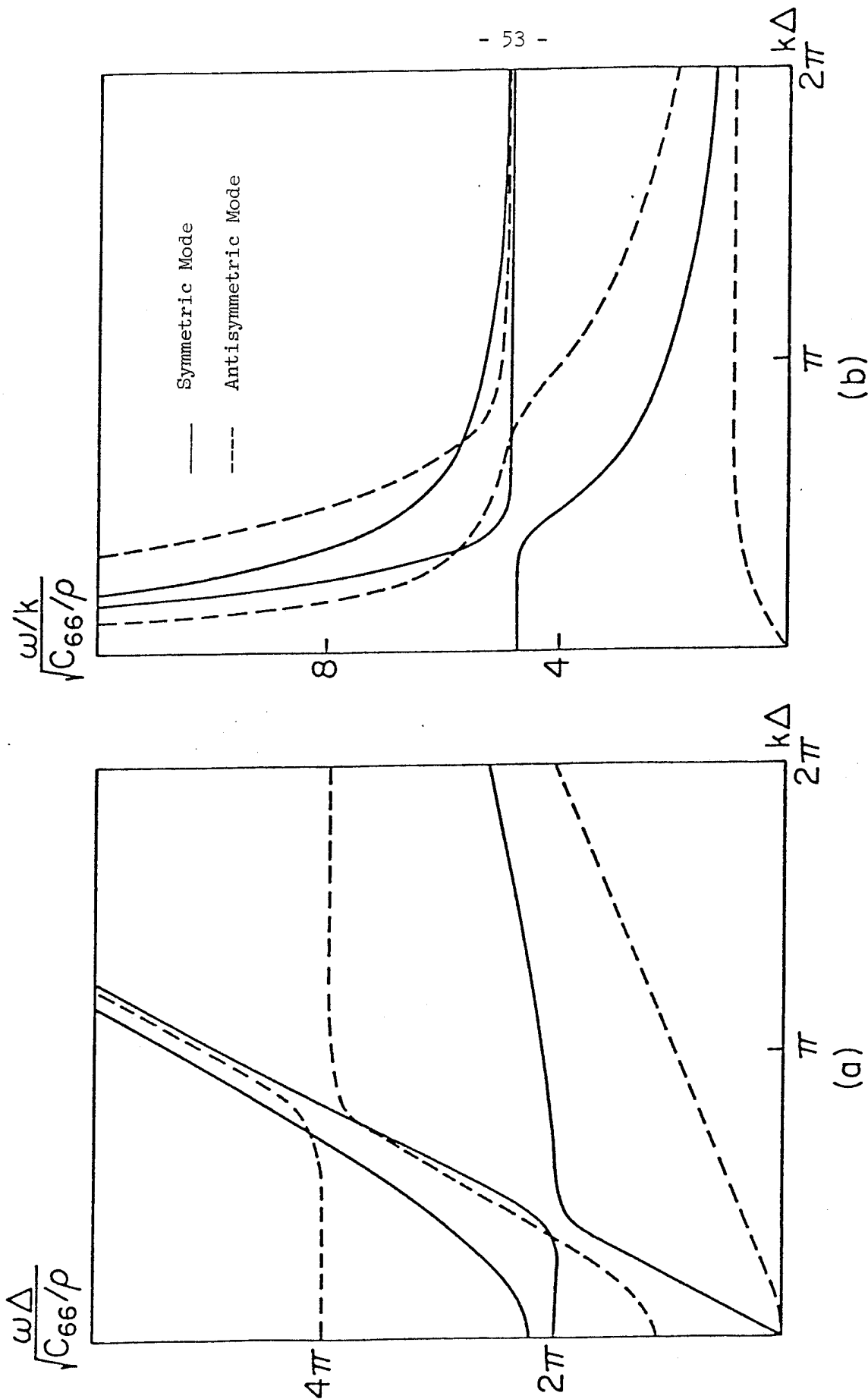


Figure 5. Dispersion Relationship and Phase Velocity of Composite Plate: Two-Layer Model (55% Graphite Fiber - Epoxy Matrix, Layup Angle = 45°)

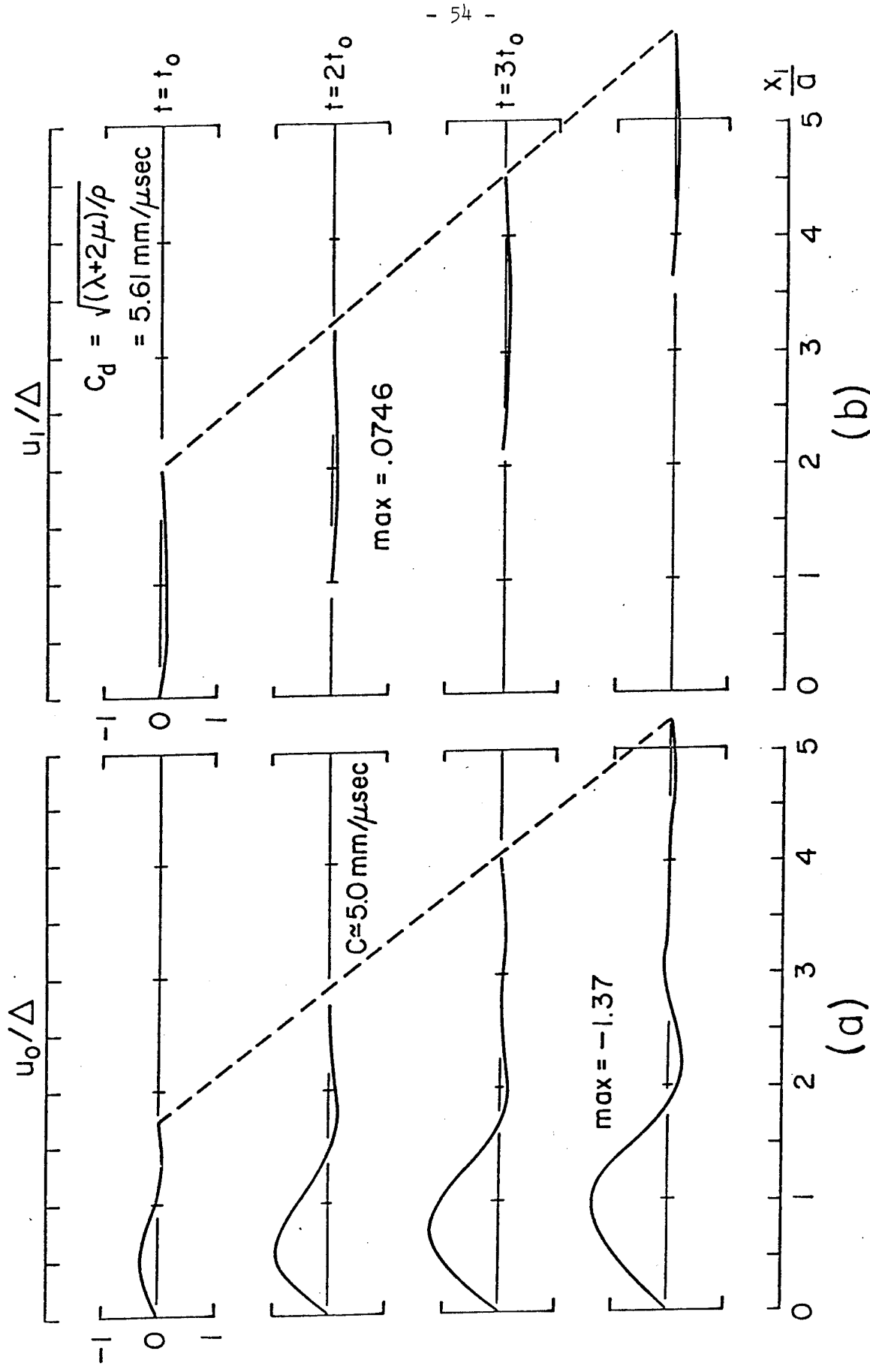


Figure 6 Longitudinal Propagation in Isotropic Plate; 2-layer Model  
 $(\lambda = \mu = 1.2 \times 10^7 \text{ psi}; \Delta = 1 \text{ cm}, t_0 = 10 \mu\text{sec}, a = 4 \text{ cm})$

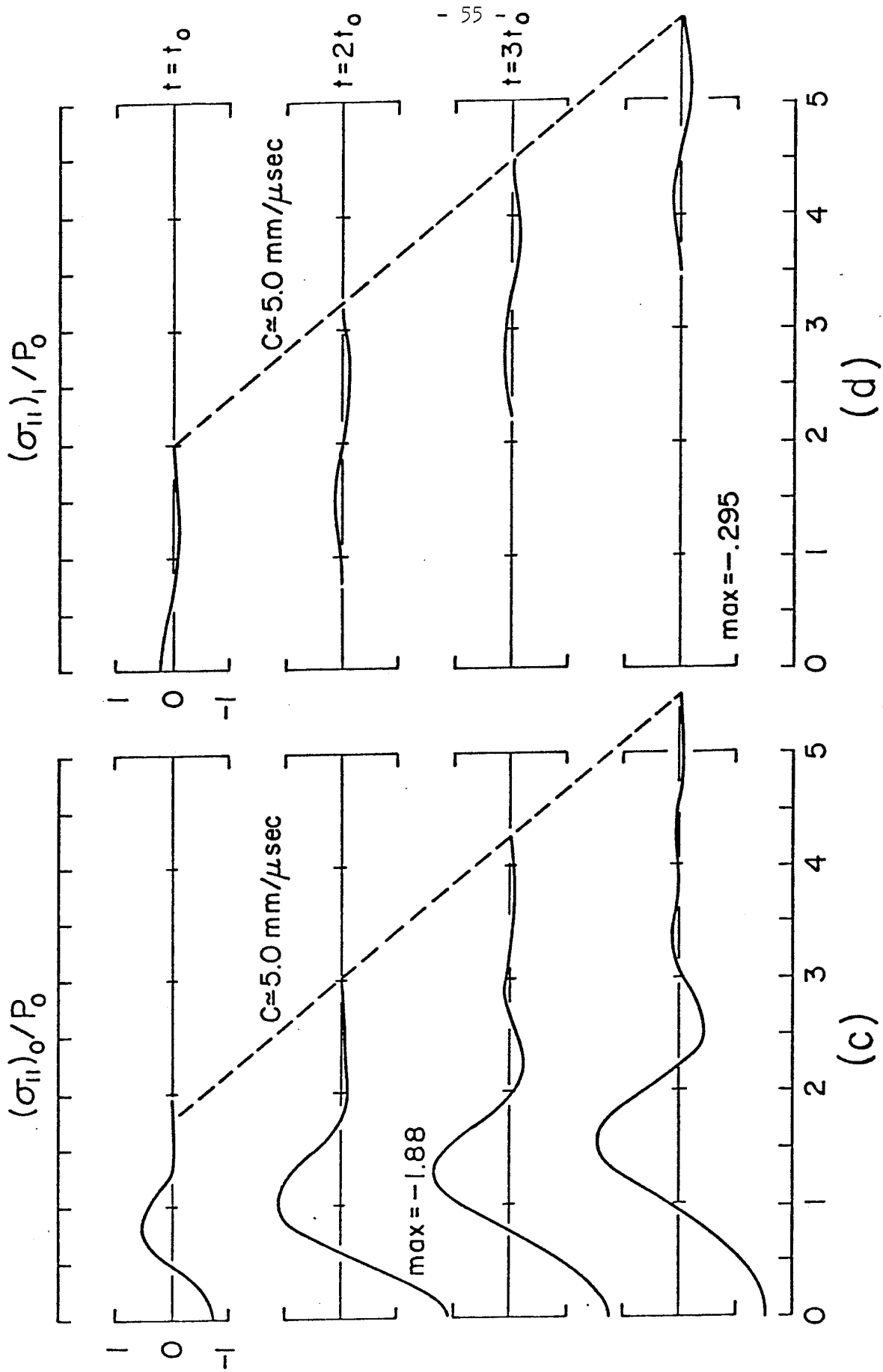


Figure 6 Continued

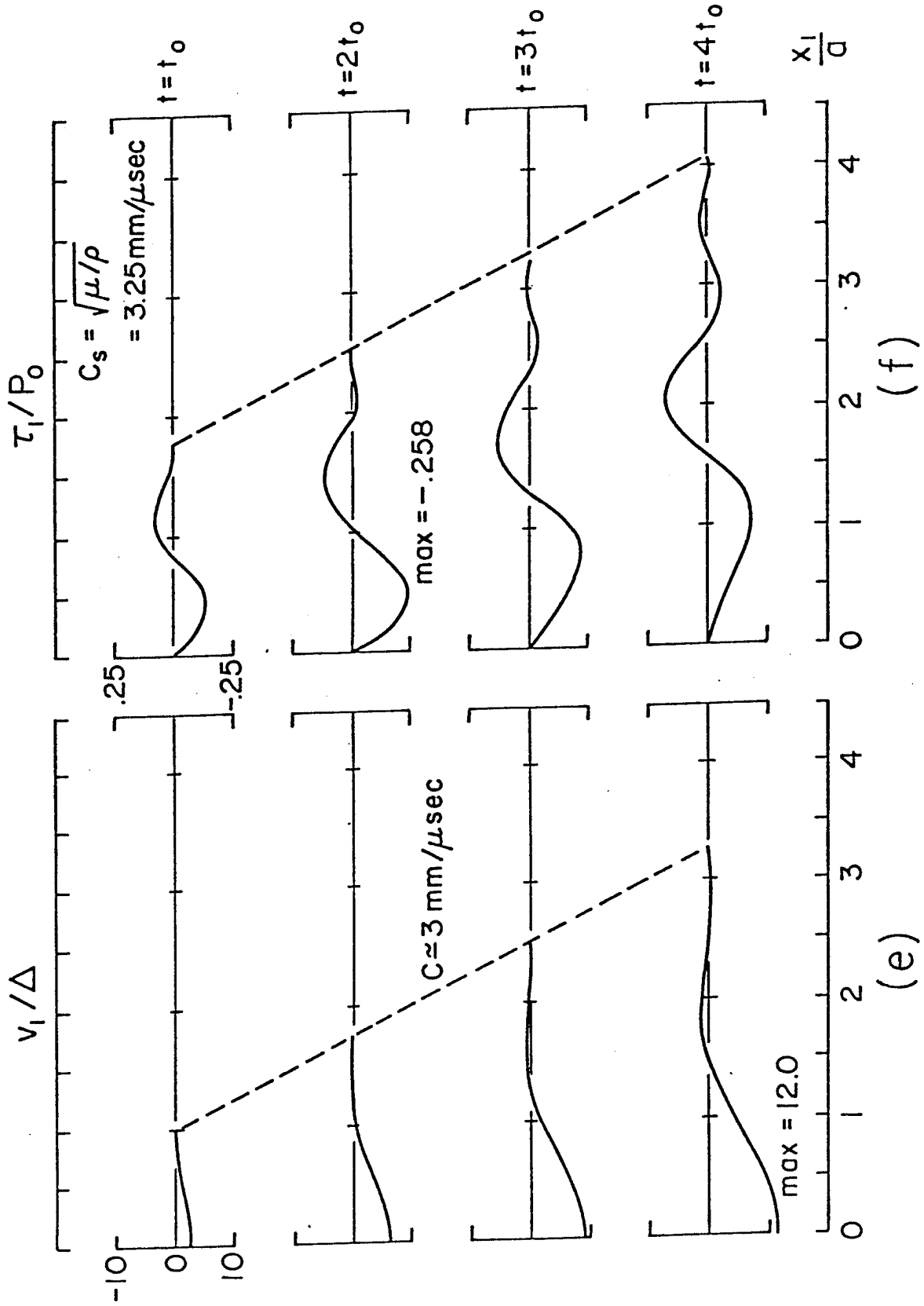


Figure 6 Continued

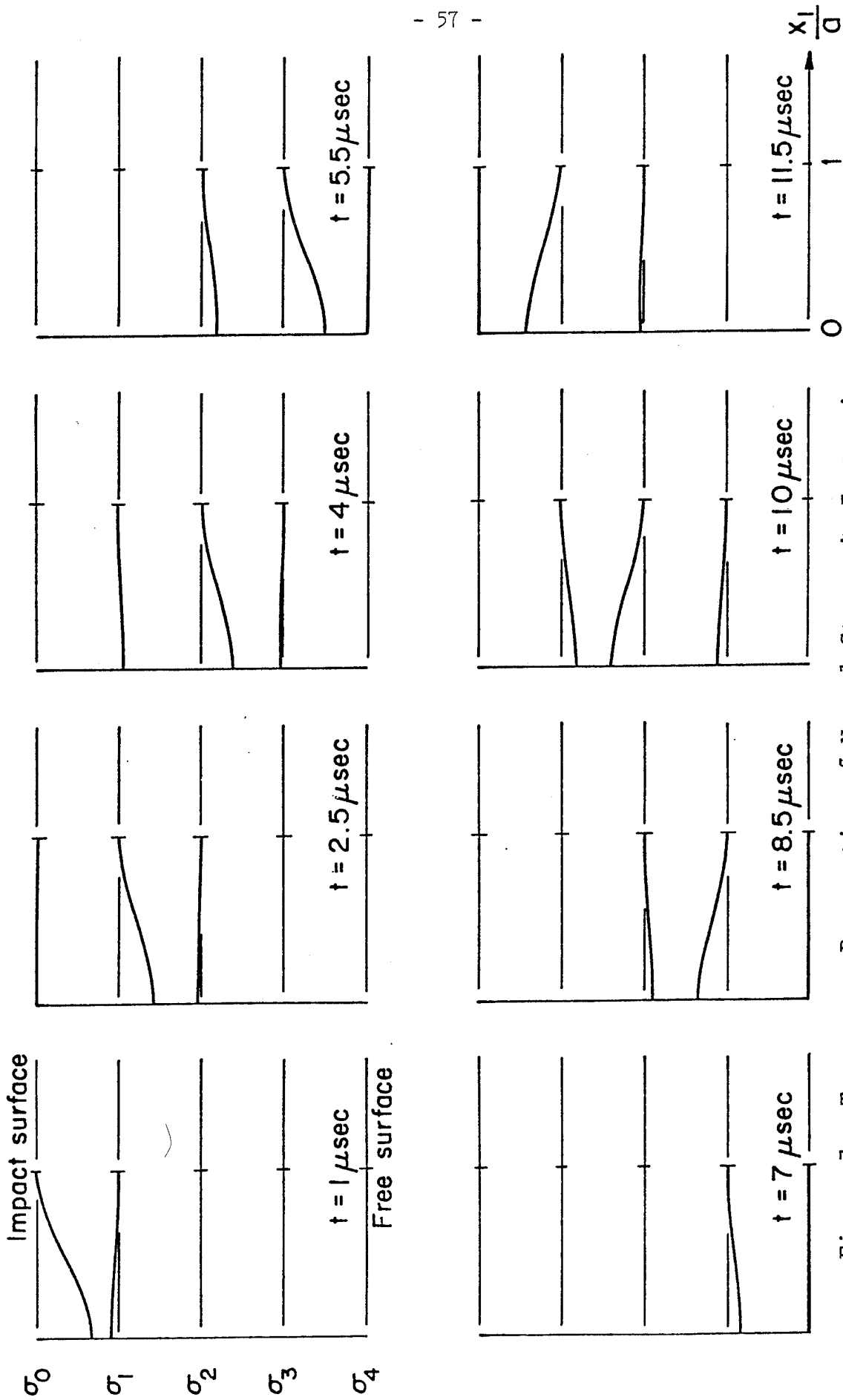


Figure 7. Transverse Propagation of Normal Stress in Isotropic Plate: 4-layer Model ( $\nu = 0.2$ ,  $\mu = 1.2 \times 10^7$  psi;  $\Delta = 4$  cm,  $t_0 = 2$   $\mu$ sec,  $a = 40$  cm)

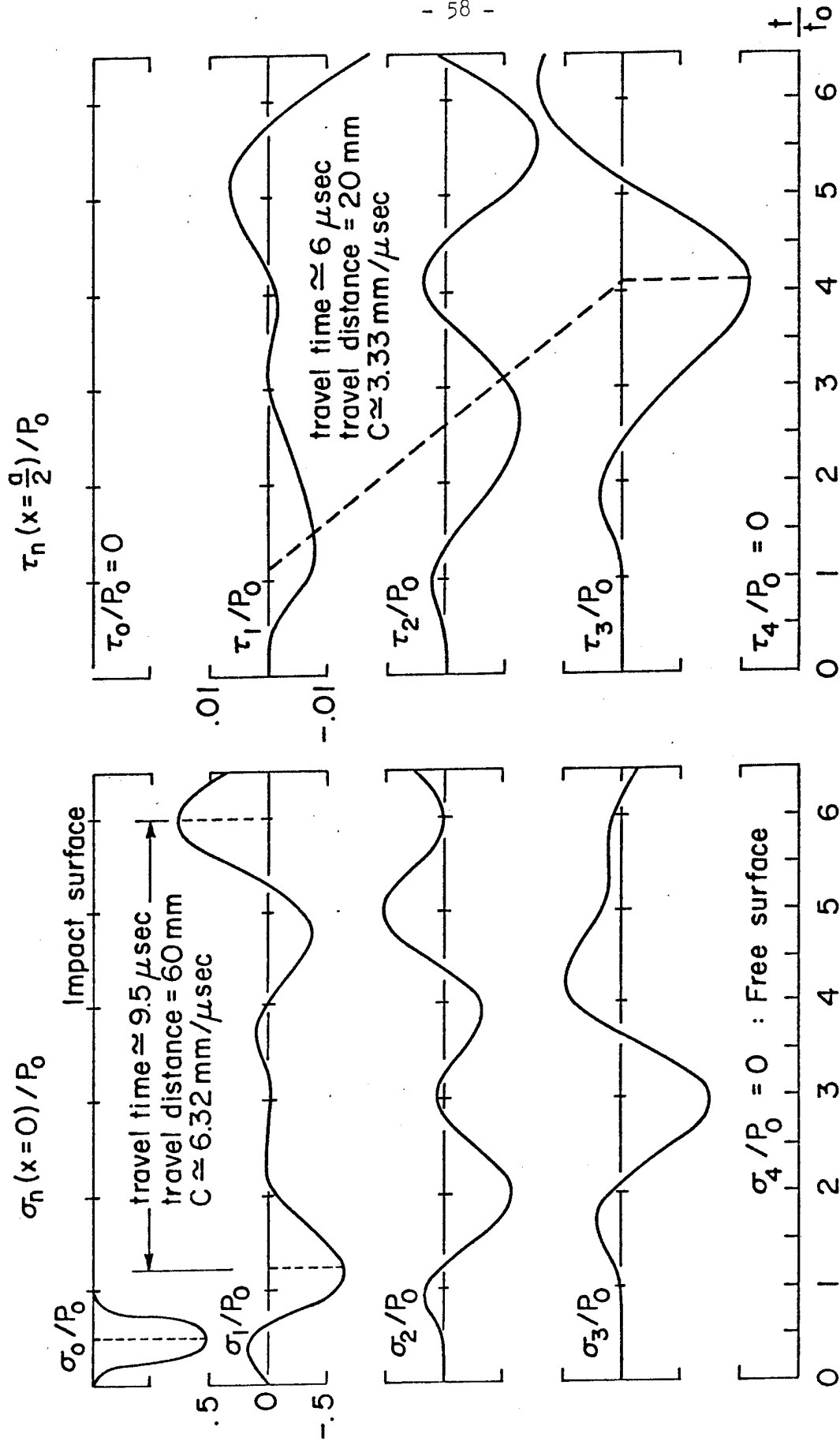


Figure 8. Transverse Propagation of Normal and Shear Stress (Same as in Figure 7)

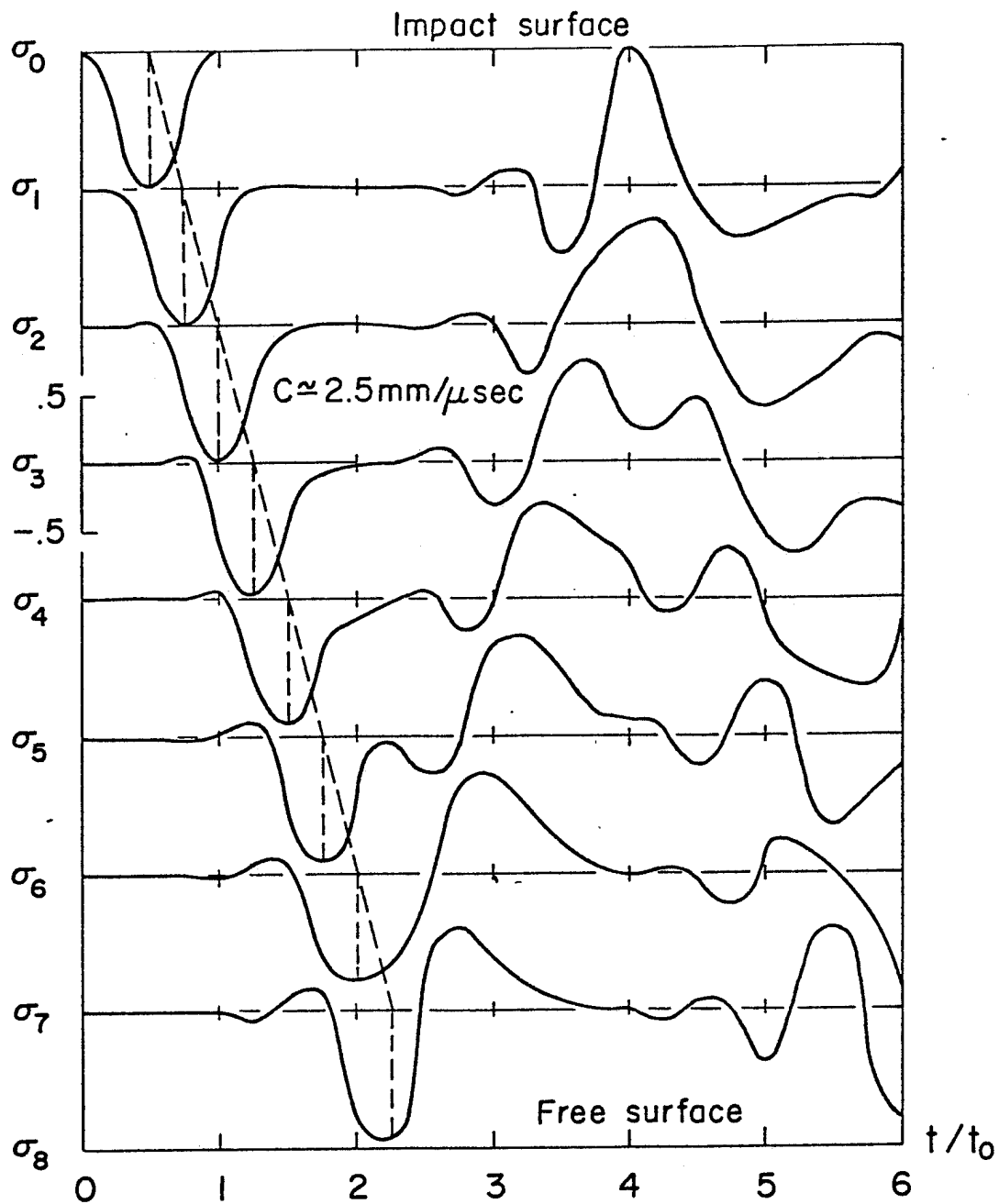


Figure 9 Transverse propagation of normal stress in composite plate; 8-layer Model (55% Graphite Fiber - Epoxy Matrix,  $\pm 15^\circ$  Layup;  $\Delta = 1 \text{ cm}$ ,  $t_0 = 2 \mu\text{sec}$ ,  $a = 2 \text{ cm}$ )

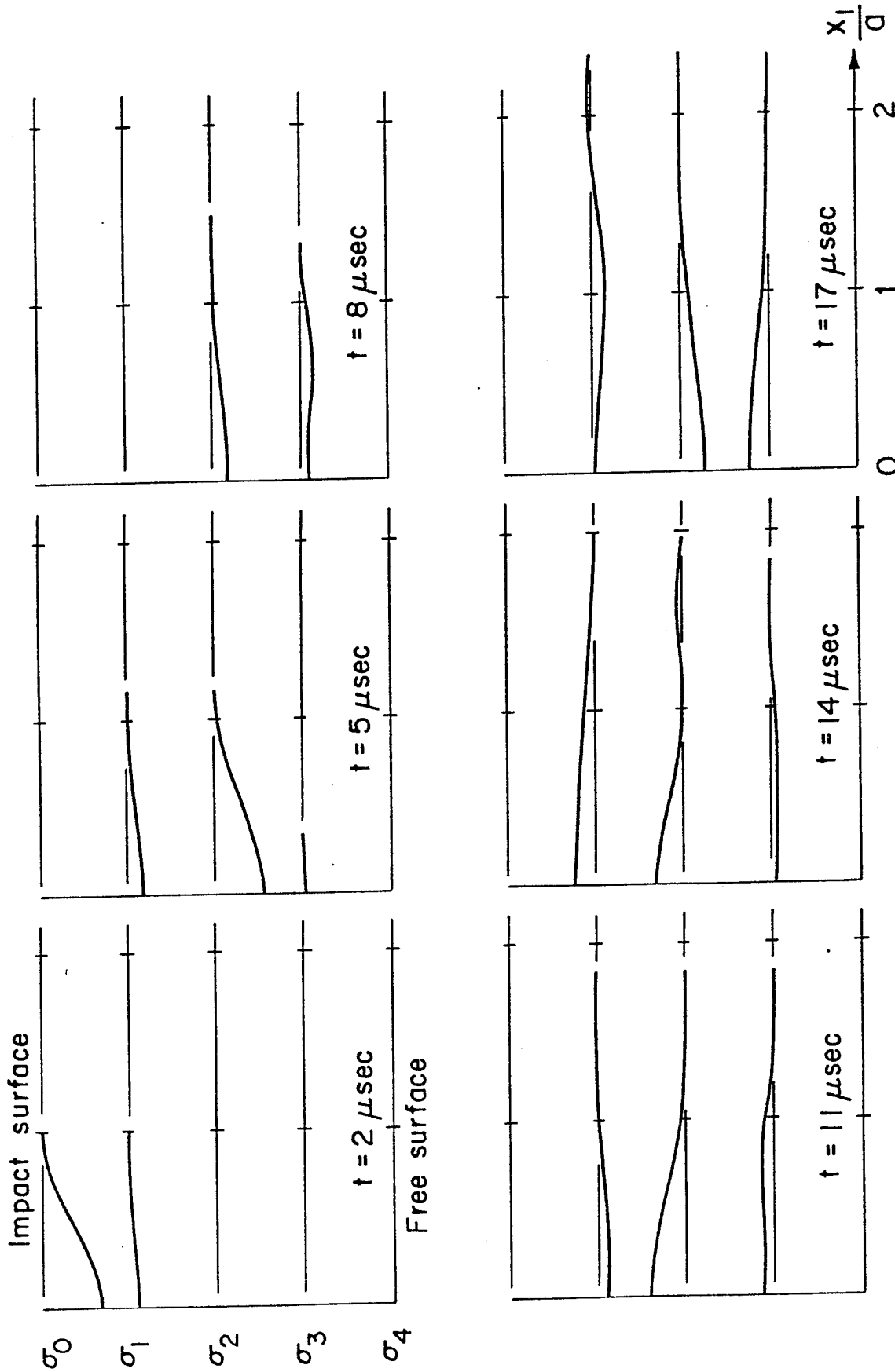


Figure 10. Two Dimensional Propagation of Normal Stress in Isotropic Plate:  
4-layer Model ( $\lambda = \mu = 1.2 \cdot 10^7$  psi;  $\Delta = 4$  cm,  $t_0 = 4 \mu\text{sec}$ ,  $a = 4$  cm)

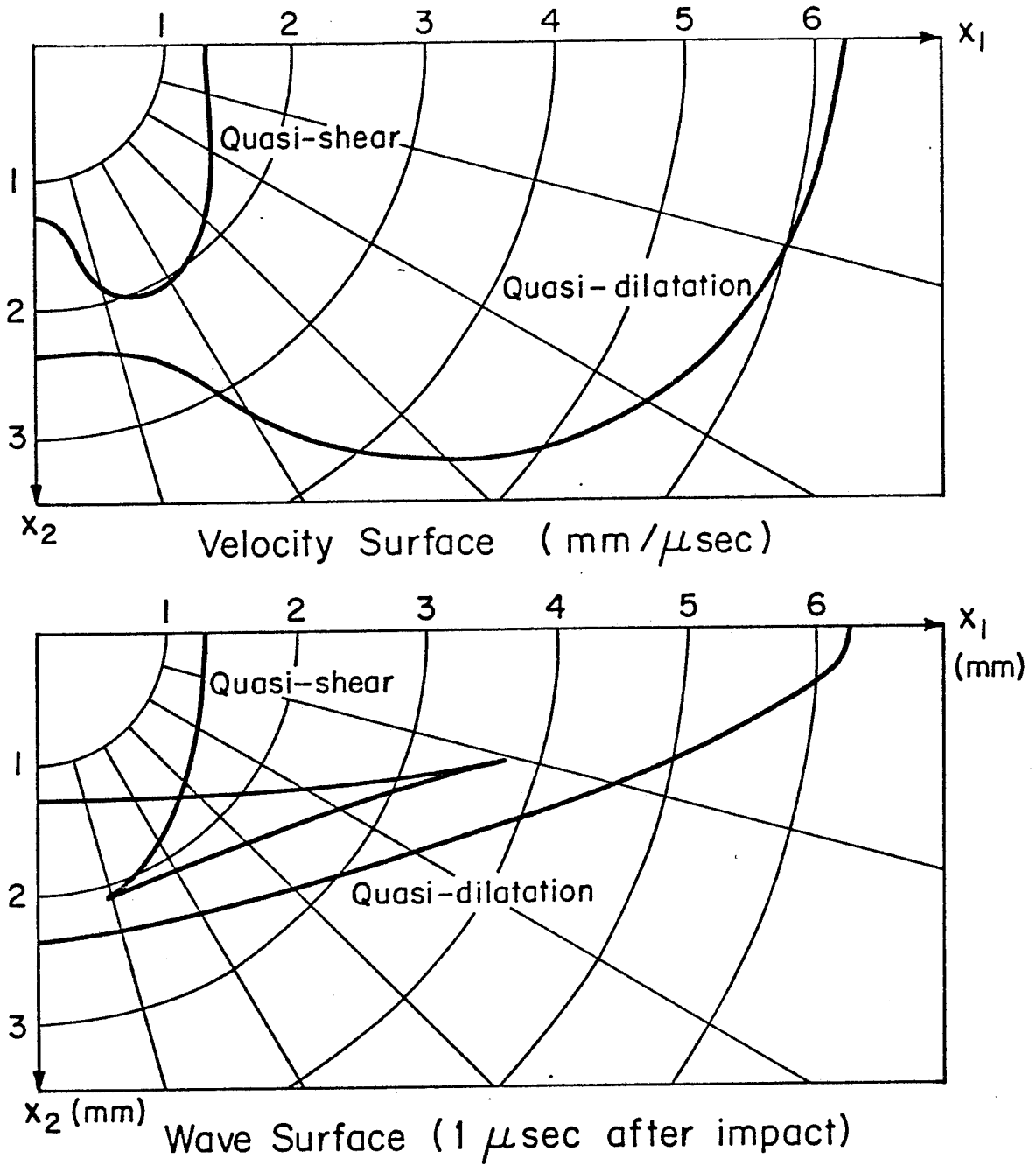


Figure 11. Velocity Surface and Wave Surface of Composite Plate (55% Graphite Fiber-Epoxy Matrix, Layup Angle  $45^\circ$ )

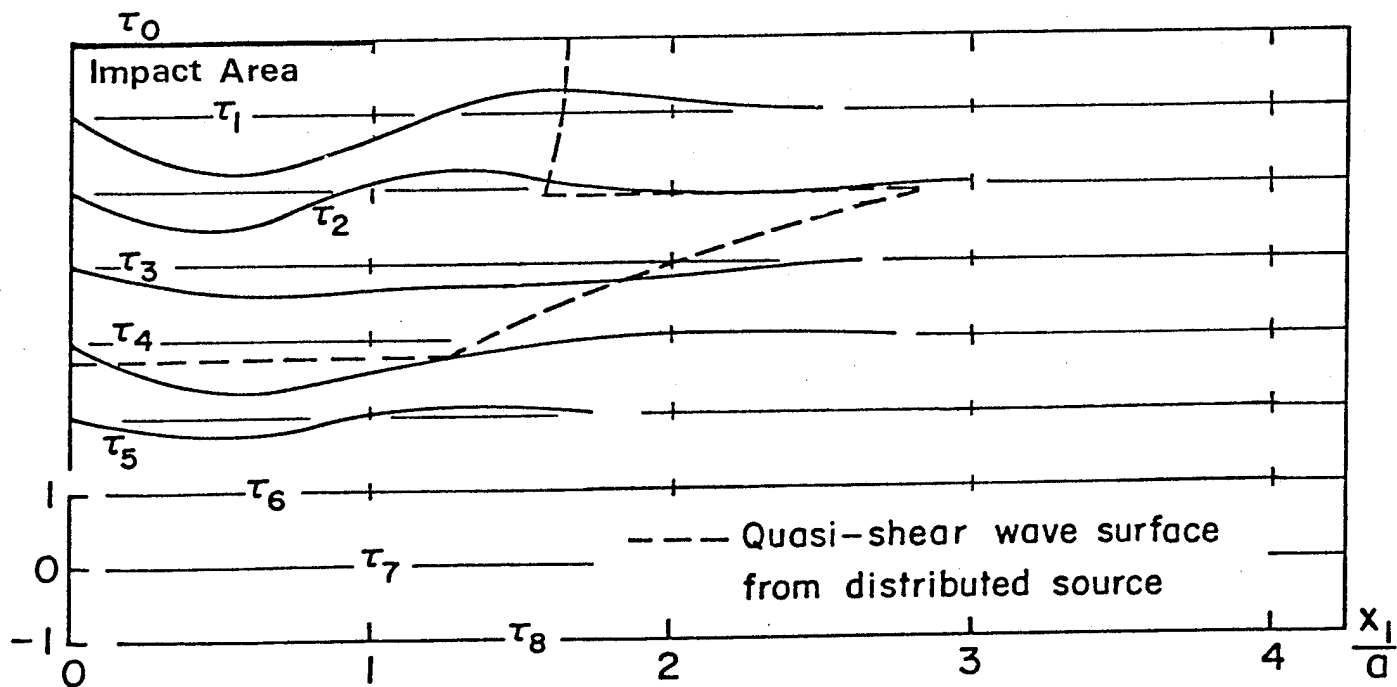
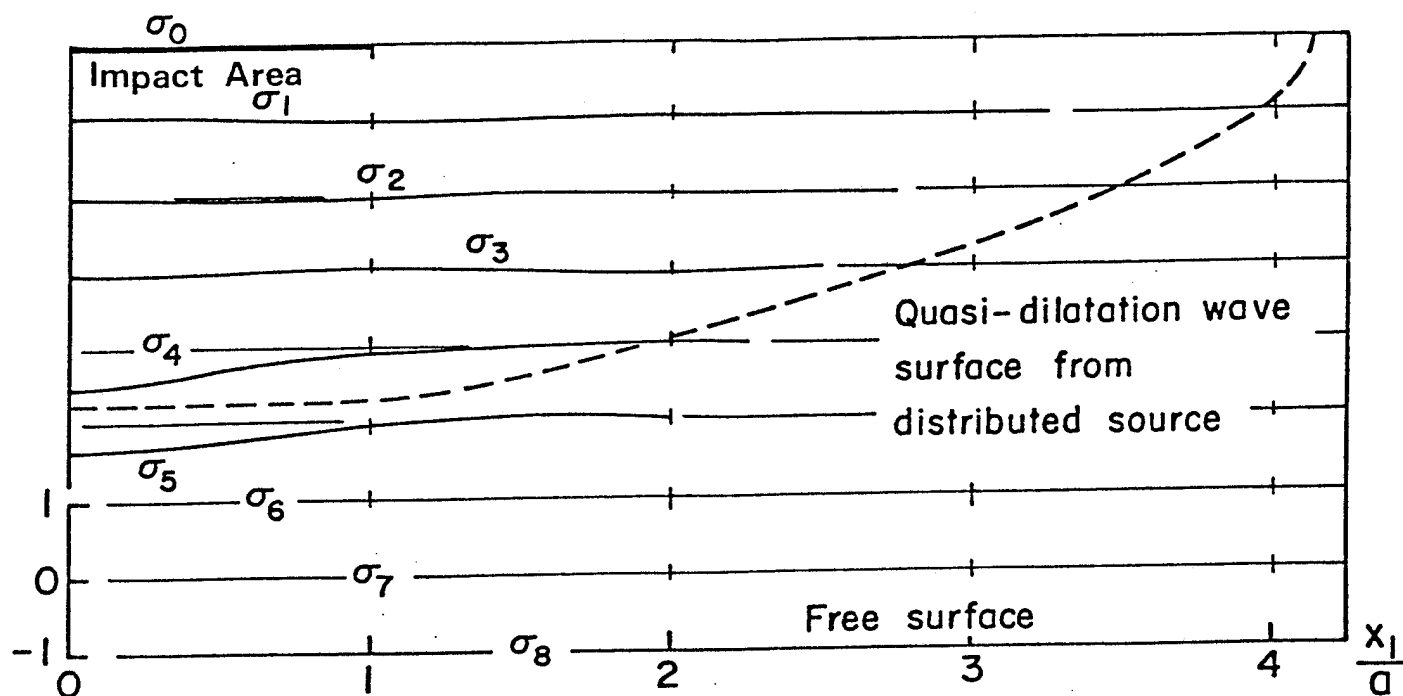


Figure 12a. Wave front 10  $\mu$ sec after impact (without correction factor)  
 (55% Graphite Fiber-Epoxy Matrix,  $\pm 45^\circ$  Layup;  $\Delta = 4$  cm,  
 8-layer Model;  $t_0 = 4$   $\mu$ sec,  $a = 2$  cm)

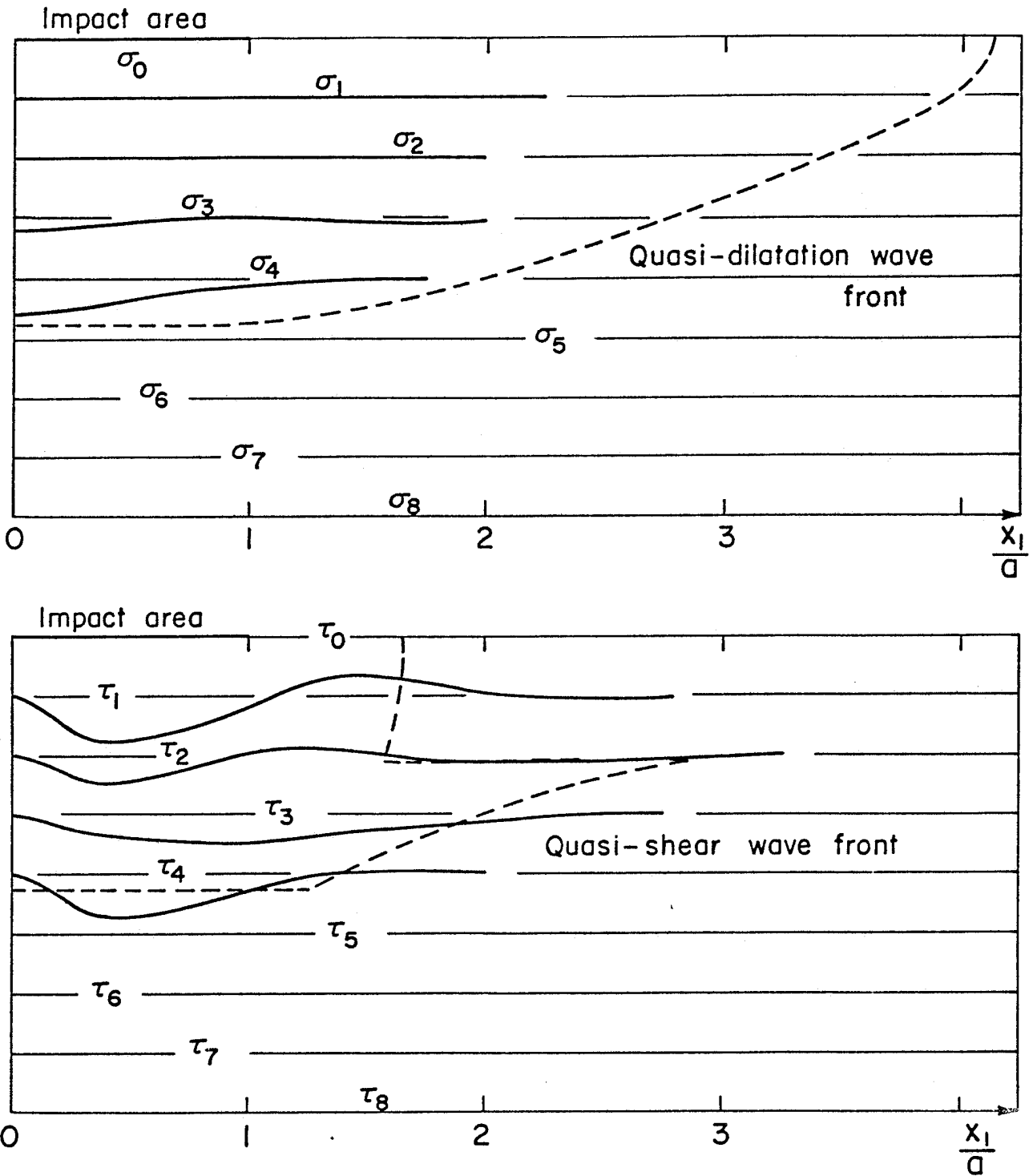


Figure 12b. Wave front 10  $\mu$ sec after impact (with correction factor)  
(55% Graphite Fiber-Epoxy Matrix,  $\pm 45^\circ$  Layup;  $\Delta = 4$  cm,  
8-layer Model;  $t = 4$   $\mu$ sec,  $a = 2$  cm)

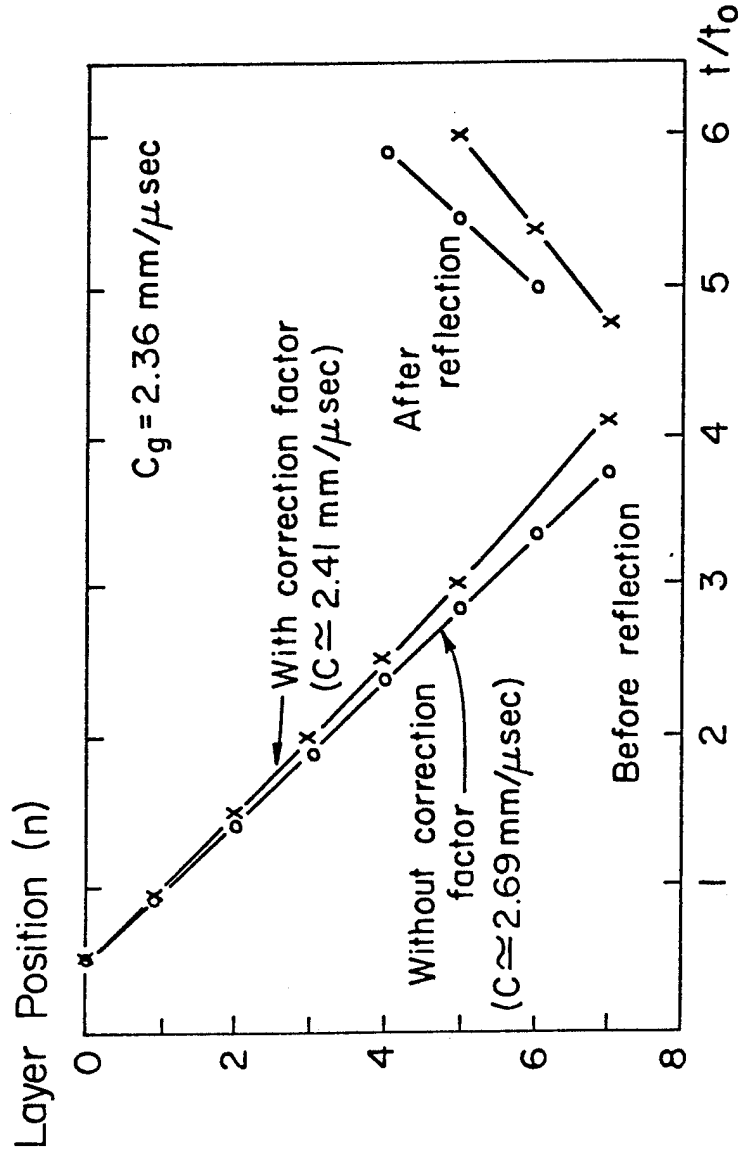


Figure 13 Effect of correction factors on transverse propagation of max  $\sigma_n$  ( $x_1 = 0$ ); 8-layer Model. (55% Graphite Fiber-Epoxy Matrix,  $\pm 45^\circ$  Layout;  $\Delta = 4 \text{ cm}$ ,  $t_0 = 4 \mu\text{sec}$ ,  $a = 2 \text{ cm}$ )

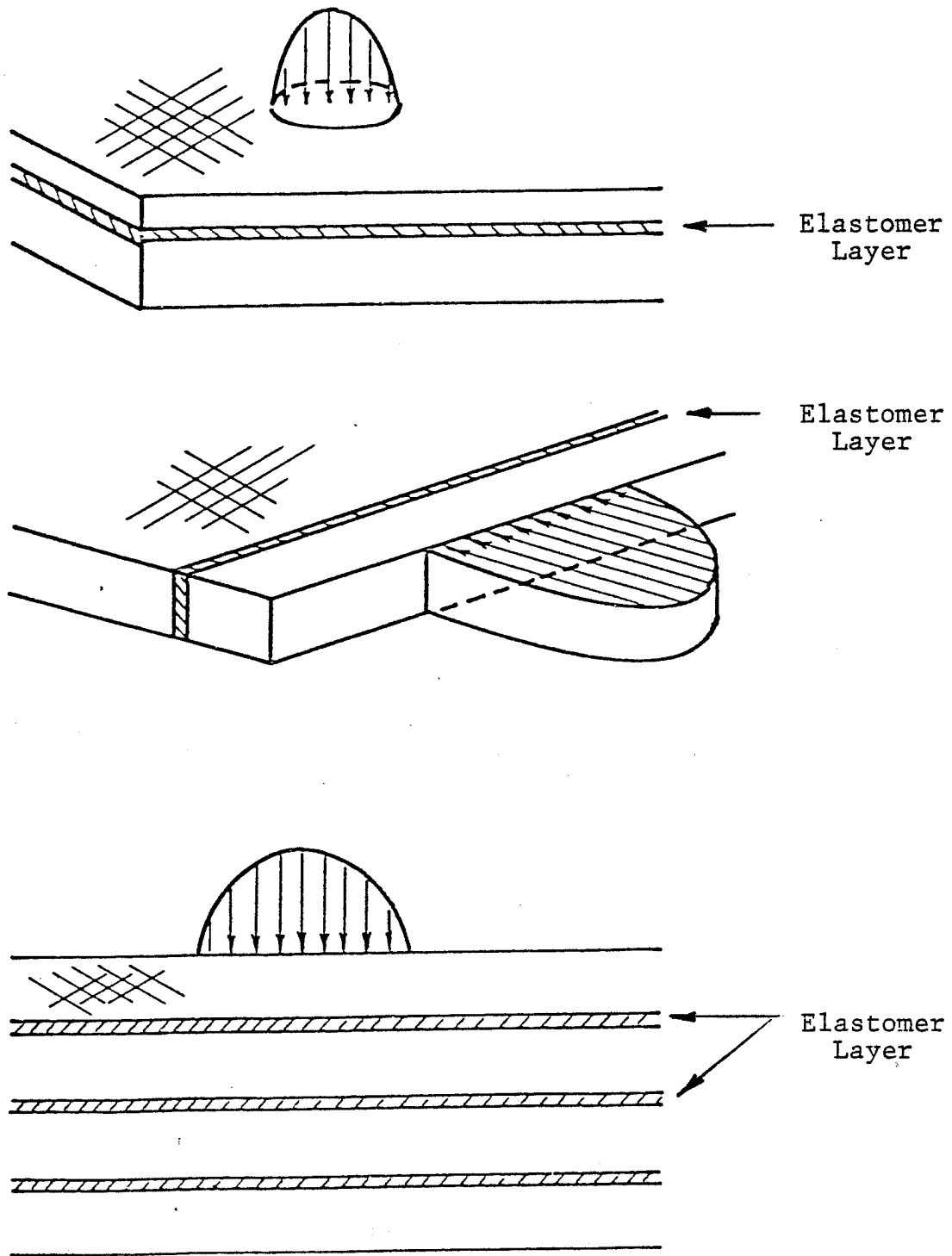


Figure 14. Viscoelastic Impact Energy Absorbing Models



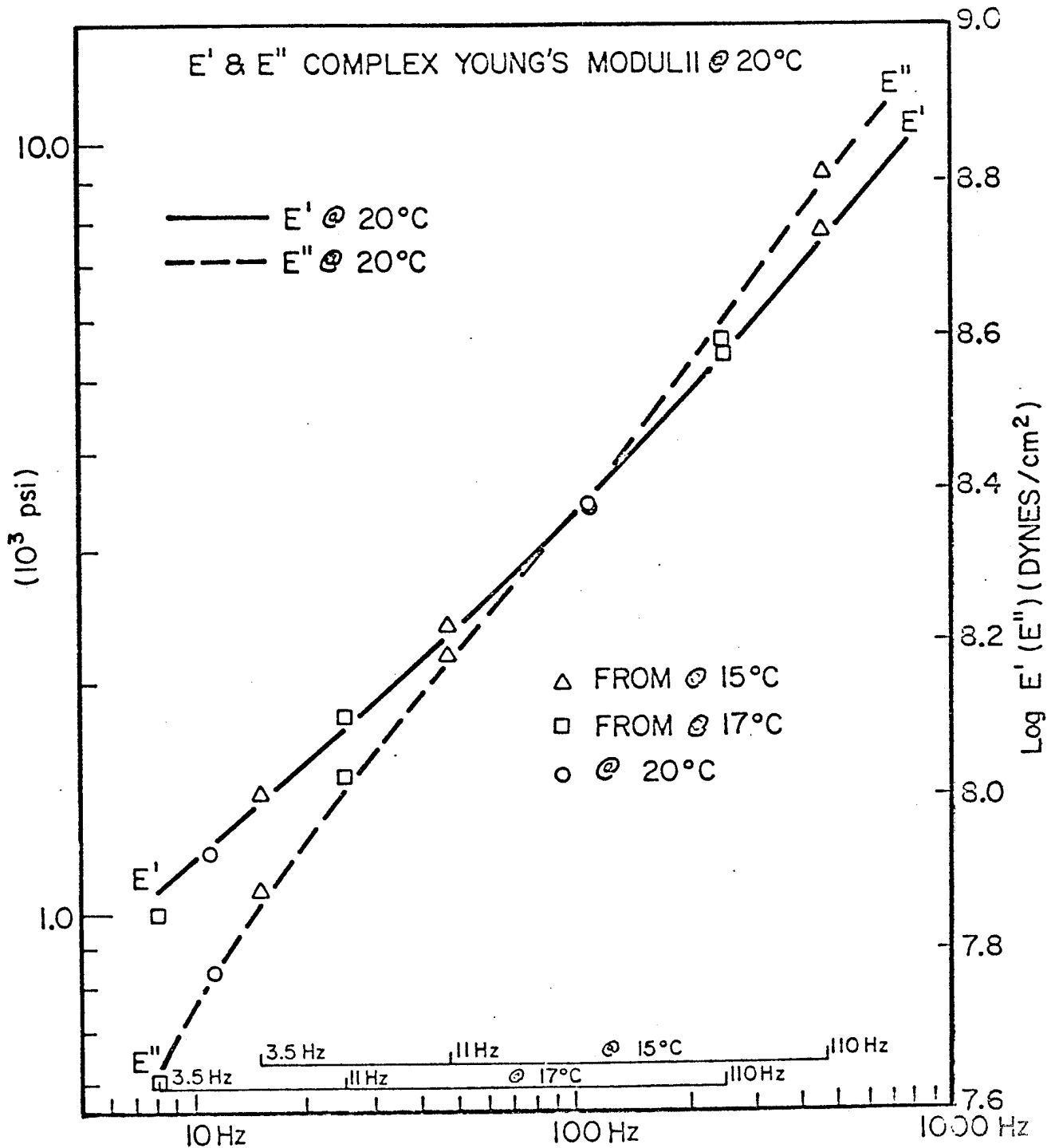


FIGURE 15b. THE COMPLEX YOUNG'S MODULUS OF LR3-604 MEASURED

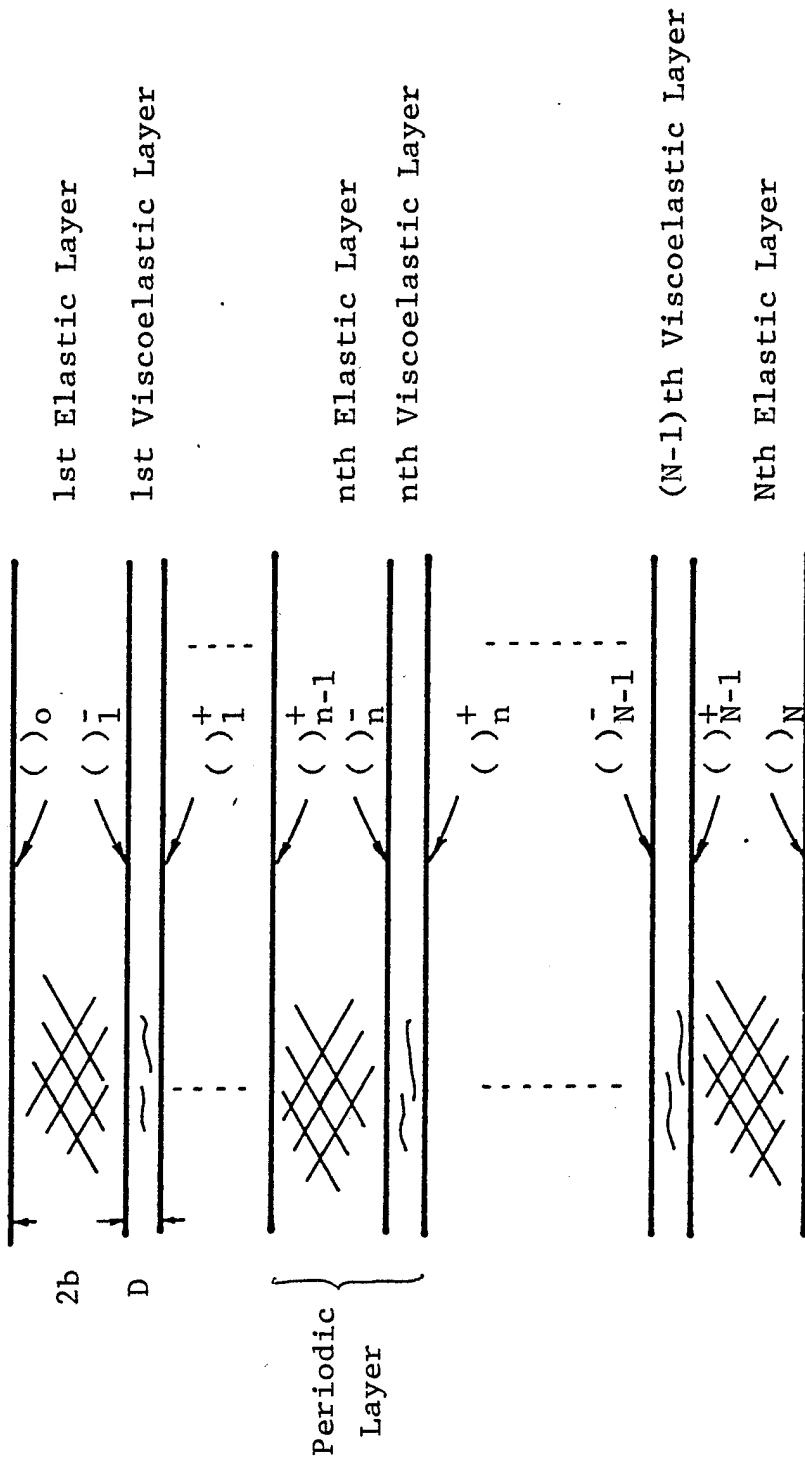


Figure 16. Plate with Viscoelastic Layers

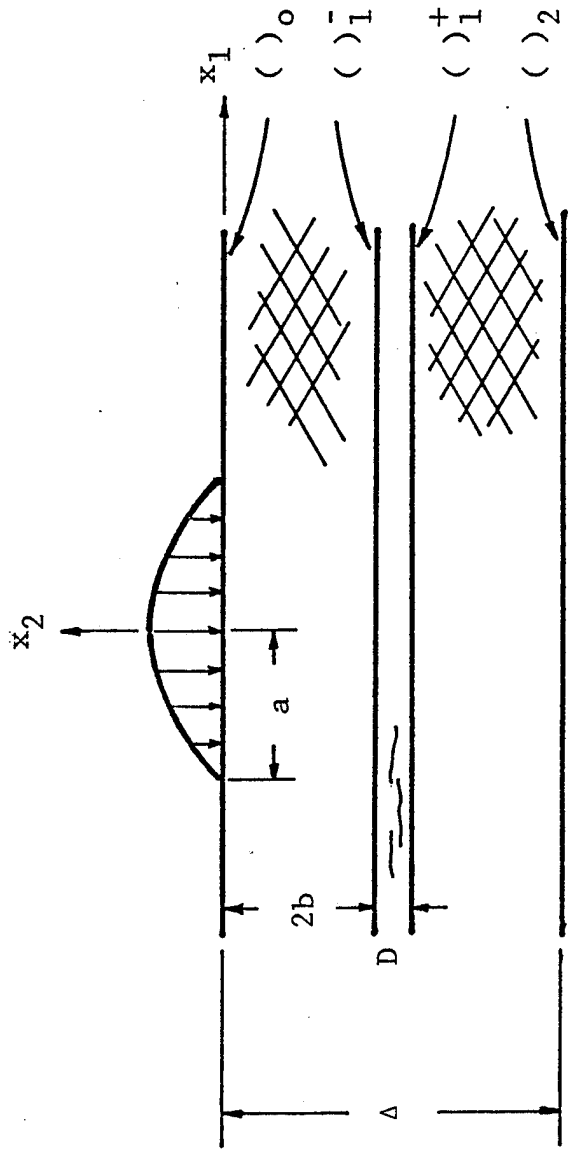


Figure 17. Impact of Plate Made of 2 Elastic Layers and a Viscoelastic Layer

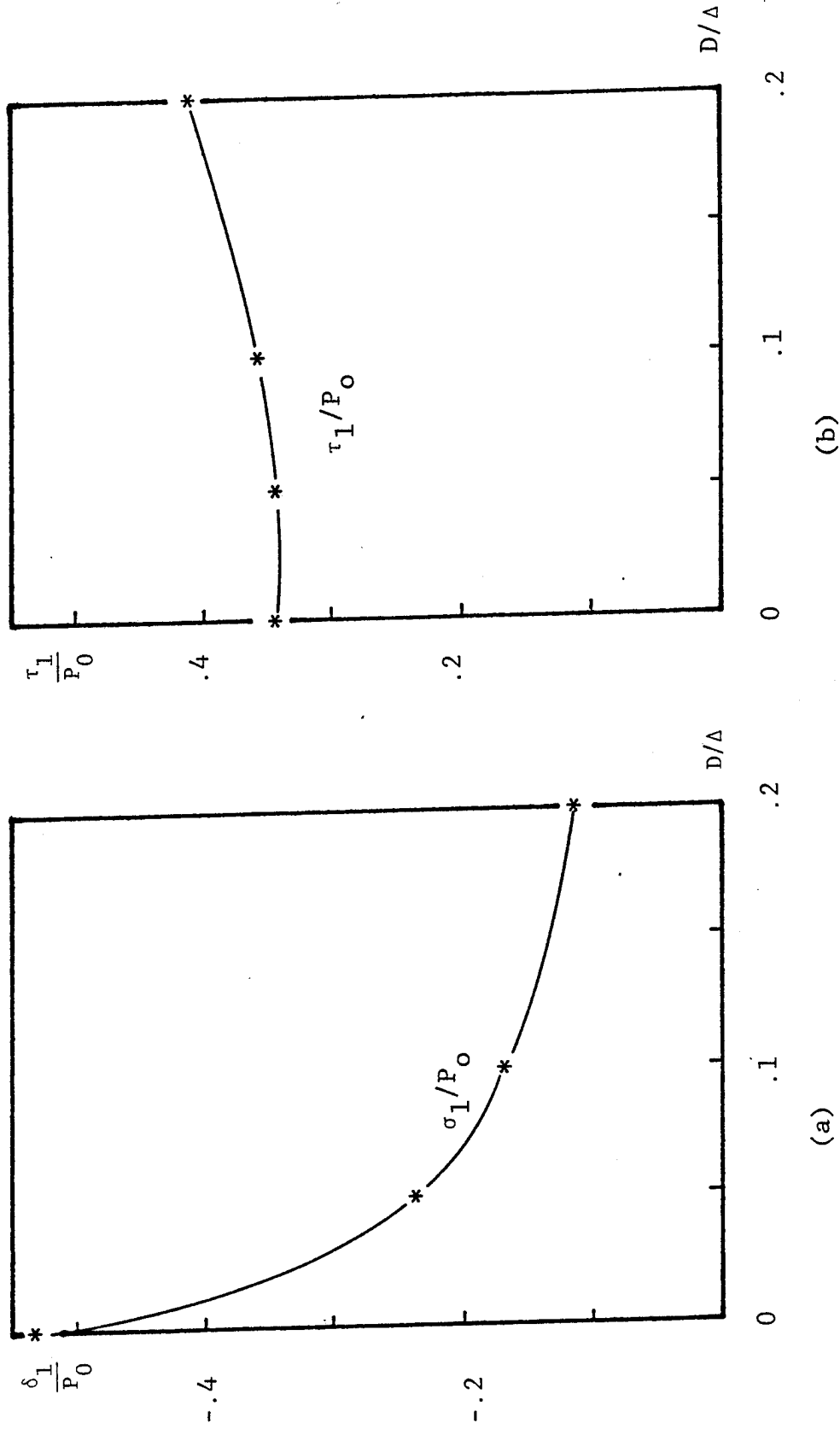


Figure 18. Peak Value of Interlaminar Stress Vs. Elastomer Thickness (two elastic layers and a viscoelastic layer;  $\Delta = 1$  cm,  $t_0 = 10$   $\mu$ sec,  $a = 4$  cm)  
\*Calculated values

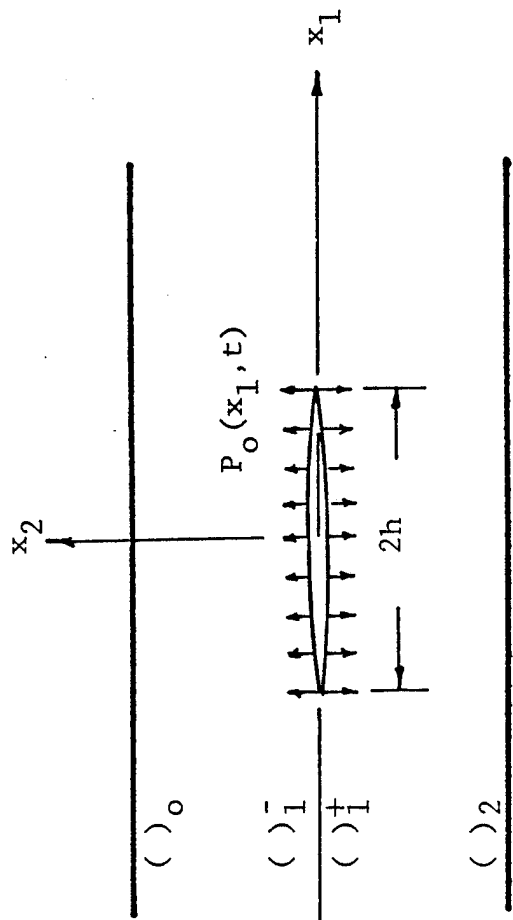
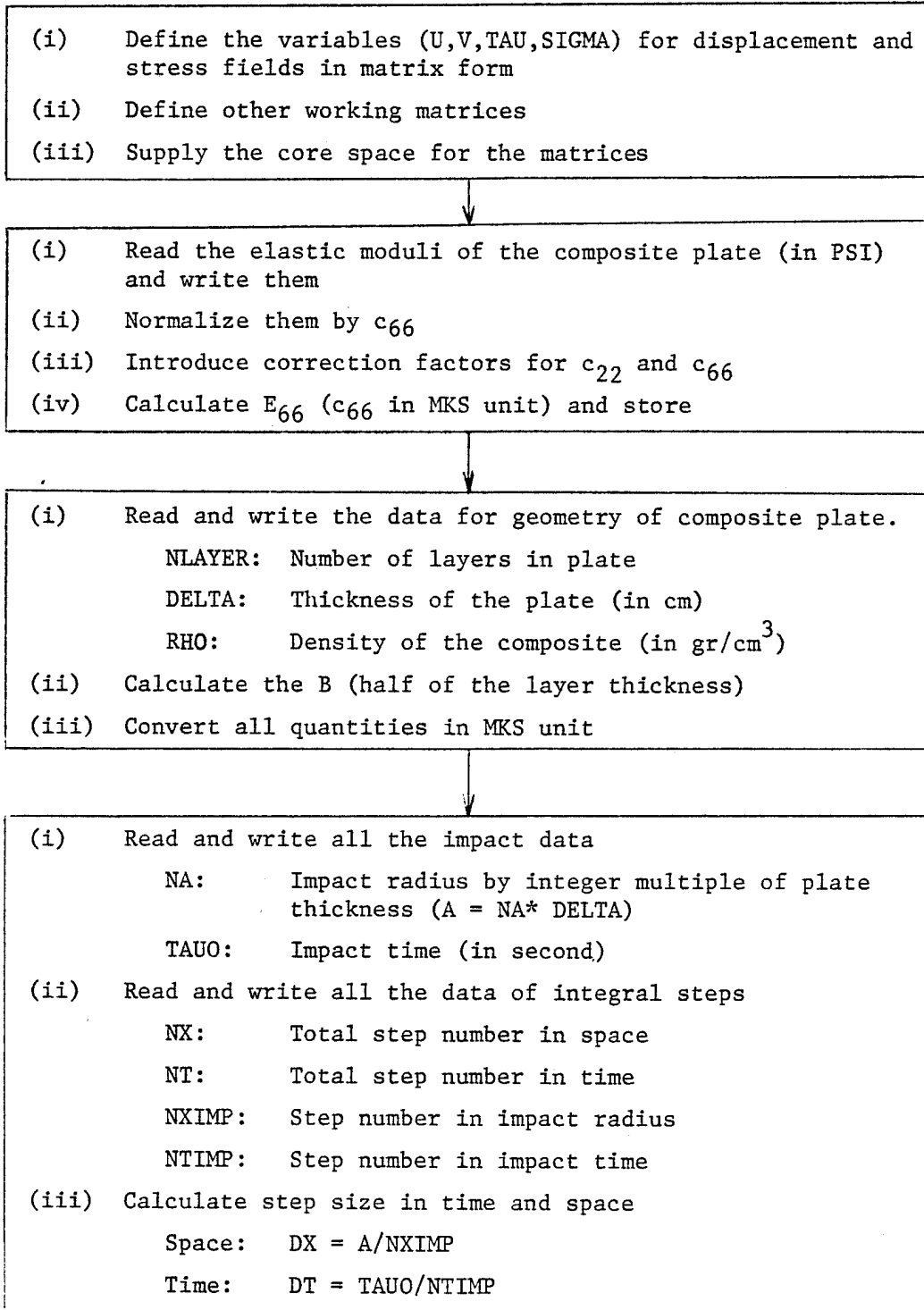


Figure 19. Composite Plate with Crack

## APPENDIX A FLOW CHART

In this flow chart and program,  $U(I,J)$ ,  $V(I,J)$ ,  $TAU(I,J)$   
 $SIGMA(I,J)$  and  $SIGMAL(I,J)$  represent  $\hat{U}$ ,  $\hat{V}$ ,  $\hat{T}$  and  $\hat{\Sigma}$  in  
Eq. (II-17,18) and integral transform of  $\sigma_{11}$

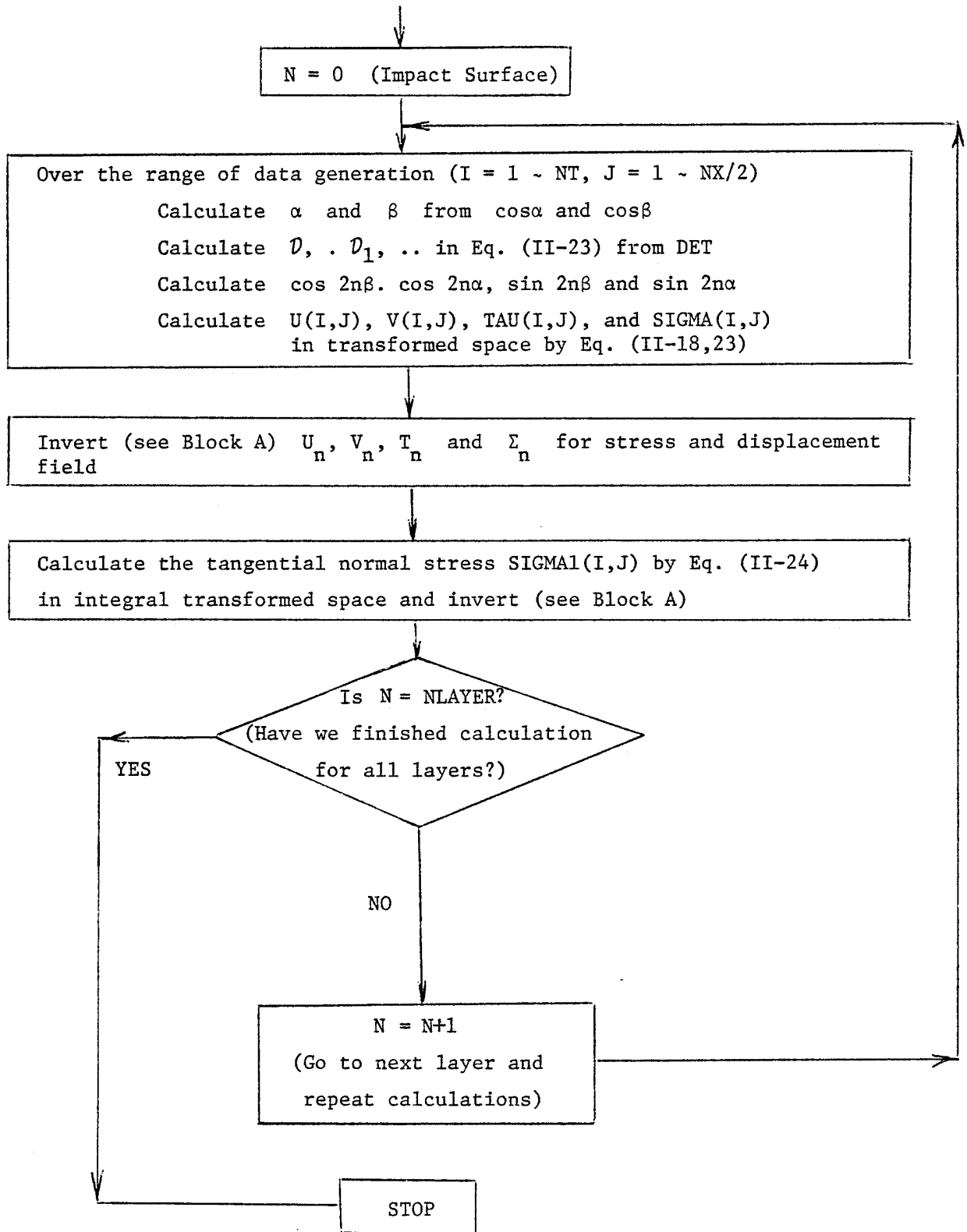


- (i) Calculate normalization units  
Space:  $UNITX = \text{DELTA}$  (Thickness of the plate)  
Time:  $UNITT = A/\sqrt{E_{66}/\text{RHO}}$  (Time required for the quasi-shear wave to travel the impact radius)
- (ii) Normalized all quantities by UNITT and UNITX
- (iii) Calculate integral limits ( $\omega_0$  and  $k_0$ ) in Fast Fourier Transform

Calculate  $QO(I,J)$ ,  $CBX(I,J)$ ,  $CAX(I,J)$ ,  $XIBX(I,J)$ ,  $YIAX(I,J)$  ....  
 $Y3AX(I,J)$ , over a half of the range of integration  
( $I = 1 \sim NT$ ,  $J = 1, NX/2$ ).

$QO$ : Impact function given in Eq. (II-22)  
 $CBX, CAX$ :  $\cos\beta$  and  $\cos\alpha$  in Eq. (II-16,17) by DPHASE  
 $X1BX, X2BX$  ...:  $X_1(\beta), X_2(\beta)$  in Eq. (II-18,19) by DELL  
 $Y1AX, Y2AX$  ...:  $Y_1(\alpha), Y_2(\alpha)$  in Eq. (II-18,19) by DELL

Invert (see Block A) and check the impact function  $\sigma_0$  with  $QO$



Block A Inversion

- (i) Data  $xx(I,J)$  in integral transformed space are generated for a half of the inverse transform range:  $I = 1 \sim NT$ ,  
 $J = 1 \sim NX/2$
- (ii) Generate full data over  $J = 1 \sim NX$  by FLIP  
Symmetric flip:  $V(I,J)$ ,  $SIGMA(I,J)$ ,  $SIGMA1(I,J)$ ,  $QO(I,J)$   
Antisymmetric flip:  $U(I,J)$ ,  $TAU(I,J)$
- (iii) Invert them for displacement and stress fields by FOURT
- (iv) Take care of the coordinate shifts and multiplication factors in FOURT by FACT
- (v) Print out by MAP







C  
C DET: CALCULATE D,D1,.. IN EQ(II-23)  
C  
C FLIP: THIS PROGLAM GENERATES ONLY A HALF OF THE DATA (X>0) DUE  
C TO SYMMETRY AND FLIP THEM TO FIND FULL DATA ALONG X AXIS  
C  
C MAP: CONTROLLS THE PRINTOUT FORMAT  
C  
C FACT: TAKES CARES OF THE COORDINATE SHIFT AND MULTIPLICATION FACTORS  
C IN FOURIER-LAPLACE DCUBLE INTEGRAL TRANSFORMS  
C  
C FOURT: IS FAST FOURIER TRANSFORM ROUTINE SUPPLIED BY IBM  
C  
C

C\*\*\*\*\*  
C  
C

IMPLICIT REAL\*8(K)  
COMPLEX DATA(32,64),SUB(32,32),CAX(32,32),CBX(32,32),Q0(32,32)  
COMPLEX SIGMA(32,32),SIGMA1(32,32),TAU(32,32)  
COMPLEX U(32,32),V(32,32),VX(32,32)  
COMPLEX Y1AX(32,32),Y2AX(32,32),Y3AX(32,32)  
COMPLEX X1BX(32,32),X2BX(32,32),X3BX(32,32)  
DIMENSION NN(2),MM(32)

REAL\*8 C11,C12,C22,C66,CHAT,E66,V66,PI,P2  
REAL\*8 DCOS,DSIN,DBLE,DSQRT,DFLOAT,DLOG  
REAL\*8 DELTA,D,RHO,FN,F,KX(32),B,TAU0,A,DX,DT,UNITT,UNITX  
REAL\*8 Q,OMEGA0,BL,C0

COMPLEX\*16 CDEXP,CDLOG,CDSQRT,CDCOS,CDSIN  
COMPLEX\*16 BETA,ALPHA,CB,CA,SB,SA,C2NB,C2NA,S2NB,S2NA  
COMPLEX\*16 S,SI,S2,D1,D2,D3,D4  
COMPLEX\*16 Y1A,Y2A,Y3A,X1B,X2B,X3B

COMMON Y1A,Y2A,Y3A,X1B,X2B,X3B,D1,D2,D3,D4,C11,C12,C22,C66,CHAT  
EQUIVALENCE (DELTA,D)  
EQUIVALENCE (DATA(1,1),SUB(1,1))

SI=(0.D 00,1.D 00)  
PI=3.1415926536D 00  
P2=PI\*2.D 00  
INDEX=0  
INDEX=1

WRITE(6,4)  
4 FORMAT('1'//////////20X,'\*\*\* WAVE PROPAGATION IN COMPOSITE P  
1LATE \*\*\*')

```

WRITE(6,5)
5  FORMAT(22X,'GRAPHITE FIBER(55%)-EPOXY MATRIX COMPOSITE')
C
C*****
C
C
C  INPUT DATA FOR ELASTIC PROPERTIES OF COMPOSITE PLATE
C  ALL THE DATA ARE SUPPLIED IN PSI UNIT BUT NORMALIZED BY C66
C  WHICH IS CONSTANT REGARDLESS THE LAYUP ANGLE
C
C
C  READ (5,101) IANGLE,C11,C12,C22,C66
101  FORMAT(I10,4D15.7)
      CHAT=C11-C12**2/C22
      IF (IANGLE.EQ.100) GO TO 200
      WRITE(6,102) IANGLE,C11,C12,C22,C66
102  FORMAT(/ 20X,'LAYUP ANGLE=',I3,3X,'DEGREE'
$ /20X,'C(1,1)=' ,D12.5,' PSI',10X,'C(1,2)=' ,D12.5,' PSI'
$ /20X,'C(2,2)=' ,D12.5,' PSI',10X,'C(6,6)=' ,D12.5,' PSI'//)
      GO TO 201
200  CONTINUE
      WRITE(6,210) C11,C12,C22,C66
210  FORMAT(/20X,' PLATE IS ISOTROPIC WITH POISSON''S RATIO 1/4'
$ /20X,'C(1,1)=' ,D12.5,' PSI',10X,'C(1,2)=' ,D12.5,' PSI'
$ /20X,'C(2,2)=' ,D12.5,' PSI',10X,'C(6,6)=' ,D12.5,' PSI'//)
201  CONTINUE
C
      E66=C66*6892.2D 00
      C11=C11/C66
      C12=C12/C66
      C22=C22/C66
      CHAT=CHAT/C66
      C66=1.D 00
C
C***** WITH CORRECTION FACTOR
C
      C66=PI**2/12.D 00
      C22=C22*C66
C
C
C  -----
C
C  INPUT DATA FOR GEOMETRY OF COMPOSITE PLATE
C  ALL THE DATA ARE FIRST SUPPLIED IN CGS UNIT BUT CONVERTED INTO MKS UNIT
C
C
C  READ(5,120) NLAYER,DELTA,RHO
120  FORMAT(I10,2D20.10)

```

```

NL1=N LAYER+1
FN=DFLOAT(N LAYER)
B=DELTA/FN
WRITE(6,121) DELTA,RHO,N LAYER,B
121  FORMAT(20X,'TOTAL THICKNESS OF COMPOSITE PLATE ; DELTA=',F10.5,
$ ' CM'/
$ 20X,'DENSITY OF COMPOSITE ; RHO=',F10.5,' GR/CM**3'/
$ 20X, 'PLATE IS MADE OF ',I3,3X, ' IDENTICAL LAYERS'/
$ 20X,'LAYER THICKNESS ; 2B=',F10.5,' CM'//)

```

```

C
DELTA=DELTA/100.D 00
RHO=RHO*1000.D 00
B=B/200.D 00

```

```

C
C
C -----

```

```

C INPUT DATA FOR IMPACT

```

```

C
C
60  READ(5,60) NA,TAUO
    FORMAT(I10,D20.10)
111 READ(5,111) NX,NT,NXIMP,NTIMP
    FORMAT(4I10)

```

```

C
112 WRITE(6,112) NX,NXIMP,NT,NTIMP
    FORMAT(20X,'TOTAL SPACE STEPS; NX=',I3,5X,'WITH',I3,2X,'STEPS FOR
$ CONTACT RADIUS'/
$ 20X,'TOTAL TIME STEPS ; NT=',I3,5X,'WITH',I3,2X,'STEPS FOR CONTAC
$ T TIME'//)

```

```

C
A=DFLOAT(NA)*DELTA
DX=A/DFLOAT(NXIMP)
DT=TAUO/DFLOAT(NTIMP)

```

```

C
61  WRITE(6,61) A,DX,TAUO,DT
    FORMAT(20X,'CONTACT RADIUS ; A=',D12.5,' M'/
$ 20X,'SPACE STEP ; DX=',D12.5,' M'/
$ 20X,'CONTACT TIME ; TAUO=',D12.5,' SECOND'/
$ 20X,'TIME STEP ; DT=',D12.5,' SECOND'//)

```

```

C
C
C -----

```

```

C NORMALIZE ALL THE INPUT DATA

```

```

C
V66=DSQRT(E66/RHO)

```

```

UNITT=A/V66
UNITX=DELTA
F=D*D*RHO/(E66*UNITT**2)/2.D 00/FN

```

C

```

NX2=NX/2
NN(1)=NT
NN(2)=NX
DX=DX/UNITX
DT=DT/UNITT
KO=PI/DX
OMEGA0=PI/DT
BL=A/D
CO=DLOG(1.D 06*2.D 00*DT)/(3.D 00*DT*DFLOAT(NT))

```

C

C

C

C\*\*\*\*\*

C

C

C

```

CALCULATE THE IMPACT INPUT FUNCTION Q0(I,J) IN EQ(II-22)
CALCULATE COS(BETA) AND COS(ALPHA) IN EQ(II-16) BY SUBROUTINE DPHASE
CALCULATE X1(BETA), Y1(ALPHA) ,.. BY SUBROUTINE DELL

```

C

C

```

DO 30 J=1,NX2
K=2.D 00*KO*(DFLOAT(J)-.5)/DFLOAT(NX)-KO
K2=K**2
KX(J)=K
Q=PI**2/DSQRT(P2)*DSIN(K*BL)/K/((K*BL)**2-PI**2)

```

C

```

DO 30 I=1,NT
S=CO+SI*OMEGA0*(1.D 00-(DFLOAT(I)-.5D 00)*2.D 00/DFLOAT(NT))
S2=S**2*F
Q0(I,J)=Q/2./S*(1.D 00-CDEXP(-S*TAUO/UNITT))*(P2*UNITT)**2
$ /((S*TAUO)**2+(P2*UNITT)**2)

```

C

```

CALL DPHASE (K,S2,CB,CA,NLAYER)
CBX(I,J)=CB
CAX(I,J)=CA

```

C

```

CALL DELL(K,S2,CB,CA,SI,NLAYER)
Y1AX(I,J)=Y1A
Y2AX(I,J)=Y2A
Y3AX(I,J)=Y3A
X1BX(I,J)=X1B
X2BX(I,J)=X2B
X3BX(I,J)=X3B

```

C

31 RELEASE 2.0

MAIN

DATE = 77139

21/11/39

30 CONTINUE

C  
C  
C

C\*\*\*\*\*

C  
C

REPRODUCE THE IMPACT FUNCTION TO CHECK INPUT

C

DO 300 I=1,NT  
DO 300 J=1,NX2  
300 SUB(I,J)=QO(I,J)  
CALL FLIP(DATA,NX,NX2,NT,+1)  
CALL FOURT(DATA,NN,2,-1,1,0)  
CALL FACT(DATA,NX,NT,CO,OMEGA0,KO,PI,SI)  
WRITE(6,301)

301 FORMAT('1'//////////20X, '\*\*\* REPRODUCTION OF IMPACT FUNCTIO  
IN \*\*\*')

CALL MAP(DATA,NX,NT,NX2,MM,INDEX)

C  
C  
C

C\*\*\*\*\*

C  
C

THIS IS THE MAIN PART OF THE PROGRAM.

C

CALCULATE D(BETA),DBAR(ALPHA),.. IN EQ(II-19,20) BY SUBROUTINE DET  
NEXT CALCULATE 1,V,.. IN EQ(II-18) IN TRANSFORMED SPACE  
AND FLIP TO FIND FULL DATA AND INVERT THEM BY MEANS OF FOURT.  
REPEAT THIS PROCESS FROM N=0 TO N LAYER

C

DO 11 N=1,NL1  
NY=N-1  
NYY=NY-1

C  
C  
C

-----

C

GENERATION OF DATA FOR DISPLACEMENTS AND STRESS IN TRANSFORMED SPACE

C

DO 100 J=1,NX2  
DO 100 I=1,NT  
CB=CBX(I,J)  
CA=CAX(I,J)  
X1B=X1BX(I,J)  
X2B=X2BX(I,J)  
X3B=X3BX(I,J)

31 RELEASE 2.0

MAIN

DATE = 77139

21/11/39

Y1A=Y1AX(I,J)  
Y2A=Y2AX(I,J)  
Y3A=Y3AX(I,J)

C

SB=CDSQRT(1.D 00-CB\*\*2)  
SA=CDSQRT(1.D 00-CA\*\*2)  
BETA=CB+SI\*SB  
ALPHA=CA+SI\*SA  
BETA=CDLOG(BETA)/SI  
ALPHA=CDLOG(ALPHA)/SI

C

CALL DET(ALPHA,BETA,SI, FN)  
C2NB=CDCOS(2.D 00\*BETA\*DFLOAT(NY))  
S2NB=CDSIN(2.D 00\*BETA\*DFLOAT(NY))  
C2NA=CDCOS(2.D 00\*ALPHA\*DFLOAT(NY))  
S2NA=CDSIN(2.D 00\*ALPHA\*DFLOAT(NY))

C

U(I,J)=(X1B\*(D1\*C2NB+SI\*D2\*S2NB)+Y1A\*(D4\*C2NA+SI\*D3\*S2NA))\*Q0(I,J)  
V(I,J)=(X2B\*(D2\*C2NB+SI\*D1\*S2NB)+Y2A\*(D3\*C2NA+SI\*D4\*S2NA))\*Q0(I,J)  
TAU(I,J)=(X3B\*(D2\*C2NB+SI\*D1\*S2NB)+(D3\*C2NA+SI\*D4\*S2NA))\*Q0(I,J)  
SIGMA(I,J)={(D1\*C2NB+SI\*D2\*S2NB)+Y3A\*(D4\*C2NA+SI\*D3\*S2NA))\*Q0(I,J)  
100 CONTINUE

100

C

C

C

C

C

INVERSION AND PRINTOUT OF HORIZONTAL DISPLACEMENT UN(I,J)

C

DO 10 I=1,NT  
DO 10 J=1,NX2  
10 SUB(I,J)=U(I,J)  
CALL FLIP(DATA,NX,NX2,NT,-1)  
CALL FOURT(DATA,NN,2,-1,1,0)  
CALL FACT(DATA,NX,NT,CO,OMEGA0,KO,PI,SI)  
WRITE(6,981) NY  
981 FORMAT('1'//////////20X,'U',I3)  
CALL MAP(DATA,NX,NT,NX2,MM,INDEX)

C

C

C

C

INVERSION AND PRINTOUT OF VERTICAL DISPLACEMENT VN(I,J)

C

DO 20 I=1,NT  
DO 20 J=1,NX2  
20 SUB(I,J)=V(I,J)  
CALL FLIP(DATA,NX,NX2,NT,+1)  
CALL FOURT(DATA,NN,2,-1,1,0)

20

```

CALL FACT(DATA,NX,NT,CO,OMEGAO,KO,PI,SI)
WRITE(6,982) NY
982  FORMAT('1'//////////20X,'V',I3)
CALL MAP(DATA,NX,NT,NX2,MM,INDEX)

```

C  
C  
C  
C  
C  
C

-----  
INVERSION AND PRINTOUT OF SHEAR STRESS TAU(I,J)

```

DO 35 I=1,NT
DO 35 J=1,NX2
35  SUB(I,J)=TAU(I,J)
CALL FLIP(DATA,NX,NX2,NT,-1)
CALL FOURT(DATA,NN,2,-1,1,0)
CALL FACT(DATA,NX,NT,CO,OMEGAO,KO,PI,SI)
WRITE(6,983) NY
983  FORMAT('1'//////////20X,'TAU',I3)
CALL MAP(DATA,NX,NT,NX2,MM,INDEX)

```

C  
C  
C  
C  
C  
C

-----  
INVERSION AND PRINTOUT OF NORMAL STRESS SIGMA(I,J)

```

DO 40 I=1,NT
DO 40 J=1,NX2
40  SUB(I,J)=SIGMA(I,J)
CALL FLIP(DATA,NX,NX2,NT,+1)
CALL FOURT(DATA,NN,2,-1,1,0)
CALL FACT(DATA,NX,NT,CO,OMEGAO,KO,PI,SI)
WRITE(6,984) NY
984  FORMAT('1'//////////20X,'SIGMA',I3)
CALL MAP(DATA,NX,NT,NX2,MM,INDEX)

```

C  
C  
C  
C  
C  
C

-----  
INVERSION AND PRINTOUT OF TANGENTIAL NORMAL STRESS SIGMA1(I,J)

```

IF (NY.EQ.0) GO TO 160
DO 50 I=1,NT
DO 50 J=1,NX2
50  SUB(I,J)=SIGMA1(I,J)+FN*C12*V(I,J)
CALL FLIP(DATA,NX,NX2,NT,+1)
CALL FOURT(DATA,NN,2,-1,1,0)
CALL FACT(DATA,NX,NT,CO,OMEGAO,KO,PI,SI)
WRITE(6,985) NY

```

31 RELEASE 2.0

MAIN

DATE = 77139

21/11/39

985 FORMAT('1'//////////20X,'SIGMA1',I3)  
CALL MAP(DATA,NX,NT,NX2,MM,INDEX)

C  
IF (NY.EQ.NLAYER) GO TO 70  
DO 51 I=1,NT

DO 51 J=1,NX2  
51 SIGMA1(I,J)=-SI\*KX(J)\*C11\*U(I,J)-FN\*C12\*VX(I,J)  
GO TO 80

C  
160 CONTINUE  
DO 161 I=1,NT  
DO 161 J=1,NT  
161 SIGMA1(I,J)=-SI\*KX(J)\*C11\*U(I,J)-FN\*C12\*V(I,J)  
GO TO 80

C  
70 CONTINUE  
DO 71 I=1,NT  
DO 71 J=1,NX2  
71 SUB(I,J)=-SI\*KX(J)\*C11\*U(I,J)+FN\*C12\*(V(I,J)-VX(I,J))  
CALL FLIP(DATA,NX,NX2,NT,+1)  
CALL FOURT(DATA,NN,2,-1,1,0)  
CALL FACT(DATA,NX,NT,CO,OMEGAO,KO,PI,SI)  
WRITE(6,985) NY  
CALL MAP(DATA,NX,NT,NX2,MM,INDEX)  
GO TO 90

C  
80 CONTINUE  
DO 81 I=1,NT  
DO 81 J=1,NX2  
81 VX(I,J)=V(I,J)

C  
90 CONTINUE

C  
C  
11 CONTINUE

C  
C\*\*\*\*\*

C  
C  
C  
C  
C  
STOP  
END

```

C
C
C*****
C
C   THIS SUBROUTINE CALCULATES THE PHASE SHIFT BETA AND ALPHA FROM
C   EQ(II-15,16) OF THE PRESENT REPORT WITH GIVEN VALUES OF
C   WAVE NUMBER K AND LAPLACE TRANSFORM VARIABLE S
C
C   CA=COS(ALPHA)
C   CB=COS(BETA)
C*****
C
C
C   SUBROUTINE DPHASE(K,S ,CB,CA,NLAYER)
C   IMPLICIT COMPLEX*16(A,X,Y)
C   COMPLEX*16 ROOTP,ROOTM,S,CDSQRT,DCMPLX,DCB,DCA
C   COMPLEX*16 D1,D2,D3,D4
C   COMPLEX*16 CB,CA
C   REAL*8 C11,C12,C22,C66,CHAT,N,K2,DFLOAT,DBLE,K
C
C   COMMON Y1A,Y2A,Y3A,X1B,X2B,X3B,D1,D2,D3,D4,C11,C12,C22,C66,CHAT
C   ROOTP(AA,AB,AC)=(-AB+CDSQRT(AB**2-4.D 00*AA*AC))/(2.D 00*AA)
C   ROOTM(AA,AB,AC)=(-AB-CDSQRT(AB**2-4.D 00*AA*AC))/(2.D 00*AA)
C
C   N=DFLOAT(NLAYER)*2.D 00
C   K2=K**2
C
C   A1=(K2*C11/N+S)*(K2*C66/N+S)
C   A2=K2*CHAT/(3.D 00*N)+N*C66+S/3.D 00-C12*C66*K2/(3.D 00*N*C22)
C   A2=A2*(-C12*K2/(3.D 00*N)+N*C22+S/3.D 00)
C   A3=N*C22+S/3.D 00-K2*C12*(C66*K2/N+S)/(9.D 00*N**2*C22)+C66*K2/
$   (3.D 00*N)
C   A3=A3*(C11*K2/N+S)-K2*(C12+C66)**2
C   A3=A3+(C66*K2/N+S)*(CHAT*K2/(3.D 00*N)+N*C66+S/3.+C12**2*K2/
$   (3.D 00*C22))
C
C   AA=A1+A2-A3
C   AB=A3-2.D 00*A2
C   AC=A2
C   DCB=ROOTP(AA,AB,AC)
C   DCA=ROOTM(AA,AB,AC)
C
C   CB=CDSQRT(DCB)
C   CA=CDSQRT(DCA)
C   RETURN
C   END

```

```

C
C
C *****
C THIS SUBROUTINE CALCULATES DELTA(BETA), DELTABAR(ALPHA), DELTA1(BETA),...
C IN EQ(II-19,20) AND X1(BETA), Y1(ALPHA) IN EQ(II-18,19,20)
C
C X1B=X1(BETA), Y1A=Y1(ALPHA)
C
C :
C
C *****
C
C SUBROUTINE DELL (K,S,CB,CA,SI,NLAYER)
C IMPLICIT REAL*8(K),COMPLEX*16(S,X,D,Y)
C COMPLEX*16 SB,CB,CDSQRT,SA,CA
C REAL*8 N,DFLOAT
C REAL*8 C11,C12,C22,C66,CHAT
C
C COMMON Y1A,Y2A,Y3A,X1B,X2B,X3E,D1,D2,D3,D4,C11,C12,C22,C66,CHAT
C
C K2=K**2
C N=DFLOAT(NLAYER)
C
C
C S11=S+C11*K2/2.D 00/N
C S66=S+C66*K2/2.D 00/N
C SA=CDSQRT(1.D 00-CA**2)
C SB=CDSQRT(1.D 00-CB**2)
C
C
C DELTAB=CB**3*S11*S66+SB**2*CB*(-C66*(C66+C12)*K2
$ +S66*(S/3.D 00+CHAT*K2/6.D 00/N+2.D 00*N*C66))
C DEL1B=SI*K*SB**2*CB*(-C66-C12+C12*S66/6.D 00/N/C22)
C DEL2B=SI*SB**3*(C12*C66*K2/6.D 00/N/C22-S/3.D 00
$ -CHAT*K2/6.D 00/N-2.D 00*N*C66)-SI*CB**2*SB*S11
C DEL3B=CB**2*SB*(C12*K*S11*S66/6.D 00/N/C22-C66*K*S11)
$ +SB**3*(C12*K*(S/3.D 00+CHAT*K2/6.D 00/N+2.D 00*N*C66)
$ -C12**2*C66*K*K2/6.D 00/N/C22)
C
C DELTAA=SI*CA**2*SA*{(C12+C66)*C66*K2-S66*(S/3.D 00+CHAT*K2
$ /6.D 00/N+2.D 00*N*C66+C12**2*K2/6.D 00/N/C22)}
$ +SI*SA**3*(S/3.D 00+2.D 00*N*C22)*(C66*C12*K2/6.D 00/N/C22
$ -S/3.D 00-CHAT*K2/6.D 00/N-2.D 00*N*C66)
C DEL1A=SA**2*CA*(-K2*C12*S66/6.D 00/6.D 00/N**2/C22+C66*K2/6.D 00/N
$ +S/3.D 00+2.D 00*N*C22)+CA**3*S66
C DEL2A=CA**2*SA*K*(C12+C66)

```

V G1 RELEASE 2.0

DELL

DATE = 77139

21/11/39

\$ +SA\*\*3\*(K/6.D 00/N\*(S/3.D 00+CHAT\*K2/6.D 00/N+2.D 00\*N\*C66)  
\$ -C66\*C12\*K\*\*3/36.D 00/C22/N\*\*2)  
DEL3A=-SI\*CA\*\*3\*C12\*K\*S66+SI\*SA\*\*2\*CA\*(C66\*K\*(S/3.D 00+2.D 00\*N  
\$ \*C22+C66\*K2/6.D 00/N)-K/6.D 00/N\*S66\*(S/3.D 00+CHAT\*K2/6.D 00  
\$ /N+2.D 00\*N\*C66))

C  
C

X1B=-DEL1B/DELTAB  
X2B=-DEL2B/DELTAB  
X3B=-DEL3B/DELTAB  
Y1A=-DEL1A/DELTA  
Y2A=-DEL2A/DELTA  
Y3A=-DEL3A/DELTA

C

RETURN  
END

```

C
C
C*****
C THIS SUBROUTINE CALCUALTES D,D1,.. IN EQ(II-23) OF THE PRESENT REPORT
C*****
C
C

```

```

SUBROUTINE DET(ALPHA,BETA,SI, FN)
IMPLICIT COMPLEX*16(D,X,Y)
COMPLEX*16 ALPHA,BETA
COMPLEX*16 C2NB,C2NA,S2NA,S2NB,CDSQRT,SI
REAL*8 FN
REAL*8 C11,C12,C22,C66,CHAT

```

```

COMMON Y1A,Y2A,Y3A,X1B,X2B,X3B,D1,D2,D3,D4,C11,C12,C22,C66,CHAT

```

```

C2NA=CDCOS(2.D 00*ALPHA*FN)
S2NA=CDSIN(2.D 00*ALPHA*FN)
C2NB=CDCOS(2.D 00*BETA*FN)
S2NB=CDSIN(2.D 00*BETA*FN)

```

```

X=Y3A*X3B*(1.D 00-C2NA*C2NB)
Y=X3B*Y3A*S2NB*C2NA-S2NA*C2NB

```

```

D=-2.D 00*X+(1.D 00+X3B**2*Y3A**2)*S2NA*S2NB
D1=-(X-S2NA*S2NB)
D2=-SI*Y
D3=SI*Y*X3B
D4=X3B*(X3B*Y3A*S2NB*S2NA+C2NA*C2NB-1.D 00)

```

```

D1=D1/D
D2=D2/D
D3=D3/D
D4=D4/D

```

```

RETURN
END

```

```
C
C
C*****
C
C
C   ALL THE DATA IN THE MAIN PROGRAM ARE GENERATED FOR ONLY HALF OF THE
C   PLATE WHEN X>0. DUE TO SYMMETRY OF THE PROBLEM WE CAN GENERATE
C   THE FULL DATA BY FLIPPING THE HALF OF THE DATA.
C
C*****
C
C
C   SUBROUTINE FLIP(DATA,NX,NX2,NT,INDEX)
C   COMPLEX DATA(NT,NX)
C   DO 10 J=1,NX2
C   JJ=NX+1-J
C   DO 10 I=1,NT
C   DATA(I,JJ)=FLOAT(INDEX)*DATA(I,J)
10 CONTINUE
C   RETURN
C   END
```

```
C
C
C*****
C
C
C   THIS SUBROUTINE TAKES CARE OF THE COORIDINATE SHIFT IN
C   LAPLACE AND FOURIER TRANSFORM IN THE PROCESS OF APPLYING
C   FAST FOURIER TRANSFORM ALGORITHM
C
C*****
C
C
C   SUBROUTINE FACT(DATA,NX,NT,CO,WO,KO,PI,SI)
C   COMPLEX DATA(NT,NX)
C   COMPLEX*16 CDEXP,SI
C   REAL*8 DEXP,DSQRT,DFLOAT
C   REAL*8 CO,WO,PI,KO,FT,FX
C   FX=DFLOAT(NX)
C   FT=DFLOAT(NT)
C   NX2=NX/2
C
C   DO 10 L=1,NX2
C   DO 10 M=1,NT
C   DATA(M,L)=DATA(M,L)*4.D 00*KO*WO/(DSQRT(2.D 00*PI)**3*FT*FX)
C   $ *DEXP(CO*PI*DFLOAT(M-1)/WO)*CDEXP(SI*PI*(1.D 00-1.D 00/FX)
C   $ *DFLOAT(L-1))*CDEXP(SI*PI*(1.D 00-1.D 00/FT)*DFLOAT(M-1))
10  CONTINUE
C   RETURN
C   END
```

```
C
C*****
C
C THIS SUBROUTINE CONTROLS THE FORMAT OF THE PRINTOUT OF THE FINAL RESULTS
C
C IF INDEX=0: ALL THE NUMERICAL VALUES ARE PRINTED
C IF INDEX=1: THE MAXIMUM AND NORMALIZED VALUES ARE PRINTED
C
C*****
C
C
C SUBROUTINE MAP(DATA,NX,NT,NX2,MM,INDEX)
C COMPLEX DATA(NT,NX),S
C DIMENSION MM(NX2)
C IF (INDEX.EQ.1) GO TO 200
C DO 44 IQ=1,NT
44 WRITE(6,15) IQ,(DATA(IQ,I),I=1,NX2)
15 FORMAT(I5,2E14.5,2X,2E14.5,2X,2E14.5,2X,2E14.5/
$ 3(5X,2E14.5,2X,2E14.5,2X,2E14.5,2X,2E14.5//)
$ 4(5X,2E14.5,2X,2E14.5,2X,2E14.5,2X,2E14.5//))
200 CONTINUE
C*** FIND THE MAXIMUM VALUE
RS= 1.E-3
NT5=NT-5
NX5=NX2-5
DO 114 I=1,NT5
DO 114 J= 1,NX5
S= DATA(I,J)
TP= REAL(S)/RS
IF (ABS(TP).LT.1.) GO TO 114
RS= REAL(S)
114 CONTINUE
WRITE (6,516) RS
516 FORMAT(20X,'*** MAXIMUM VALUE =',E12.5,' ***'//)
DO 119 I=1,NT5
DO 113 J=1,NX5
S= DATA(I,J)
113 MM(J)= REAL(S)/RS*100
WRITE(6,515) (MM(KIM),KIM=1,27)
119 CONTINUE
515 FORMAT(10X,27I3)
RETURN
END
```

1 RELEASE 2.0

FOURT

DATE = 77139

21/11/39

```
SUBROUTINE FOURT(DATA,NN,NDIM,ISIGN,IFORM,WORK)
DIMENSION DATA(1),NN(1),IFACT(32),WORK(1)
TWOPI=6.283185307
IF(NDIM-1)920,1,1
1  NTOT=2
DO 2 IDIM=1,NDIM
IF(NN(IDIM))920,920,2
2  NTOT=NTOT*NN(IDIM)
C
C  MAIN LOOP FOR EACH DIMENSION
C
NP1=2
DO 910 IDIM=1,NDIM
N=NN(IDIM)
NP2=NP1*N
IF(N-1)920,900,5
C
C  FACTOR N
C
5  M=N
NTWO=NP1
IF=1
IDIV=2
10  IQUOT=M/IDIV
IREM=M-IDIV*IQUOT
IF(IQUOT-IDIV)50,11,11
11  IF(IREM)20,12,20
12  NTWO=NTWO+NTWO
M=IQUOT
GO TO 10
20  IDIV=3
30  IQUOT=M/IDIV
IREM=M-IDIV*IQUOT
IF(IQUOT-IDIV)60,31,31
31  IF(IREM)40,32,40
32  IFACT(IF)=IDIV
IF=IF+1
M=IQUOT
GO TO 30
40  IDIV=IDIV+2
GO TO 30
50  IF(IREM)60,51,60
51  NTWO=NTWO+NTWO
GO TO 70
60  IFACT(IF)=M
C
C  SEPARATE FOUR CASES--
C  1. COMPLEX TRANSFORM OR REAL TRANSFORM FOR THE 4TH, 5TH,ETC.
```

```
FFTT000
FFTT077
FFTT078
FFTT079
FFTT080
FFTT081
FFTT082
FFTT083
FFTT084
FFTT085
FFTT086
FFTT087
FFTT088
FFTT089
FFTT090
FFTT091
FFTT092
FFTT093
FFTT094
FFTT095
FFTT096
FFTT097
FFTT098
FFTT099
FFTT100
FFTT101
FFTT102
FFTT103
FFTT104
FFTT105
FFTT106
FFTT107
FFTT108
FFTT109
FFTT110
FFTT111
FFTT112
FFTT113
FFTT114
FFTT115
FFTT116
FFTT117
FFTT118
FFTT119
FFTT120
FFTT121
FFTT122
FFTT123
```

1 RELEASE 2.0

FOURT

DATE = 77139

21/11/39

```

C          DIMENSIONS. FFTT124C
C          2. REAL TRANSFORM FOR THE 2ND OR 3RD DIMENSION. METHOD-- FFTT125C
C          TRANSFORM HALF THE DATA, SUPPLYING THE OTHER HALF BY CON- FFTT126C
C          JUGATE SYMMETRY. FFTT127C
C          3. REAL TRANSFORM FOR THE 1ST DIMENSION, N ODD. METHOD-- FFTT128C
C          TRANSFORM HALF THE DATA AT EACH STAGE, SUPPLYING THE OTHER FFTT129C
C          HALF BY CONJUGATE SYMMETRY. FFTT130C
C          4. REAL TRANSFORM FOR THE 1ST DIMENSION, N EVEN. METHOD-- FFTT131C
C          TRANSFORM A COMPLEX ARRAY OF LENGTH N/2 WHOSE REAL PARTS FFTT132C
C          ARE THE EVEN NUMBERED REAL VALUES AND WHOSE IMAGINARY PARTS FFTT133C
C          ARE THE ODD NUMBERED REAL VALUES. SEPARATE AND SUPPLY FFTT134C
C          THE SECOND HALF BY CONJUGATE SYMMETRY. FFTT135C
C          FFTT136C
70      NON2=NP1*(NP2/NTWO) FFTT137C
        ICASE=1 FFTT138C
        IF(IDIM-4)71,90,90 FFTT139C
71      IF(IFORM)72,72,90 FFTT140C
72      ICASE=2 FFTT141C
        IF(IDIM-1)73,73,90 FFTT142C
73      ICASE=3 FFTT143C
        IF(NTWO-NP1)90,90,74 FFTT144C
74      ICASE=4 FFTT145C
        NTWO=NTWO/2 FFTT146C
        N=N/2 FFTT147C
        NP2=NP2/2 FFTT148C
        NTOT=NTOT/2 FFTT149C
        I=3 FFTT150C
        DO 80 J=2,NTOT FFTT151C
          DATA(J)=DATA(I) FFTT152C
80      I=I+2 FFTT153C
90      I1RNG=NP1 FFTT154C
        IF(ICASE-2)100,95,100 FFTT155C
95      I1RNG=NP0*(1+NPREV/2) FFTT156C
C          FFTT157C
C          SHUFFLE ON THE FACTORS OF TWO IN N. AS THE SHUFFLING FFTT158C
C          CAN BE DONE BY SIMPLE INTERCHANGE, NO WORKING ARRAY IS NEEDED FFTT159C
C          FFTT160C
100     IF(NTWO-NP1)600,600,110 FFTT161C
110     NP2HF=NP2/2 FFTT162C
        J=1 FFTT163C
        DO 150 I2=1,NP2,NON2 FFTT164C
          IF(J-I2)120,130,130 FFTT165C
120     I1MAX=I2+NON2-2 FFTT166C
        DO 125 I1=I2,I1MAX,2 FFTT167C
        DO 125 I3=I1,NTOT,NP2 FFTT168C
        J3=J+I3-I2 FFTT169C
        TEMPR=DATA(I3) FFTT170C
        TEMPI=DATA(I3+1) FFTT171C

```

1 RELEASE 2.0

FOURT

DATE = 77139

21/11/39

```
DATA(I3)=DATA(J3) FFTT172
DATA(I3+1)=DATA(J3+1) FFTT173
DATA(J3)=TEMPR FFTT174
125 DATA(J3+1)=TEMPI FFTT175
130 M=NP2HF FFTT176
140 IF(J-M)150,150,145 FFTT177
145 J=J-M FFTT178
M=M/2 FFTT179
IF(M-NON2)150,140,140 FFTT180
150 J=J+M FFTT181
C FFTT182
C MAIN LOOP FOR FACTORS OF TWO. PERFORM FOURIER TRANSFORMS OF FFTT183
C LENGTH FOUR, WITH ONE OF LENGTH TWO IF NEEDED. THE TWIDDLE FACTOR FFTT184
C W=EXP(ISIGN*2*PI*SQRT(-1)*M/(4*MMAX)). CHECK FOR W=ISIGN*SQRT(-1) FFTT185
C AND REPEAT FOR W=ISIGN*SQRT(-1)*CONJUGATE(W). FFTT186
C FFTT187
NON2T=NON2+NON2 FFTT188
IPAR=NTWO/NP1 FFTT189
310 IF(IPAR-2)350,330,320 FFTT190
320 IPAR=IPAR/4 FFTT191
GO TO 310 FFTT192
330 DO 340 I1=1,I1RNG,2 FFTT193
DO 340 J3=I1,NON2,NP1 FFTT194
DO 340 K1=J3,NTOT,NON2T FFTT195
K2=K1+NON2 FFTT196
TEMPR=DATA(K2) FFTT197
TEMPI=DATA(K2+1) FFTT198
DATA(K2)=DATA(K1)-TEMPR FFTT199
DATA(K2+1)=DATA(K1+1)-TEMPI FFTT200
DATA(K1)=DATA(K1)+TEMPR FFTT201
340 DATA(K1+1)=DATA(K1+1)+TEMPI FFTT202
350 MMAX=NON2 FFTT203
360 IF(MMAX-NP2HF)370,600,600 FFTT204
370 LMAX=MAX0(NON2T,MMAX/2) FFTT205
IF(MMAX-NON2)405,405,380 FFTT206
380 THETA=-TWOPI*FLOAT(NON2)/FLOAT(4*MMAX) FFTT207
IF(ISIGN)400,390,390 FFTT208
390 THETA=-THETA FFTT209
400 WR=COS(THETA) FFTT210
WI=SIN(THETA) FFTT211
WSTPR=-2.*WI*WI FFTT212
WSTPI=2.*WR*WI FFTT213
405 DO 570 L=NON2,LMAX,NON2T FFTT214
M=L FFTT215
IF(MMAX-NON2)420,420,410 FFTT216
410 W2R=WR*WR-WI*WI FFTT217
W2I=2.*WR*WI FFTT218
W3R=W2R*WR-W2I*WI FFTT219
```

1 RELEASE 2.0

FOURT

DATE = 77139

21/11/39

	W3I=W2R*WI+W2I*WR	FFTT2200
420	DO 530 I1=1,I1RNG,2	FFTT2210
	DO 530 J3=I1,NON2,NP1	FFTT2220
	KMIN=J3+IPAR*M	FFTT2230
	IF(MMAX-NGN2)430,430,440	FFTT2240
430	KMIN=J3	FFTT2250
440	KDIF=IPAR*MMAX	FFTT2260
450	KSTEP=4*KDIF	FFTT2270
	DO 520 K1=KMIN,NTOT,KSTEP	FFTT2280
	K2=K1+KDIF	FFTT2290
	K3=K2+KDIF	FFTT2300
	K4=K3+KDIF	FFTT2310
	IF(MMAX-NGN2)460,460,480	FFTT2320
460	U1R=DATA(K1)+DATA(K2)	FFTT2330
	U1I=DATA(K1+1)+DATA(K2+1)	FFTT2340
	U2R=DATA(K3)+DATA(K4)	FFTT2350
	U2I=DATA(K3+1)+DATA(K4+1)	FFTT2360
	U3R=DATA(K1)-DATA(K2)	FFTT2370
	U3I=DATA(K1+1)-DATA(K2+1)	FFTT2380
	IF(ISIGN)470,475,475	FFTT2390
470	U4R=DATA(K3+1)-DATA(K4+1)	FFTT2400
	U4I=DATA(K4)-DATA(K3)	FFTT2410
	GO TO 510	FFTT2420
475	U4R=DATA(K4+1)-DATA(K3+1)	FFTT2430
	U4I=DATA(K3)-DATA(K4)	FFTT2440
	GO TO 510	FFTT2450
480	T2R=W2R*DATA(K2)-W2I*DATA(K2+1)	FFTT2460
	T2I=W2R*DATA(K2+1)+W2I*DATA(K2)	FFTT2470
	T3R=WR*DATA(K3)-WI*DATA(K3+1)	FFTT2480
	T3I=WR*DATA(K3+1)+WI*DATA(K3)	FFTT2490
	T4R=W3R*DATA(K4)-W3I*DATA(K4+1)	FFTT2500
	T4I=W3R*DATA(K4+1)+W3I*DATA(K4)	FFTT2510
	U1R=DATA(K1)+T2R	FFTT2520
	U1I=DATA(K1+1)+T2I	FFTT2530
	U2R=T3R+T4R	FFTT2540
	U2I=T3I+T4I	FFTT2550
	U3R=DATA(K1)-T2R	FFTT2560
	U3I=DATA(K1+1)-T2I	FFTT2570
	IF(ISIGN)490,500,500	FFTT2580
490	U4R=T3I-T4I	FFTT2590
	U4I=T4R-T3R	FFTT2600
	GO TO 510	FFTT2610
500	U4R=T4I-T3I	FFTT2620
	U4I=T3R-T4R	FFTT2630
510	DATA(K1)=U1R+U2R	FFTT2640
	DATA(K1+1)=U1I+U2I	FFTT2650
	DATA(K2)=U3R+U4R	FFTT2660
	DATA(K2+1)=U3I+U4I	FFTT2670

1 RELEASE 2.0

FOURT

DATE = 77139

21/11/39

```
DATA(K3)=U1R-U2R FFTT2680
DATA(K3+1)=U1I-U2I FFTT2690
DATA(K4)=U3R-U4R FFTT2700
520 DATA(K4+1)=U3I-U4I FFTT2710
KMIN=4*(KMIN-J3)+J3 FFTT2720
KDIF=KSTEP FFTT2730
IF(KDIF-NP2)450,530,530 FFTT2740
530 CONTINUE FFTT2750
M=MMAX-M FFTT2760
IF(ISIGN)540,550,550 FFTT2770
540 TEMPR=WR FFTT2780
WR=-WI FFTT2790
WI=-TEMPR FFTT2800
GO TO 560 FFTT2810
550 TEMPR=WR FFTT2820
WR=WI FFTT2830
WI=TEMPR FFTT2840
560 IF(M-LMAX)565,565,410 FFTT2850
565 TEMPR=WR FFTT2860
WR=WR*WSTPR-WI*WSTPI+WR FFTT2870
570 WI=WI*WSTPR+TEMPR*WSTPI+WI FFTT2880
IPAR=3-IPAR FFTT2890
MMAX=MMAX+MMAX FFTT2900
GO TO 360 FFTT2910
C FFTT2920
C MAIN LOOP FOR FACTORS NOT EQUAL TO TWO. APPLY THE TWIDDLE FACTOR FFTT2930
C W=EXP(ISIGN*2*PI*SQRT(-1)*(J2-1)*(J1-J2)/(NP2*IFP1)), THEN FFTT2940
C PERFORM A FOURIER TRANSFORM OF LENGTH IFACT(IF), MAKING USE OF FFTT2950
C CONJUGATE SYMMETRIES. FFTT2960
C FFTT2970
600 IF(NTWO-NP2)605,700,700 FFTT2980
605 IFP1=NON2 FFTT2990
IF=1 FFTT3000
NP1HF=NP1/2 FFTT3010
610 IFP2=IFP1/IFACT(IF) FFTT3020
J1RNG=NP2 FFTT3030
IF(ICASE-3)612,611,612 FFTT3040
611 J1RNG=(NP2+IFP1)/2 FFTT3050
J2STP=NP2/IFACT(IF) FFTT3060
J1RG2=(J2STP+IFP2)/2 FFTT3070
612 J2MIN=1+IFP2 FFTT3080
IF(IFP1-NP2)615,640,640 FFTT3090
615 DO 635 J2=J2MIN,IFP1,IFP2 FFTT3100
THETA=-TWOPI*FLOAT(J2-1)/FLOAT(NP2) FFTT3110
IF(ISIGN)625,620,620 FFTT3120
620 THETA=-THETA FFTT3130
625 SINTH=SIN(THETA/2.) FFTT3140
WSTPR=-2.*SINTH*SINTH FFTT3150
```

RELEASE 2.0

FOURT

DATE = 77139

21/11/39

	WSTPI=SIN(THETA)	FFTT3160
	WR=WSTPR+1.	FFTT3170
	WI=WSTPI	FFTT3180
	J1MIN=J2+IFP1	FFTT3190
	DO 635 J1=J1MIN,J1RNG,IFP1	FFTT3200
	I1MAX=J1+I1RNG-2	FFTT3210
	DO 630 I1=J1,I1MAX,2	FFTT3220
	DO 630 I3=I1,NTOT,NP2	FFTT3230
	J3MAX=I3+IFP2-NP1	FFTT3240
	DO 630 J3=I3,J3MAX,NP1	FFTT3250
	TEMPR=DATA(J3)	FFTT3260
	DATA(J3)=DATA(J3)*WR-DATA(J3+1)*WI	FFTT3270
630	DATA(J3+1)=TEMPR*WI+DATA(J3+1)*WR	FFTT3280
	TEMPR=WR	FFTT3290
	WR=WR*WSTPR-WI*WSTPI+WR	FFTT3300
635	WI=TEMPR*WSTPI+WI*WSTPR+WI	FFTT3310
640	THETA=-TWOPI/FLOAT(IFACT(IF))	FFTT3320
	IF(ISIGN)650,645,645	FFTT3330
645	THETA=-THETA	FFTT3340
650	SINTH=SIN(THETA/2.)	FFTT3350
	WSTPR=-2.*SINTH*SINTH	FFTT3360
	WSTPI=SIN(THETA)	FFTT3370
	KSTEP=2*N/IFACT(IF)	FFTT3380
	KRANG=KSTEP*(IFACT(IF)/2)+1	FFTT3390
	DO 698 I1=1,I1RNG,2	FFTT3400
	DO 698 I3=I1,NTOT,NP2	FFTT3410
	DO 690 KMIN=1,KRANG,KSTEP	FFTT3420
	J1MAX=I3+J1RNG-IFP1	FFTT3430
	DO 680 J1=I3,J1MAX,IFP1	FFTT3440
	J3MAX=J1+IFP2-NP1	FFTT3450
	DO 680 J3=J1,J3MAX,NP1	FFTT3460
	J2MAX=J3+IFP1-IFP2	FFTT3470
	K=KMIN+(J3-J1+(J1-I3)/IFACT(IF))/NP1HF	FFTT3480
	IF(KMIN-1)655,655,665	FFTT3490
655	SUMR=0.	FFTT3500
	SUMI=0.	FFTT3510
	DO 660 J2=J3,J2MAX,IFP2	FFTT3520
	SUMR=SUMR+DATA(J2)	FFTT3530
660	SUMI=SUMI+DATA(J2+1)	FFTT3540
	WORK(K)=SUMR	FFTT3550
	WORK(K+1)=SUMI	FFTT3560
	GO TO 680	FFTT3570
665	KCONJ=K+2*(N-KMIN+1)	FFTT3580
	J2=J2MAX	FFTT3590
	SUMR=DATA(J2)	FFTT3600
	SUMI=DATA(J2+1)	FFTT3610
	OLDSR=0.	FFTT3620
	OLDSI=0.	FFTT3630

1 RELEASE 2.0

FOURT

DATE = 77139

21/11/39

```
670 J2=J2-IFP2 FFTT364
    TEMPR=SUMR FFTT365
    TEMPI=SUMI FFTT366
    SUMR=TWOWR*SUMR-OLDSR+DATA(J2) FFTT367
    SUMI=TWOWR*SUMI-OLDSI+DATA(J2+1) FFTT368
    OLDSR=TEMPR FFTT369
    OLDSI=TEMPI FFTT370
    J2=J2-IFP2 FFTT371
    IF(J2-J3)675,675,670 FFTT372
675 TEMPR=WR*SUMR-OLDSR+DATA(J2) FFTT373
    TEMPI=WI*SUMI FFTT374
    WORK(K)=TEMPR-TEMPI FFTT375
    WORK(KCONJ)=TEMPR+TEMPI FFTT376
    TEMPR=WR*SUMI-OLDSI+DATA(J2+1) FFTT377
    TEMPI=WI*SUMR FFTT378
    WORK(K+1)=TEMPR+TEMPI FFTT379
    WORK(KCONJ+1)=TEMPR-TEMPI FFTT380
680 CONTINUE FFTT381
    IF(KMIN-1)685,685,686 FFTT382
685 WR=WSTPR+1. FFTT383
    WI=WSTPI FFTT384
    GO TO 690 FFTT385
686 TEMPR=WR FFTT386
    WR=WR*WSTPR-WI*WSTPI+WR FFTT387
    WI=TEMPR*WSTPI+WI*WSTPR+WI FFTT388
690 TWOWR=WR+WR FFTT389
    IF(ICASE-3)692,691,692 FFTT390
691 IF(IFP1-NP2)695,692,692 FFTT391
692 K=1 FFTT392
    I2MAX=I3+NP2-NP1 FFTT393
    DO 693 I2=I3,I2MAX,NP1 FFTT394
    DATA(I2)=WORK(K) FFTT395
    DATA(I2+1)=WORK(K+1) FFTT396
693 K=K+2 FFTT397
    GO TO 698 FFTT398
C FFTT399
C COMPLETE A REAL TRANSFORM IN THE 1ST DIMENSION, N ODD, BY CON- FFTT400
C JUGATE SYMMETRIES AT EACH STAGE. FFTT401
C FFTT402
695 J3MAX=I3+IFP2-NP1 FFTT403
    DO 697 J3=I3,J3MAX,NP1 FFTT404
    J2MAX=J3+NP2-J2STP FFTT405
    DO 697 J2=J3,J2MAX,J2STP FFTT406
    J1MAX=J2+J1RG2-IFP2 FFTT407
    J1CNJ=J3+J2MAX+J2STP-J2 FFTT408
    DO 697 J1=J2,J1MAX,IFP2 FFTT409
    K=1+J1-I3 FFTT410
    DATA(J1)=WORK(K) FFTT411
```

RELEASE 2.0

FOURT

DATE = 77139

21/11/39

	DATA(J1+1)=WORK(K+1)	FFTT4120
	IF(J1-J2)697,697,696	FFTT4130
696	DATA(J1CNJ)=WORK(K)	FFTT4140
	DATA(J1CNJ+1)=-WORK(K+1)	FFTT4150
697	J1CNJ=J1CNJ-IFP2	FFTT4160
698	CONTINUE	FFTT4170
	IF=IF+1	FFTT4180
	IFP1=IFP2	FFTT4190
	IF(IFP1-NP1)700,700,610	FFTT4200
		FFTT4210
C		FFTT4220
C	COMPLETE A REAL TRANSFORM IN THE 1ST DIMENSION, N EVEN, BY CON-	FFTT4230
C	JUGATE SYMMETRIES.	FFTT4240
C		FFTT4250
700	GO TO (900,800,900,701),ICASE	FFTT4260
701	NHALF=N	FFTT4270
	N=N+N	FFTT4280
	THETA=-TWOPI/FLOAT(N)	FFTT4290
	IF(ISIGN)703,702,702	FFTT4300
702	THETA=-THETA	FFTT4310
703	SINTH=SIN(THETA/2.)	FFTT4320
	WSTPR=-2.*SINTH*SINTH	FFTT4330
	WSTPI=SIN(THETA)	FFTT4340
	WR=WSTPR+1.	FFTT4350
	WI=WSTPI	FFTT4360
	IMIN=3	FFTT4370
	JMIN=2*NHALF-1	FFTT4380
	GO TO 725	FFTT4390
710	J=JMIN	FFTT4400
	DO 720 I=IMIN,NTOT,NP2	FFTT4410
	SUMR=(DATA(I)+DATA(J))/2.	FFTT4420
	SUMI=(DATA(I+1)+DATA(J+1))/2.	FFTT4430
	DIFR=(DATA(I)-DATA(J))/2.	FFTT4440
	DIFI=(DATA(I+1)-DATA(J+1))/2.	FFTT4450
	TEMPR=WR*SUMI+WI*DIFR	FFTT4460
	TEMPI=WI*SUMI-WR*DIFR	FFTT4470
	DATA(I)=SUMR+TEMPR	FFTT4480
	DATA(I+1)=DIFI+TEMPI	FFTT4490
	DATA(J)=SUMR-TEMPR	FFTT4500
	DATA(J+1)=-DIFI+TEMPI	FFTT4510
720	J=J+NP2	FFTT4520
	IMIN=IMIN+2	FFTT4530
	JMIN=JMIN-2	FFTT4540
	TEMPR=WR	FFTT4550
	WR=WR*WSTPR-WI*WSTPI+WR	FFTT4560
	WI=TEMPR*WSTPI+WI*WSTPR+WI	FFTT4570
725	IF(IMIN-JMIN)710,730,740	FFTT4580
730	IF(ISIGN)731,740,740	FFTT4590
731	DO 735 I=IMIN,NTOT,NP2	

1 RELEASE 2.0

FOURT

DATE = 77139

21/11/39

```
735 DATA(I+1)=-DATA(I+1) FFTT4600
740 NP2=NP2+NP2 FFTT4610
      NTOT=NTOT+NTOT FFTT4620
      J=NTOT+1 FFTT4630
      IMAX=NTOT/2+1 FFTT4640
745 IMIN=IMAX-2*NHALF FFTT4650
      I=IMIN FFTT4660
      GO TO 755 FFTT4670
750 DATA(J)=DATA(I) FFTT4680
      DATA(J+1)=-DATA(I+1) FFTT4690
755 I=I+2 FFTT4700
      J=J-2 FFTT4710
      IF(I-IMAX)750,760,760 FFTT4720
760 DATA(J)=DATA(IMIN)-DATA(IMIN+1) FFTT4730
      DATA(J+1)=0. FFTT4740
      IF(I-J)770,780,780 FFTT4750
765 DATA(J)=DATA(I) FFTT4760
      DATA(J+1)=DATA(I+1) FFTT4770
770 I=I-2 FFTT4780
      J=J-2 FFTT4790
      IF(I-IMIN)775,775,765 FFTT4800
775 DATA(J)=DATA(IMIN)+DATA(IMIN+1) FFTT4810
      DATA(J+1)=0. FFTT4820
      IMAX=IMIN FFTT4830
      GO TO 745 FFTT4840
780 DATA(1)=DATA(1)+DATA(2) FFTT4850
      DATA(2)=0. FFTT4860
      GO TO 900 FFTT4870
C FFTT4880
C COMPLETE A REAL TRANSFORM FOR THE 2ND OR 3RD DIMENSION BY FFTT4890
C CONJUGATE SYMMETRIES. FFTT4900
C FFTT4910
800 IF(I1RNG-NP1)805,900,900 FFTT4920
805 DO 860 I3=1,NTOT,NP2 FFTT4930
      I2MAX=I3+NP2-NP1 FFTT4940
      DO 860 I2=I3,I2MAX,NP1 FFTT4950
      IMIN=I2+I1RNG FFTT4960
      IMAX=I2+NP1-2 FFTT4970
      JMAX=2*I3+NP1-IMIN FFTT4980
      IF(I2-I3)820,820,810 FFTT4990
810 JMAX=JMAX+NP2 FFTT5000
820 IF(IDIM-2)850,850,830 FFTT5010
830 J=JMAX+NPO FFTT5020
      DO 840 I=IMIN,IMAX,2 FFTT5030
      DATA(I)=DATA(J) FFTT5040
      DATA(I+1)=-DATA(J+1) FFTT5050
840 J=J-2 FFTT5060
850 J=JMAX FFTT5070
```

1 RELEASE 2.0

FOURT

DATE = 77139

21/11/39

	DO 860 I=IMIN,IMAX,NPO	FFTT5080
	DATA(I)=DATA(J)	FFTT5090
	DATA(I+1)=-DATA(J+1)	FFTT5100
860	J=J-NPO	FFTT5110
C		FFTT5120
C	END OF LOOP ON EACH DIMENSION	FFTT5130
C		FFTT5140
900	NPO=NP1	FFTT5150
	NP1=NP2	FFTT5160
910	NPREV=N	FFTT5170
920	RETURN	FFTT5180
	END	FFTT5190

\*\*\* WAVE PROPAGATION IN COMPOSITE PLATE \*\*\*  
GRAPHITE FIBER(55%)-EPOXY MATRIX COMPOSITE

LAYUP ANGLE= 15 DEGREE  
C(1,1)= 0.24560D+08 PSI  
C(2,2)= 0.11700D+07 PSI  
C(1,2)= 0.40000D+06 PSI  
C(6,6)= 0.35520D+06 PSI

TOTAL THICKNESS OF COMPOSITE PLATE ; DELTA= 1.00000 CM  
DENSITY OF COMPOSITE ; RHO= 1.44000 GR/CM\*\*3  
PLATE IS MADE OF 8 IDENTICAL LAYERS  
LAYER THICKNESS ; 2B= 0.12500 CM

TOTAL SPACE STEPS; NX= 64 WITH 8 STEPS FOR CONTACT RADIUS  
TOTAL TIME STEPS ; NT= 32 WITH 24 STEPS FOR CONTACT TIME

CONTACT RADIUS ; A= 0.20000D-01 M  
SPACE STEP ; DX= 0.25000D-02 M  
CONTACT TIME ; TAU0= 0.60000D-05 SECOND  
TIME STEP ; DT= 0.25000D-06 SECOND



















